ABSTRACT

TAYLOR, ELLIOTT McDONALD. Two-way Behavior and Fatigue Performance of 3-D GFRP Sandwich Panels.

This research presents the two-way bending and fatigue behavior of an innovative 3-D glass fiber reinforced polymer (GFRP) pultruded sandwich panel. The panels consist of two GFRP face sheets separated by a foam core with through thickness GFRP fiber insertions to achieve the composite action between the top and bottom layers of the panel.

The panels tested under two-way bending include six different configurations to consider the effect of number of skin plies, fiber insertion patterns, panel thicknesses, and the foam type. All panels were simply supported at the four edges, loaded by a single concentrated load at mid span, and tested subjected to a quasi-static loading condition up to failure. The parameters under consideration for testing the two-way panels were also used in a one way configuration under two fatigue loading condition. The fatigue test consists of three point flexural loading configuration in which the panel is subjected to cyclic loading for a minimum of 600,000 cycles or up to failure.

The research also presents the finite element analysis (FEA) which was used to describe the behavior of the 3-D GFRP sandwich panel under the effect of the applied load used in the experimental program. The effect of the various parameters including: the aspect ratio, thickness, skin strength, and insertion density were considered. The experimental results were used to calibrate the analysis and produce design guidelines for practitioners. The proposed design guidelines can be used for design of the panels for various applications.

Two-Way Behavior and Fatigue Performance of 3-D GFRP Sandwich Panels

by
Elliott McDonald Taylor

A thesis submitted to the Graduate Faculty of
North Carolina State University
in partial fulfillment of the
requirements for the Degree of
Master of Science

Civil Engineering

Raleigh, NC

2009

APPROVED BY:

Dr. Vernon Matzen

Dr. Emmett Sumner

Dr. Sami Rizkalla
Chairman of Advisory Committee

DEDICATION

to my grandparents, Ismail and Clara McDonald

BIOGRAPHY

Elliott McDonald Taylor was born to Stuart and Linda Taylor on August 19, 1985 in Pinehurst, North Carolina. Growing up in North Carolina, Elliott was persuaded by his mother, a UNC grad, to become a Tarheel fan. However, his allegiance quickly changed when he enrolled at North Carolina State University in Raleigh, NC during the fall of 2003. Unsure of what he wanted to major in, Elliott enrolled in the First Year College program at NC State. Elliott quickly found his academic niche in civil engineering. In the spring of 2007, Elliott graduated valedictorian of his class with a Bachelor's of Science in Civil Engineering. His love of NC State athletics and academics lead him to stay in Raleigh and pursue a Master's of Science Degree in Structural Engineering. Under the direction of Dr. Sami Rizkalla, Elliott studied the two-way behavior and fatigue performance of 3-D GFRP sandwich panels at the Constructed Facilities Laboratory on NC State's Centennial Campus. On July, 5th 2008, Elliott married his loving wife, Tiffany, in Salisbury NC. Elliott first met Tiffany in 2005 in Mann Hall, the civil engineering building on NC State's main campus where Elliott spent most of his academic career. Few things can compare to his passion for North Carolina State University, it's where he found two of his greatest loves, engineering and Tiffany.

ACKNOWLEDGEMENTS

I can not express enough appreciation to everyone who has assisted me during my graduate career. This opportunity would not have been possible without the profound leadership of my graduate advisor, Dr. Sami Rizkalla. Dr. Rizkalla has provided me with great advice both professionally and personally. He truly cares about each of his students and always makes himself available when needed. Also, I would like to thank the other members of my advisory committee, Dr. Emmett Sumner and Dr. Vernon Matzen. Dr. Sumner has been great in providing guidance in my research and career objectives, including his involvement with the MTS software update.

I am fortunate to have been able to perform experimental research at the Constructed Facilities Laboratory (CFL) located on North Carolina State University's Centennial Campus. This laboratory is a result of the joint venture between the National Science Foundation and the University Cooperative Research Center on Repair of Buildings and Bridges with Composites. I would like to thank Martin Marietta Composites for providing the research funding and test specimens. It was a pleasure to work with Wes Ballew on the testing and modeling of the sandwich panels.

All of the experimental testing could not have been accomplished without the help of the CFL staff: Jerry Atkinson, Jonathan McEntire, Greg Lucier, Lee Nelson, Bill Dunleavy, and Diana Lotito. Also, I would like to thank Dr. Mina Dawood for his timely help with the presentation of this thesis and the other graduate students that provided a fun and eventful work environment.

TABLE OF CONTENTS

LIST OF FIGURES

LIST OF TABLES

Chapter 1

1 Introduction

1.1 Introduction

The competitive construction and industrial market demands continuous innovation and the use of more efficient and economical structural systems and new innovative construction materials. Development of new structural systems and materials typically require significant research and basic understanding of the mechanism and ingredient of these materials so they can be used effectively. In the past decades various sandwich panels have been implemented in aerospace, marine, architectural and transportation industry. This has lead to the increasing amount of interest in lightweight structural systems such as sandwich panels. In recent years the introduction of other new lightweight high-strength materials, such as fiber reinforced polymers (FRP), have changed the way sandwich structures are designed and fabricated.

Sandwich panels consist of two stiff face sheets separated by a lighter and more flexible core material. Core materials range from different types of foam to wood, while the face sheets can be made from a larger variety of materials such as FRP or concrete. While each of these components provide unique structural advantages, when combined the resulting structural system represents a unique type of member with several excellent properties. These properties include thermal insulation, acoustics, and high strength to weight ratios. The face skins act similar to the flanges of an I-beam providing resistance to the induced tensile and compressive internal forces from bending. The core plays the role of the web, separating

the face skins and carrying the shear forces. The faces are typically bonded to the core to achieve the composite action and to transfer the forces between the components

1.2 Research Objective

Recently, a new type of sandwich panel has been developed which incorporates different patterns of through thickness fiber insertions in the core of the panel. These insertions provide the composite action between the skins of the panel and help to resist shear stress in the core. Previous research conducted at North Carolina State University's Constructed Facilities Laboratory showed that various parameters affect the fundamental characteristics of this innovative 3-D GFRP sandwich panels. These include fiber insertion density, fiber insertion pattern and test direction, panel thickness, and GFRP laminate skin thickness. The main objective of this research is to determine the performance of the two-way flexural behavior of these types of GFRP sandwich panels and the behavior under fatigue loading conditions.

The research included a major experimental program consisting of two phases. In the first phase various types of panel configurations were tested in a two way bending configuration to determine the two-way action of these types of sandwich panels. The panels tested under two-way bending include six different configurations to consider the effect of number of skin plies, fiber insertion patterns, panel thicknesses, and the foam type. The measured results were used to calibrate a finite element (FE) analysis which was used to model the two-way behavior. The FE model was then used to study the effect of various parameters believed to affect the sandwich panel's behavior.

The second phase of the experimental program explored the one-way fatigue behavior of the panels. Each panel was subjected to at least 600,000 cycles or until failure. The same panel configurations that were considered in the two-way study were also used in a one way configuration under a fatigue loading condition. The parameters considered include the core shear strain, span length, and fiber insertion density. Based on the measured behavior of the sandwich panels recommendations are provided for the design of the 3-D GFRP sandwich panels.

1.3 Scope and Content

This thesis describes the details of the experimental and analytical program that was conducted to study the two-way bending and fatigue behavior of innovative 3-D GFRP sandwich panels. The thesis consists of six chapters. In addition to this introduction the thesis consists of:

Chapter 2 provides a review of the analysis, design, manufacturing, and applications of sandwich panels. The main findings of previous research conducted on similar 3-D GFRP sandwich panels are discussed.

Chapter 3 provides a detailed description of the experimental program used to determine the two-way behavior and fatigue performance of the proposed 3-D GFRP sandwich panels.

Chapter 4 presents the experimental results obtained for the two-way testing program. Based on the experimental results a finite element model was created to verify the analysis and evaluate the effect of the panel's parameters on the two-way behavior.

Chapter 5 describes the experimental results obtained from the fatigue testing program described in Chapter 3. A power law model is recommended to determine the overall fatigue performance of the sandwich panels throughout their service life and determine the effect of the span length and applied shear stress level.

Chapter 6 highlights the conclusions of both phases of the research program and the recommended design limitations are presented. Recommendations regarding possible future work on the 3-D GFRP sandwich panels are also provided.

Chapter 2

2 Literature Review

2.1 History of Sandwich Panels

On July 20th, 1969 the first successful landing of a spaceship on the moon was the result of the successful application of several new technologies including, rocketry, computers, and sandwich construction. While public interest was centered mainly on the advances in rocketry and computer technology it was with the help of sandwich technology that a space craft shell could be constructed which was light in weight but could be sufficiently strong to sustain the stresses induced from acceleration and landing of the space craft. Prior to 1960, most sandwich technology was limited to aerospace engineering applications. The World War II Mosquito bomber aircraft, which used sandwich panels in parts of the airframe, is known as the first major application of sandwich panels. However there were numerous earlier uses of the sandwich principal (Davies, 2001).

At various times in history the concept of sandwich construction has been considered by many inventors and engineers. Some of the earliest sandwich panel drawings can be found in the works of Leonardo da Vinci. However, the first person to formally describe and record the concept of using two cooperating faces separated by a distance is accredited to a Frenchman, Duleau, in 1820 (Zenkert, 1997). In 1845, the first known sandwich structure was a bridge built in Whales, in which two plates were separated by a wooden egg crate core. Sandwich panels use in aviation started in 1919 when the pontoons of a seaplane were primarily constructed of a mahogany faced sandwich panel with a balsa wood core. The first

all aluminum sandwich panel was constructed in 1945, made of two aluminum facings bonded to an aluminum honeycomb core structure. A honeycomb core is made from very thin sheets of material formed into numerous small cells, usually hexagonal in shape, bonded to each other. The creation of good adhesives allowed for this breakthrough in sandwich technology by creating a sufficient bond between the skins and the core of the sandwich panels. The early adhesives had lower viscosities and would fill the honeycomb cells and would not allow for the skin to be properly bonded to the core (Bitzer, 1997).

The strength and stability of sandwich panels was widely researched during the world wars as well as the late 1940's. However, beside their use in secondary elements the practical application of sandwich structures delayed due to the deficient core materials, bonding methods, and the sandwich structures inspection and repair procedures (Plantema, 1966). Also during this period, Reissner published his well known theory on sandwich plates in which he derives the differential equation for the deflection of a sandwich panel. Libove and Batdorf derived differential equations for the shear forces and deflections of orthotropic panels with thin faces. Hoff, considering the strain energy of a sandwich panel, derived the governing differential equation for an isotropic panel with respect to thick faces. Mindlin derived the governing equation of motion for an isotropic plate accounting for both transverse shear deflections and rotational inertia. These theories provided the basis of the two important books on sandwich constructions published in the 1960's by Plantema and Allen (Zenkert, 1997).

In 1960 a break though occurred, when the utilization of poly-vinyl chloride (PVC) and polyurethane (PUR) foam core materials was discovered. The softness of the foam delayed their use as a core material when they were first produced in the 1940's by the Germans. While foam cores have lesser strength to weight ratios compared to metallic honeycomb cores they offer their share of advantages. Foam cores are typically lower in cost than honeycomb cores, as well as, having better workability. Foam can be easily distorted and uncomplicated surface preparation allows for an improved bond between the core and skin layers. Also, foams utilize greater thermal insulation, acoustical damping, and the closed cell structure ensures buoyancy and prevents water penetration. Polyurethane foams can also be made fire resistant by using additives containing phosphorus (Zenkert, 1997).

Recently, fiber reinforced polymers (FRP) have been used as an alternate material for the skins. FRP offers a greatly increased strength to weight ratio when compared to metallic or wooden facings, as well as, improved corrosion resistance, lower thermal conductivity, and ease of installation. Much of today's research involves the use of computer simulated methods, such as finite element analysis (FEA), to allow for modeling the behavior with great accuracy for specific applications. The existing analytical solutions include approximations and assumptions, which can be excluded from FEA, to provide good accuracy in predicting the behavior. The main application of sandwich structures research has primarily been around the areas of impact resistance, and fatigue.

2.2 Practical Applications

Sandwich construction provides efficient utilization of the materials used for each component to its ultimate limit (Zenkert, 1997). The sandwich structure offers also a very high stiffness-to-weight ratio. It enhances the flexural rigidity of a structure without adding a substantial weight and making it more advantageous as compared to composite materials. Sandwich constructions have superior fatigue strength and exhibit superior acoustical and thermal insulation. Sandwich composites can be used in a wide variety of applications shown in Figure 2.1 to Figure 2.4.

Sandwich composites are increasingly being used in the aerospace industry because of their high strength to weight ratio and enhanced fatigue resistance. Sandwich panels designed for aircraft structures always employ metal faces with metal honeycomb or corrugated cores. Smooth metallic skins are desirable for low wind resistance while the honeycomb core offers excellent fatigue characteristics. Floorboards, composite wings, horizontal stabilizers, composite rudders, landing gear doors, speed brakes, flap segments, aircraft interiors and wingspans are typically made of sandwich composites.

Sandwich composites are well suited for the marine industry's most demanding designs, including stealth naval vessels. Foam cores meet the critical requirements of strength, buoyancy and low water absorption while non-metallic skins offer high corrosion resistance. The main application of sandwich construction with GFRP faces are in boat construction and offshore oil and gas rigs. Other applications include the construction of bulkheads, hulls, decks, and furniture (Allen, 1998).

High strength-to-weight ratios of sandwich composites offer great advantages to the transportation industry. Structural components of freight trailers made from sandwich panels can greatly decrease the weight of the trailer. Thus, allowing for greater amounts of goods to be shipped or a decrease in gas consumption for a similar load. The insulating, sound damping, and low cost characteristics make them an appropriate choice for walls, floors, doors, panels and roofs for vans, trucks, trailers and trains.

Excellent thermal and acoustical insulation provided by foam cores makes sandwich construction an attractive option for the architectural industry. Typical applications include portable buildings, office partitions, roof panels, building facades, and freezer liners.

2.3 Principles of a Sandwich Panel

The three characteristic components of a sandwich panel are illustrated in Figure 2.5. The two thin rigid skins, with relatively high modulus of elasticity, are adhesively bonded to a thick flexible core. Each component alone is relatively weak but when working together they can provide a strong yet lightweight structure. The cores separation of the skins allows for an increased moment of inertia than the skins would be able to provide by themselves. Another important part of the sandwich panel, is the adhesive bond between the foam and skin layers. The adhesive bond is required to transfer shear forces between the layers and achieve the composite action of the material. In certain types of structures weight savings can be as much as 30 %. Other advantages of sandwich panels include: good fatigue properties, good thermal and acoustical insulation, and ease of mass production (Plantema, 1966).

Thin, high strength sheets are commonly used for the skins of the panel. The skins primary purpose is to carry the high tensile and compressive forces induced in the structure. Steel, aluminum, FRP, and even concrete are commonly used as materials for the facings.

The core's main function is to separate the face sheets at a constant distance from each other in an effort to maximize the moment of inertia for the section. In addition, the core should be able to provide enough resistance to the induced shear stresses. Furthermore, the core should be stiff enough to keep the face sheets flat so as to prevent them from buckling out of plane under induced compressive forces.

In a sandwich beam, typically the core material is not rigid; therefore, the shear deflection within the core is insignificant in most cases. The shear deflection in the faces can be also neglected. The effect of shear rigidity in the core is shown in Figure 2.6. Figure 2.6 (a) shows an ideal sandwich beam using relatively stiff core, therefore the two faces cooperate without sliding relative to each other. Figure 2.6 (b) shows a sandwich beam using weak core, therefore the faces are no longer coupled together effectively and each face works independently as plates in bending. Use of a weak core in shear results in significant loss of the efficiency of the sandwich structures.

2.4 Proposed GFRP Sandwich Panels

The proposed 3-D GFRP sandwich panels in this study consist of a polyisocyanurate foam core sandwiched between two glass fiber reinforced polymer (GFRP) face sheets which are bond together by through thickness GFRP insertions, as show in Figure 2.7. The through

thickness fibers are added to the traditional sandwich structure to attempt to improve the deficiencies associated with sandwich panels.

Like with any material there are disadvantages for their use in certain cases. Disadvantages associated with the design of conventional sandwich panels can be related to the various failure modes of sandwich panels, as illustrated in Figure 2.8. Debonding of the skins from the core is the most common problem in GFRP sandwich structures. The initiation of the damage can be caused by manufacturing imperfections or by impact forces applied to a sandwich panel. The though thickness fibers are used in addition to an adhesive layer between the facing and core layers to prevent a debonding mechanism from forming.

Another common problem relating to sandwich panels occurs when the core is very flexible in shear, as is the case for the proposed panels. Polyurethane foam cores are typically much weaker than equivalent density honeycomb counterparts. Table 2.1 provides some typical properties of various core materials. Also, weaker, less dense foam cores may allow sudden failures when the face sheets buckle on the compression side (Bitzer, 1997). Because of the flexible core deflections now become a function of not only bending, but are also dependent on shear. In certain cases, the contribution of shear deformation to the total deflection can exceed that of bending (Allen, 1998). Introduction of the through thickness fibers creates a much stiffer core in shear, thus decreasing the amount of deflection due to shear. However, shear deflections may still be large enough to contribute to the overall behavior of the beam and should be considered.

The panels are fabricated using a pultrusion process, shown in Figure 2.9, where the through thickness fibers are injected through the panels before the thermoset resin has cured. To begin the pultrusion process, varying layers of stitched fabrics are pulled together to produce the desired top and bottom skin thicknesses. The urethane foam core is inserted between the top and bottom layers to form the sandwich panel and maintain spacing. 3-D fibers are then inserted through the entire panel and cut to the desired length. Finally, epoxy resin infuses throughout the glass fibers of the panel which is then pulled through a heated die forming the cured composite structural member. The width of the panels can vary from 6 in. to 8 ft. 6 in. while the thickness can vary from ½ to 4 in. The fiber insertion density can vary from 0 to 16 fibers per square inch (fipsi). Skin ply thickness can vary from 0.1 to 0.5 in. The fibers can be oriented in a variety of patterns, as shown in Figure 2.10. Patterns 1 and 2 are regular arrays with 4 and 8 fiber insertions per square inch (fipsi), respectively. Patterns 3a, 3b, and 4 are wall type patterns; the one-way walls are effective in resisting the shear force similar to a web of a steel W shape. Patterns 5 and 6 are also wall patterns but contain walls in two directions rather than only one for patterns 3 and 4. Only patterns 1, 2, 5, and 6 will be investigated in this study because of the limited number of panels available for testing.

2.5 Current Knowledge

The Constructed facilities laboratory at North Carolina State University has conducted extensive testing on the 3-D GFRP sandwich panels described in the previous section. Hundreds of specimens were tested to determine the material properties of the

panels and how various parameters affected their behavior. Parameters considered included fiber insertion pattern and test direction, panel thickness, and GFRP skin thickness (Reis, 2005).

Experimental results of the compression strength of the panels at NCSU showed that the compression strength was directly related to the density of fiber insertions but independent of fiber insertion pattern. Testing also showed that decreasing the thickness of the panel increased their compressive strength by increasing the buckling load of the 3-D fibers. Through testing of the panels with the foam core removed results indicate the importance of the foam core in providing lateral support to the 3-D fibers thus providing an increased stiffness of the fibers in compression and shear (Reis, 2005).

Tension testing of the GFRP laminate skins showed a bilinear stress-strain relationship which is due to the effect of the though thickness fibers perpendicular to the direction of the fibers in tension with the initial elastic modulus about 25% higher than the second (Patrick, 2006). An increase in fiber insertion density resulted in decreased in-plane tension strength of the skins. Results indicated that the fiber pattern, density, nor test direction had an effect on the elastic modulus. However, the test direction resulted and fiber pattern resulted in varying the skins rupture failure modes and strength. The ultimate strength of the skins is also dependent on the configuration and test direction of the insertion patters. These results suggest that the through thickness fibers can create areas of imperfections, and discontinuities, which may cause premature failure at these locations.

The shear behavior consisted of a near linear shear stress-strain relationship until initiation of the first crack in the foam layer which is followed by a continued reduction in stiffness up to failure. This reduction in stiffness can be accredited to the diagonal shear cracks forming throughout the foam core and the formation of plastic hinges at the ends of the through thickness fibers. Testing of the panels subjected to pure shear showed a considerable effect in the shear behavior from fiber insertion patterns and test direction. The presence of a wall of through thickness fibers creates a shear wall and thus significantly increases the shear modulus of the panel by decreasing the stress at the joint between the skin and fiber insertion. Wall patterns tested in the parallel to the wall insertions had a 200% increase in shear stiffness when compared to the perpendicular direction. It was also shown that the thickness of the panel exhibited negligible effect on shear stiffness but did show a decrease in ultimate strength with increasing panel thickness.

Load vs. deflection plots for flexural tests on the panels exhibited a linear relationship until the initial of shear cracking in the core followed by a gradual decease in stiffness until failure. Failure of the panels was usually defined as excessive deflection at midspan, although some specimens failed due to rupture of the GFRP skins in compression. Experimental results show that the shear characteristics of the core have considerable influence on the panel's flexural behavior. Testing of panels with identical parameters but with different widths showed that doubling the width would double the ultimate load of the panel. Therefore, design guidelines could use a unit width approach when determining ultimate strength of a panel (Patrick, 2006).

Figure 2.1 Outer shell of airplane made from aluminum sandwich panels

.

Figure 2.2 Fusion of the FRP skin of a boat hull

Figure 2.3 Full scale trailer tested at CFL

Figure 2.4 Architectural Sandwich Panels

Figure 2.5 Sandwich Panel Components

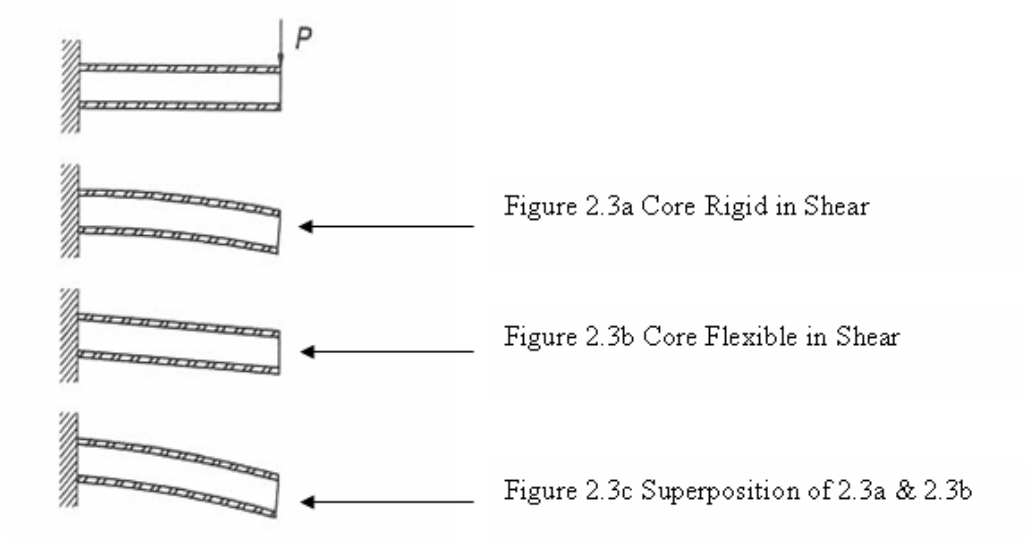

Figure 2.6 Behavior of typical sandwich beam

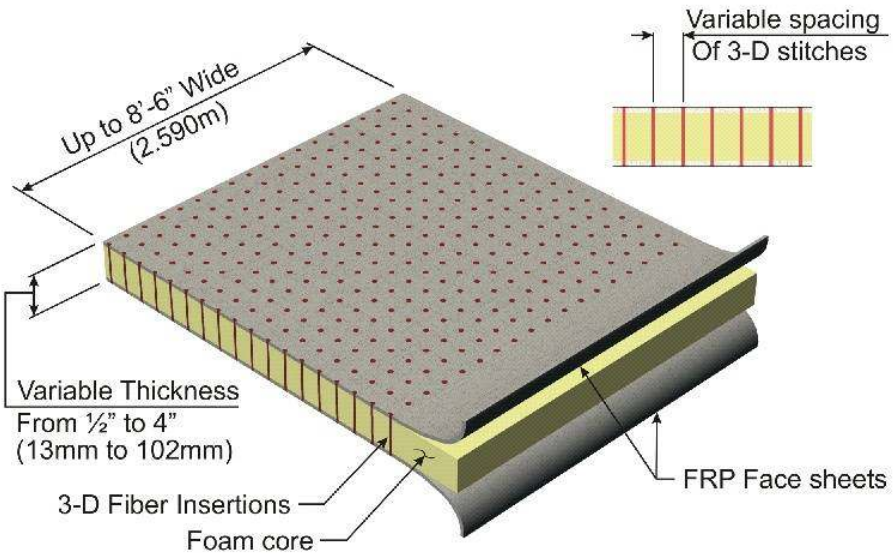

Figure 2.7 Proposed sandwich panels

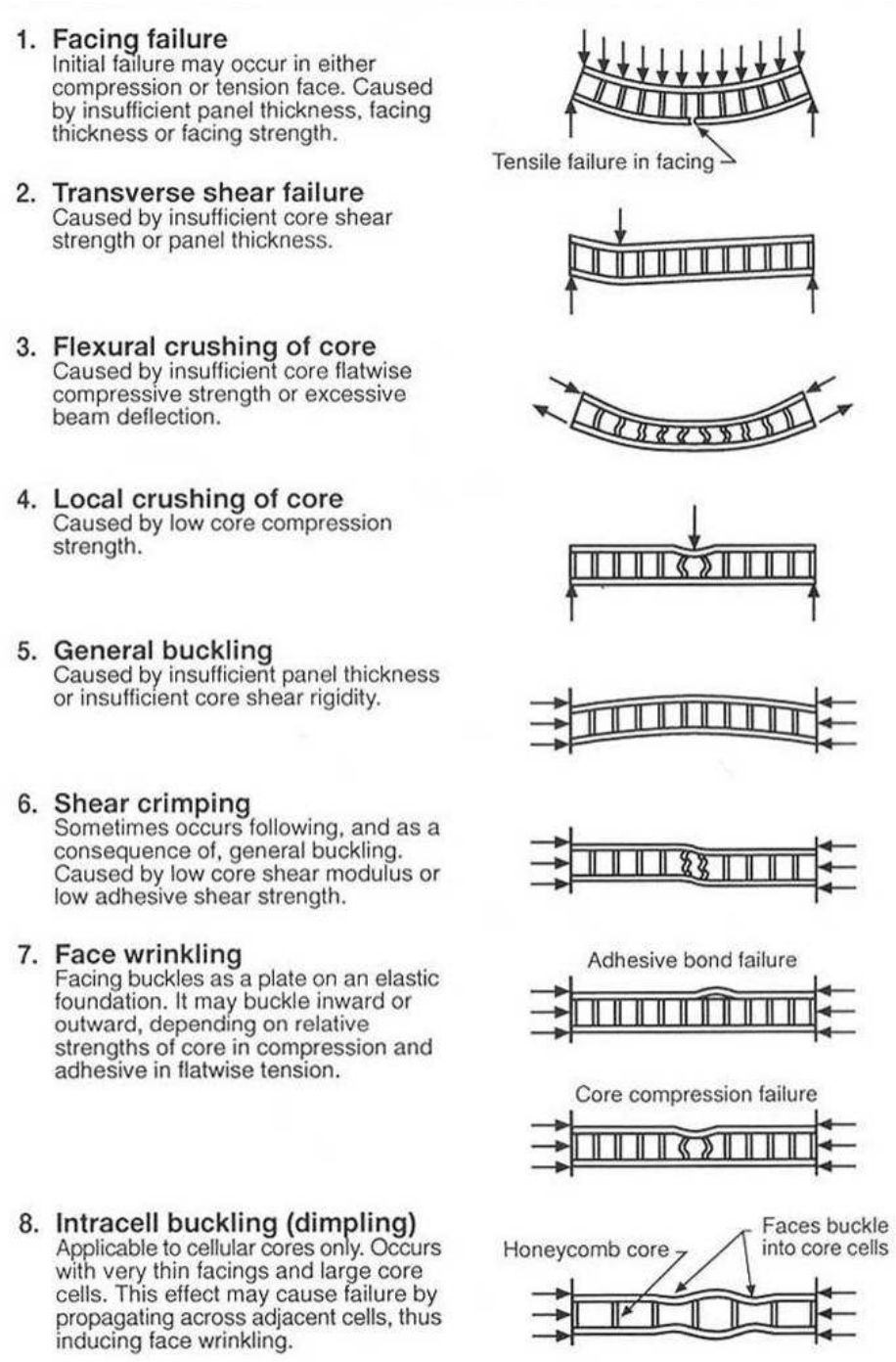

Figure 2.8 Typical failure modes of GFRP Sandwich Beams

Material	Density (pcf)	Bending Strength (psi)	Bending Modulus (ksi)	Shear Strength (psi)	Shear Modulus (ksi)
Aluminum Honeycomb	3.1	300	75	210	45
Nomex Honeycomb	3	325	20	175	6
Fiberglass Honeycomb	3	410	23	195	19
Rohacell Foam	3.1	128	10	114	3
Klegecell Foam	3	69	2.7	51	1.1
Rigicell Foam	3	80	2.5	70	2.5
Divinycell Foam	3.1	100	10.2	73	2.5

Table 2-1 Core material comparison

Figure 2.9 Manufacturing Process

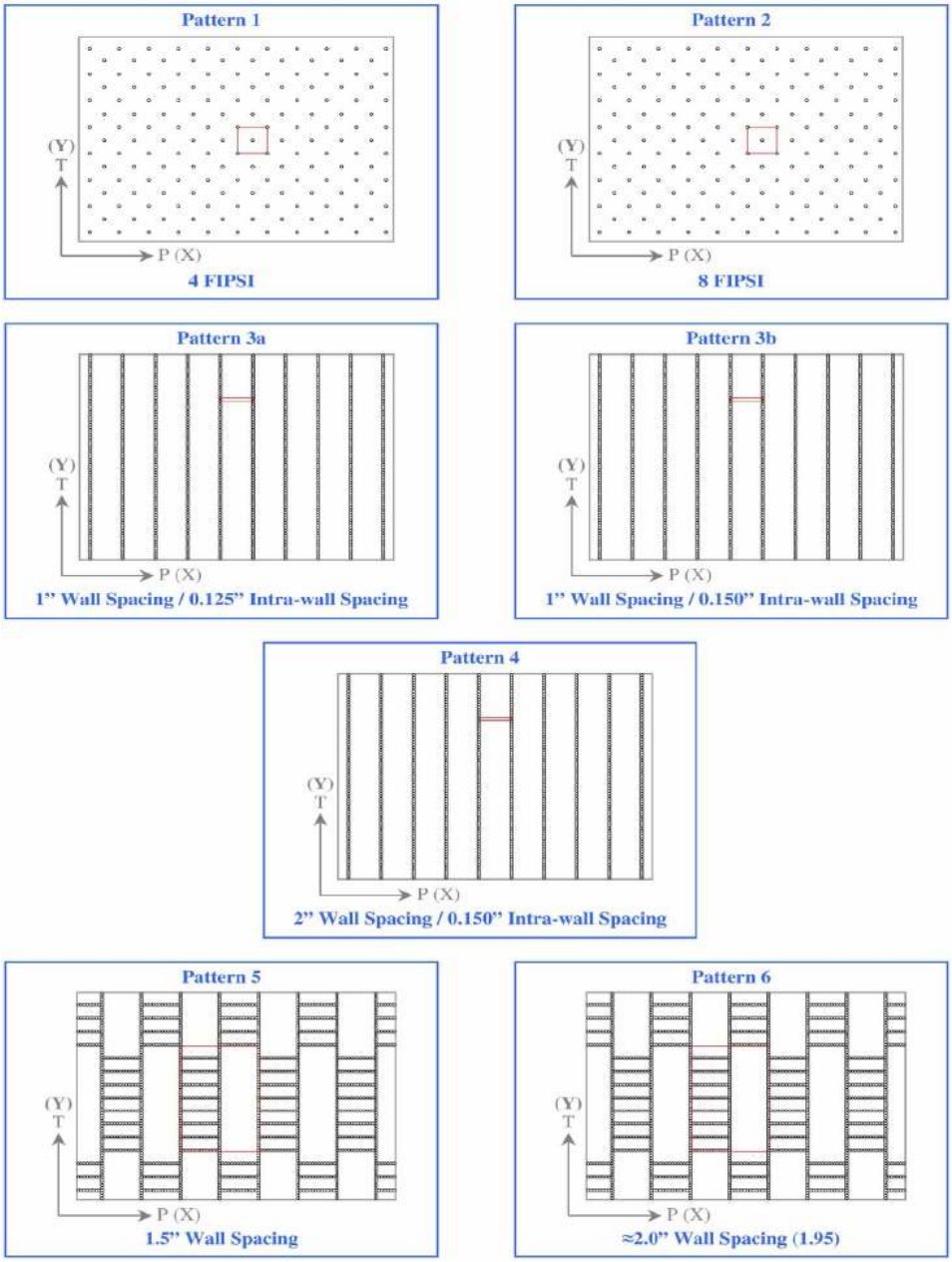

Figure 2.10 Fiber insertion patterns

Chapter 3

3 Experimental Program

3.1 Introduction

This chapter describes the research program conducted at the Constructed Facilities Laboratory at North Carolina State University to determine structural characteristics of new and innovative 3-D GFRP pultruded sandwich panels. The experimental program is designed to determine the behavior of the panels subjected to static two-way bending, as well as, the response to fatigue loadings under one-way bending conditions.

The experimental program examines different geometric properties of the panel and their effect on the structural behavior of the panel. Each unique panel consists of different properties such as the number of skin plies, panel thickness, fiber insertion pattern, and type of foam. Each specimen for the two-way bending and fatigue tests was cut from a 4 ft. by 8 ft. panel using a wet saw with a concrete cutting blade in the configuration shown in Figure 3.1, and assigned a letter for which area of the panel the specimen was cut. Cutting each specimen from the same panel ensures the same properties for each panel of the same type is achieved and minimizes the effect of variability between panel productions. The GFRP skins are constructed using glass fibers woven together using a two way weave pattern and then several layers may be epoxied together to form thicker GFRP skins. The skins in this experiment range from 2 to 4 individual plies with ply thicknesses ranging from 0.15 in. to 0.18 in. thick. Thickness of the panels can be up to 4 in. this study will focus on panel 3 different thicknesses of 1, 1.5, and 2 in. Increasing the thickness of the panel is mainly

achieved through increasing the thickness of the foam core. The primary foam used in the tested panels was TRYMER 200L polyisocyanurate foam. TRYMER 200L foam is extensively used in composite panel applications because it is easily fabricated into sheets and is less brittle than conventional foams, for improved handling. One other foam type was used in the construction of one of the test specimens; the alternate foam was of the same type as the TRYMER foam but made from a different brand. The fiber insertion patterns studied in this program were identified according to the manufacturer's designation. Four different fiber patterns were considered in the current study as shown in Figure 3.2. The fiber patterns under investigation can be categorized into two main types. Patterns 1 and 2 are continuous arrays in which the fiber insertions are distributed evenly in the X and Y directions with two different fiber insertion densities, 4 fipsi and 8 fipsi. Patterns 5 and 6 are in a "checkerboard" configuration in which discontinuous wall sets of fiber insertions in the X direction are separated by continuous walls in the Y direction. The through thickness fibers in Pattern 1 are spaced at 0.333 in. in the X direction while Y direction spacing is slightly larger at 0.375 in. Pattern 2 has equal spacing of fibers in both X and Y directions at 0.25 in. Patterns 5 and 6 walls remain continuous in the y-direction whereas in the x-direction sets of shorter walls are offset in an alternating, checkerboard like pattern, as shown in Figure 3.2. The only difference between Patterns 5 and 6 is the spacing of the continuous walls in the x-direction. The inter-wall spacing in Pattern 5 is 1.5 in. compared to 1.95 in. for Pattern 6. With these fundamental understandings of the types of sandwich panels

considered in this program, the experimental research programs for the two-way bending behavior and the one-way fatigue performance are discussed in the following sections.

3.2 Two-Way Bending

The main objective of the experimental program for the two-way flexural testing was to determine the flexural behavior of the panels and the effect of the panels properties had during testing. These results provided essential information for an accurate analysis of the flexural two-way bending behavior. A total of 6 different specimens were tested until failure with variations in panel thickness, number of skin plies, foam type, and fiber insertion pattern. A nomenclature for the two way bending specimens was developed by the manufacturer as follows: PT-(RDPS2-2-1)-A, where "PT" represents the type of test in this case "Panel Test", RDPS2 refers to **R**esearch and **D**evelopment **P**anel **S**et **2**, 2 is the number of skin plies if less than 4, if 4 skin plies are used this field is left blank, 1 is the fiber insertion pattern, and A refers to the location from which the specimen was cut from the original 8 ft. x 4 ft. panel, as shown in Figure 3.1. Nomenclature and panel properties are shown in Table 3-1.

The test setup for a typical 4 ft. x 4 ft. two-way bending specimen is shown in Figure 3.3 and Figure 3.4. The panels were simply supported on all four sides in a two-way bending configuration and loaded in the out of plane Z-direction until failure occurred. The panel was supported by 4 in. wide by ½ in. thick neoprene pads, which were resting on stiff steel beams, to allow for end translation and rotation of the panel. A 4 in. spaced grid was drawn

on top of the specimen to better show the deflection of the specimen as shown in Figure 3.5. The loading was applied on a 4 in. square area at the midpoint of the panel by a 200 kip hydraulic actuator on a 1 in. thick steel plate resting on a 1 ½ in. thick neoprene pad in displacement control at a quasi static rate. Strain was measured using, Vishay C2A-06-250LW-120 series, 120 ohm electric resistance strain gages located at two quarter points in the X and Y directions on the top and bottom of each specimen, shown in Figure 3.6, as well as at the center of the specimen on the bottom skin. Deflection was measured from the bottom of the panel at the quarter points as well as at the center using 3 string potentiometers, as shown in Figure 3.3. Load was recorded using a 200 kip load cell built in the actuator. Data was acquired from the instrumentation using a Vishay Model 5100b scanner and Vishay Strain Smart v. 4.01 data acquisition software.

3.3 Fatigue

The fatigue response of the panels is considered in this research program to determine the inherent changes in behavior of the panels throughout their service lifetime. The main objective is to determine the difference in the panel properties after it has been in use for an extended period of time. Using the same six panel types as used in the two-way bending tests, four 4 ft. x 1 ft. specimens were cut from each of the larger 4 ft. x 8 ft. original panels giving 24 total flexural fatigue specimens. The 24 specimen had varying panel thickness, number of skin plies, foam type, and fiber insertion pattern similar to the two way bending tests. Two different spans and loading magnitudes of loading were considered in the fatigue

study. The maximum applied loads, P_1 and P_2, were calculated using Elementary Sandwich Theory (EST) for predicted core shear strains of 1% and 2%, respectively, for each panel type. The maximum load was limited to 2% core shear strain to simulate a range of typical service loads and to prevent cracking of the foam core under the service load. One specimen was tested with a maximum loading equivalent to a predicted core shear strain of 0.5%. Original testing called for maximum loadings predicting core shear strains of 0.5% and 1%, however, the 0.5% maximum loading was increased to 2% after testing showed negligible fatigue effects due to the lower level of shear stress. The maximum loading, in each case, was within the linear portion of the load-deflection relationship, for simply supported panels subjected to 3 point bending, which was determined through previous conducted at the CFL on NCSU's Centennial Campus.

EST uses Bernoulli-Euler Beam Theory with adaptations for the composite nature of the cross-section. The transverse displacement of a composite sandwich beam can be separated into two independent components: deformation due to bending (Δ_B) and deformation due to shear (Δ_S). The flexural deflection component can be calculated based on the ordinary beam theory relationship:

$$\frac{d^2\Delta_B}{dx^2} = \frac{M(x)}{D} \tag{3.1}$$

where M is the bending moment induced by loading and D is the flexural rigidity of the sandwich panel. Neglecting the bending resistance of the flexible foam core the shear

rigidity of the panel is dependent on the elastic modulus of the GFRP skins and the moment of inertia of the skins about the panels neutral axis, as follows:

$$D = E_{skin}\frac{bt^3}{6} + E_{skin}\frac{btd^2}{2} \tag{3.2}$$

For a simply supported beam with span length (L) and subjected to a concentrated point load P at midspan the maximum deflection due to bending is given by:

$$\Delta_B = \frac{PL^3}{48D} \tag{3.3}$$

The elastic modulus of the GFRP skin was determined through previous testing, also conducted at the CFL, and was found to be 2700 ksi.

The shear deflection of the sandwich panels can be calculated similarly, based on the following EST expression described by Allen (1969):

$$\frac{d\Delta_S}{dx} = \frac{V(x)}{AG} \tag{3.4}$$

where A is the shear area of the sandwich panel and G is the shear modulus. The product AG is denoted the shear stiffness of the sandwich panels which is analogous to the flexural stiffness, D. For a simply supported panel with span length (L) and subjected to a concentrated load P at midspan the maximum deflection at midspan due to shear is given as follows:

$$\Delta_S = \frac{PL}{4AG} \tag{3.5}$$

Therefore, the total deflection due to the applied load is the sum of the flexural and shear deflections given by:

$$\Delta_{total} = \frac{PL^3}{48D} + \frac{PL}{4AG} \tag{3.6}$$

Based on this relationship and the load-deflection behavior of the statically tested 3-point bending specimens, the shear modulus (G), given in Table 3-2, was calculated for each panel type. The shear modulus was assumed to be constant up to 2% shear strain since the initial load-deflection behavior of the flexural specimens was linear. The maximum load for each panel was determined using these calculated shear moduli. Since the foam core is relatively weak the shear stress in the core (τ) can be assumed to be constant (Patrick, 2006) and is given by the following expression:

$$\tau = \frac{\mathrm{V}}{\mathrm{bd}} \tag{3.7}$$

where V is the shear force induced by the concentrated load P, b is the width of the panel and d is the effective depth measured between the centerline of the panel's skins. In the case of a panel subjected to 3-point bending the shear force in the panel is equal to half the applied load P. Therefore, the shear stress can be calculated directly using the following equation:

$$\tau = \frac{\mathrm{P}}{\mathrm{2bd}} \tag{3.8}$$

and the core shear strain (γ) as:

$$\gamma = \frac{\tau}{G} \tag{3.9}$$

Based on Equation 3.8 and 3.9 the maximum loads (P_1 and P_2) for the two levels of shear strain, 1% and 2%, for the fatigue testing program were calculated as follows:

$$P_1 = 2(.01)Gbd \tag{3.10}$$

$$P_2 = 2(.02)Gbd \tag{3.11}$$

Nomenclature for the fatigue testing, also specified by the manufacturer, follows the same order as the two-way bending nomenclature. Therefore, FT-(RDPS2-2-1)-B denotes a **F**atigue **T**est (FT) on a **R**esearch and **D**evelopment **P**anel **S**et **2**, with **2** skin plies, fiber insertion pattern **1**, and cut from location **B** of the 8 ft. x 4 ft. original panel, as shown in Figure 3.1. Table 3-3 outlines the experimental program and gives each test's nomenclature. Also, Table 3-4 lists the maximum and minimum applied loadings for the 1% and 2% core shear strain conditions.

The fatigue specimens were cut into 4 ft. x 1 ft. rectangular panels. Panels with fiber insertion patterns 5 and 6 were cut such that the Y direction would run in the long (testing) direction of the pane1. Due to geometric constraints no panels were tested in the X direction. The panels were tested in a simply supported 3-point bending configuration. The pinned and roller supports were distributed across the entire with of the specimen. The pinned support was simulated by adhesively bonding the steel plate shown in Figure 3.8 to the bottom of the sandwich panel. The roller was simulated by allowing the panel to slide along the steel plate. Likewise, the load was distributed across the full width of the panel by a similar steel plate as shown in Figure 3.9. Two different spans of 40 and 28 in. were considered in the experimental program, as shown in Figure 3.10 and Figure 3.11, to determine the effect of

the span length on the panel's fatigue performance. The supports were bolted to a double channel fixture which allowed for the supports to easily be moved. The pinned support which was a steel plate was connected to the specimen using a two part prevented the specimen from "walking" off the support in the longitudinal, Y-direction, during testing. Wooden braces were also constructed to prevent the panel from moving in the lateral, X direction. Teflon pads were used to prevent friction between the wooden braces and the specimen. A 1 kip Interface fatigue rated load cell, shown in Figure 3.12, was used to control the MTS actuator. The MTS actuator applied the load through a steel double channel spreader beam, shown in Figure 3.13, to the pin and roller supports through the panel and into the load cell above the central loading point. Each panel was loaded up to its predicted core shear strain loading and unloaded to 20% of the panel's maximum loading at a maximum frequency of 2 Hz for a minimum of 600,000 cycles or until failure. Loading the specimen to the same load each cycle allows for the deflection and strain to change with respect to the number of loading cycles. Deflection was measured using the internal LVDT in the MTS machine. Also, strain was recorded on the extreme tension fibers at mid-span using a Vishay C2A-06-250LW-120 series, linear strain gage shown in Figure 3.14. The deflection and strain data were recorded under the maximum and minimum loading at different stages throughout the fatigue loading program. Data was acquired through the MTS controller using Flextest SE version 3.4B software.

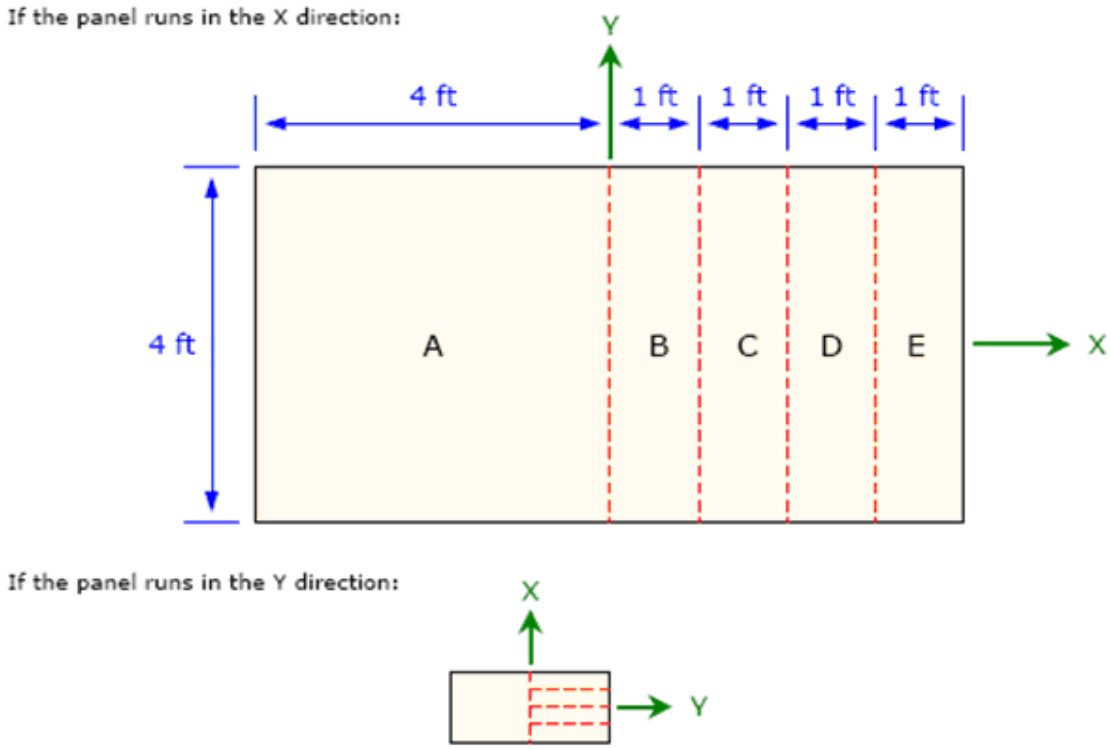

Figure 3.1 Panel Sections to be Cut

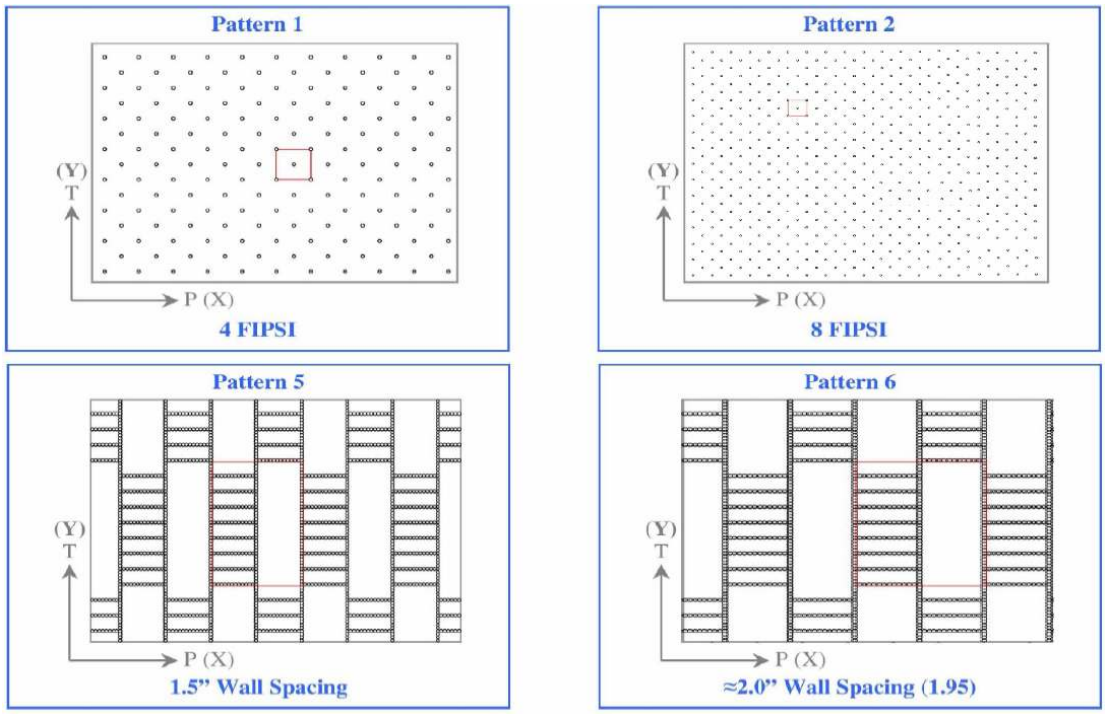

Figure 3.2 Fiber Insertion Pattern

Table 3-1 Two-Way Testing Nomenclature

Panel Set	Skin Plies	Insertion Pattern	Foam Type	Panel Height	Nomenclature
RDPS2	2	1	1	1.5"	PT-(RDPS2-2-1)-A
RDPS3	4	5	1	1"	PT-(RDPS3-5)-A
RDPS3	4	6	1	1"	PT-(RDPS3-6)-A
RDPS4	4	1	1	2"	PT-(RDPS4-1)-A
RDPS4	4	2	1	2"	PT-(RDPS4-2)-A
RDPS4	4	1	2	2"	PT-(RDPS4-7)-A*

***RDPS4-7 refers to the insertion pattern 1, with the alternate foam type.**

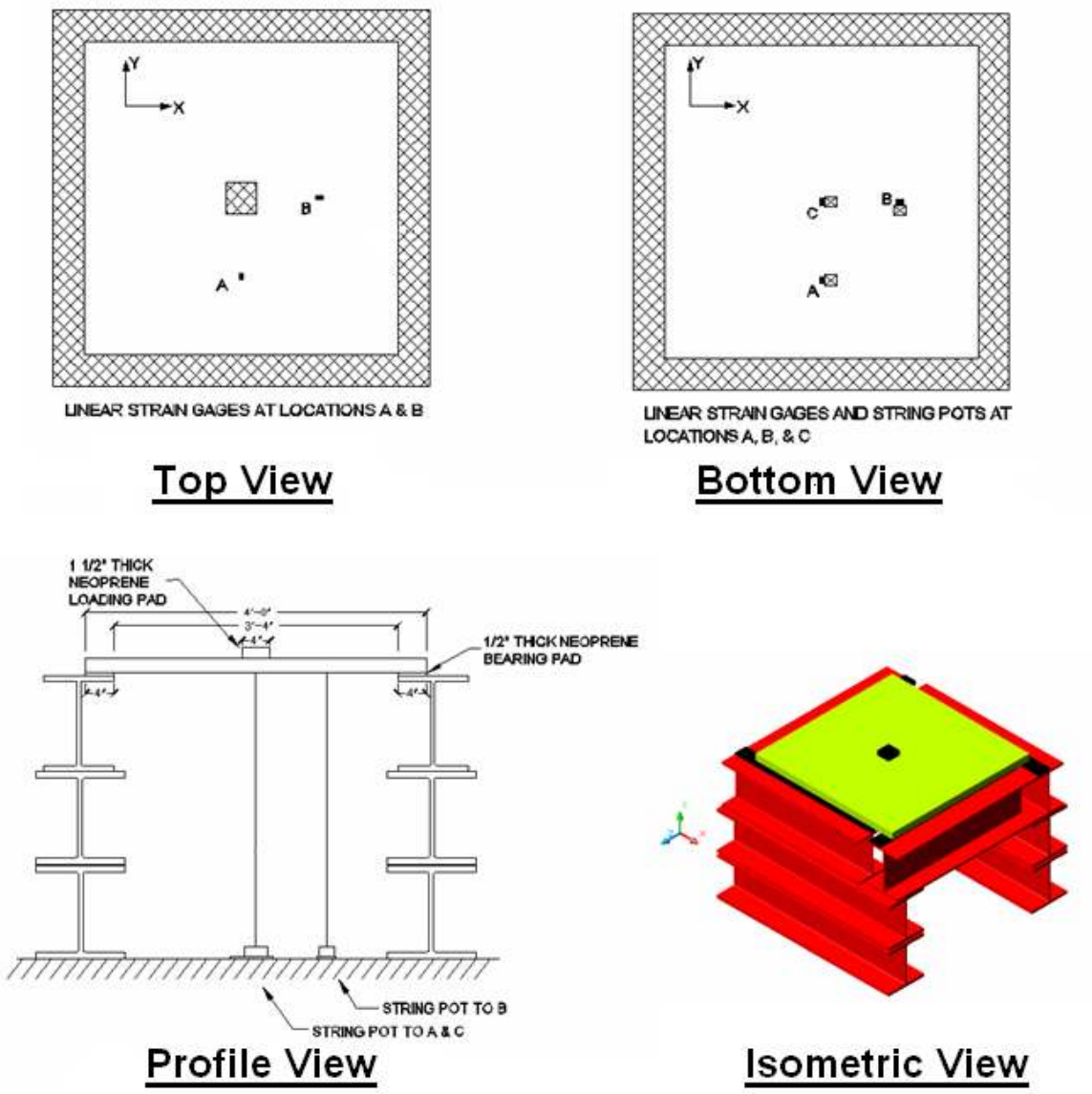

Figure 3.3 Two-Way Test Setup

Figure 3.4 Two-Way Bending Supports

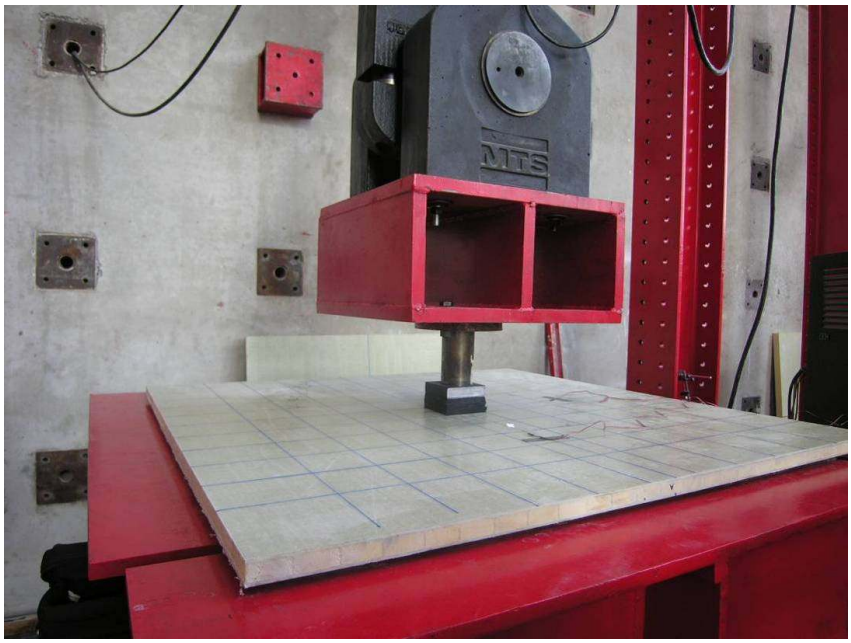

Figure 3.5 Two-Way Test with Grid

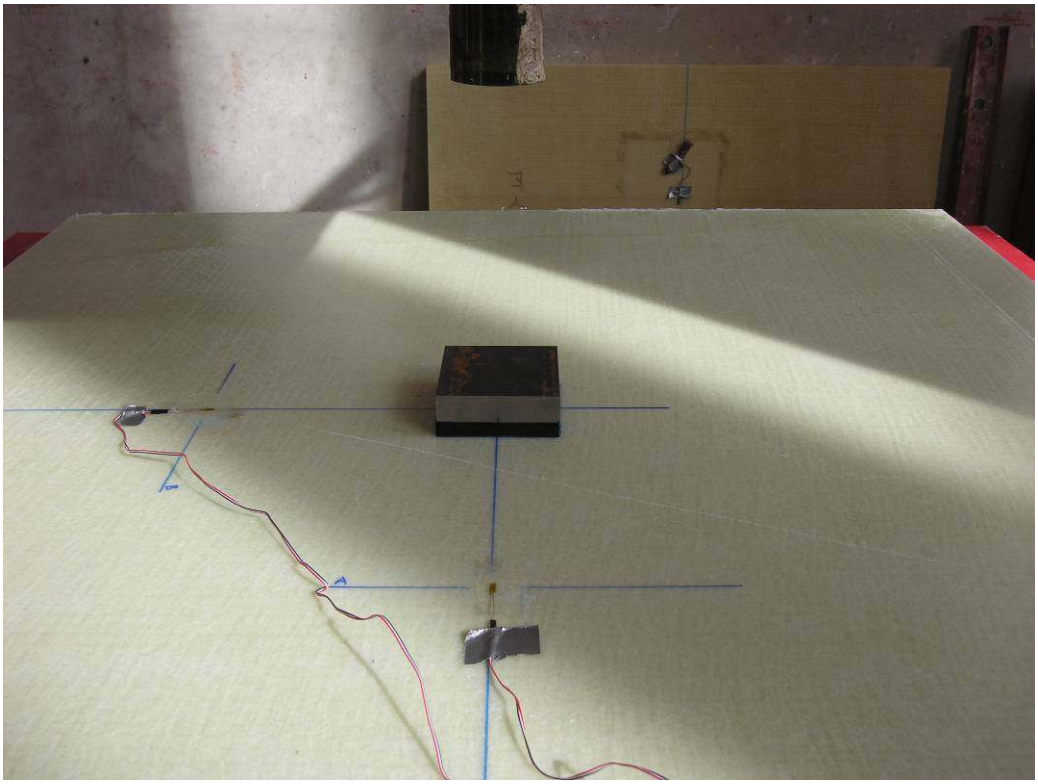

Figure 3.6 Strain Gages at Locations A and C

Table 3-2 Effective Shear Modulus G

Panel Set	Skin Plies	Insertion Pattern	Foam Type	Panel Height	Effective Shear Modulus, G (psi)
RDPS2-2-1	2	1	1	1.5"	1100
RDPS4-1	4	1	1	2"	735
RDPS4-7	4	1	2	2"	735
RDPS4-2	4	2	1	2"	1185
RDPS3-5	4	5	1	1"	1830
RDPS3-6	4	6	1	1"	1670

Table 3-3 Fatigue Testing Experimental Program

Loading	Span (in)	Pattern	Density (fipsi)	Thickness (in)	Skin Plies	Foam Type	Specimen
γ = 1%	28	Wall	8.53	1	4	1	FT-RDPS(3-5)-C
			7.59	1	4	1	FT-RDPS(3-6)-C
		Array	4	1.5	2	1	FT-RDPS(2-2-1)-C
				2	4	1	FT-RDPS(4-1)-C
				2	4	2	FT-RDPS(4-7)-C
			8	2	4	1	FT-RDPS(4-2)-C
	40	Wall	8.53	1	4	1	FT-RDPS(3-5)-B
			7.59	1	4	1	FT-RDPS(3-6)-B
		Array	4	1.5	2	1	FT-RDPS(2-2-1)-B
				2	4	1	FT-RDPS(4-1)-B
				2	4	2	FT-RDPS(4-7)-B
			8	2	4	1	FT-RDPS(4-2)-B
γ = 2%	28	Wall	8.53	1	4	1	FT-RDPS(3-5)-E
			7.59	1	4	1	FT-RDPS(3-6)-E
		Array	4	1.5	2	1	FT-RDPS(2-2-1)-E
				2	4	1	FT-RDPS(4-1)-E
				2	4	2	FT-RDPS(4-7)-E
			8	2	4	1	FT-RDPS(4-2)-E
	40	Wall	8.53	1	4	1	FT-RDPS(3-5)-D
			7.59	1	4	1	FT-RDPS(3-6)-D
		Array	4	1.5	2	1	FT-RDPS(2-2-1)-D
				2	4	1	FT-RDPS(4-1)-D
				2	4	2	FT-RDPS(4-7)-D
			8	2	4	1	FT-RDPS(4-2)-D

Table 3-4 Fatigue Loading Conditions

Specimen	Span	Core Shear Strain	Max Load (lb)	Min Load = 20% Max Load
FT-(RDPS2-2-1)-B	40"	1%	390	78
FT-(RDPS2-2-1)-C	28"	1%	390	78
FT-(RDPS2-2-1)-D	40"	2%	780	156
FT-(RDPS2-2-1)-E	28"	2%	780	156
FT-(RDPS3-5)-B	40"	1%	377	75
FT-(RDPS3-5)-C	28"	1%	377	75
FT-(RDPS3-5)-D	40"	0.5%	189	38
FT-(RDPS3-5)-E	28"	2%	754	151
FT-(RDPS3-6)-B	40"	1%	349	70
FT-(RDPS3-6)-C	28"	1%	349	70
FT-(RDPS3-6)-D	40"	2%	698	140
FT-(RDPS3-6)-E	28"	2%	698	140
FT-(RDPS4-1)-B	40"	1%	330	66
FT-(RDPS4-1)-C	28"	1%	330	66
FT-(RDPS4-1)-D	40"	2%	660	132
FT-(RDPS4-1)-E	28"	2%	660	132
FT-(RDPS4-2)-B	40"	1%	530	106
FT-(RDPS4-2)-C	28"	1%	530	106
FT-(RDPS4-2)-D	40"	2%	1059	212
FT-(RDPS4-2)-E	28"	2%	1059	212
FT-(RDPS4-7)-B	40"	1%	330	66
FT-(RDPS4-7)-C	28"	1%	330	66
FT-(RDPS4-7)-D	40"	2%	660	132
FT-(RDPS4-7)-E	28"	2%	660	132

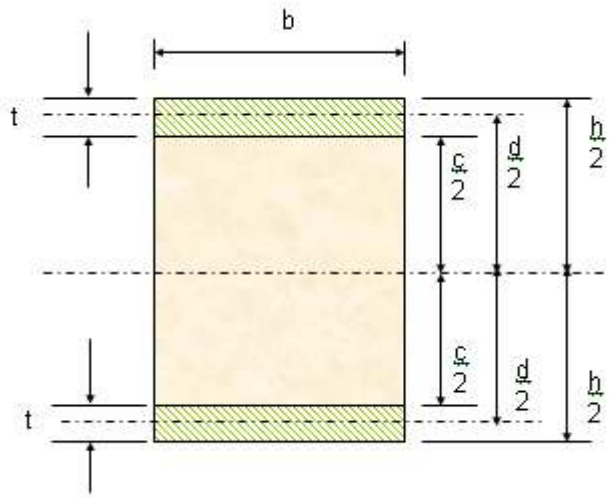

Figure 3.7 Sandwich Panel Cross Section

Figure 3.8 Fatigue Testing Supports

Figure 3.9 Loading Plate at Mid-Span

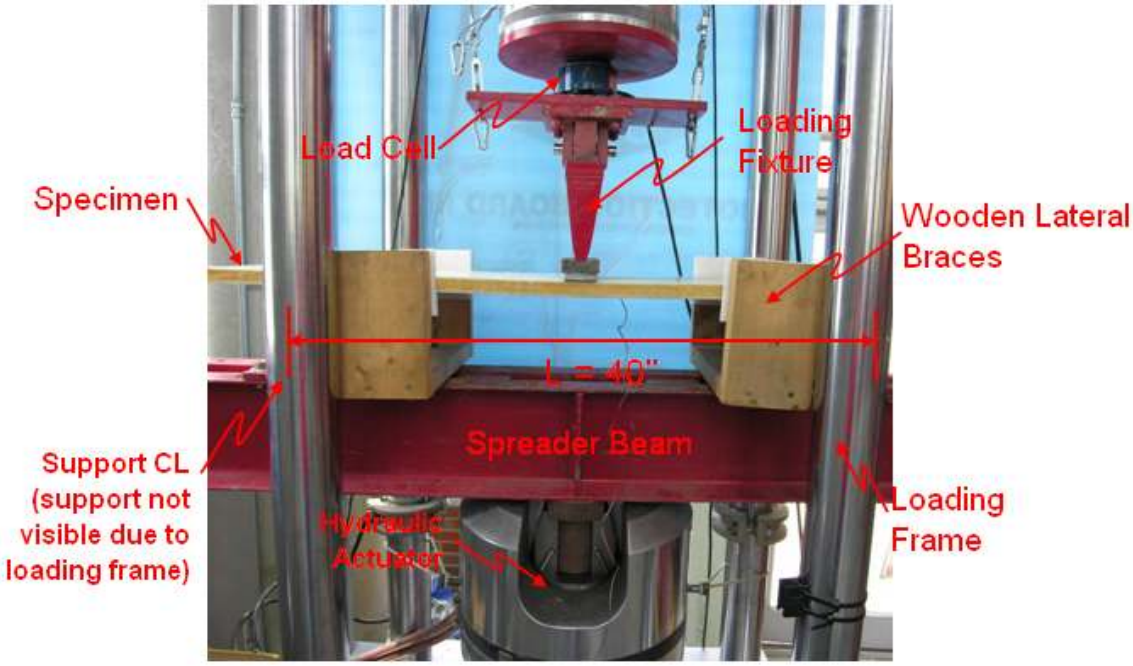

Figure 3.10 Fatigue Test Setup 40" Span

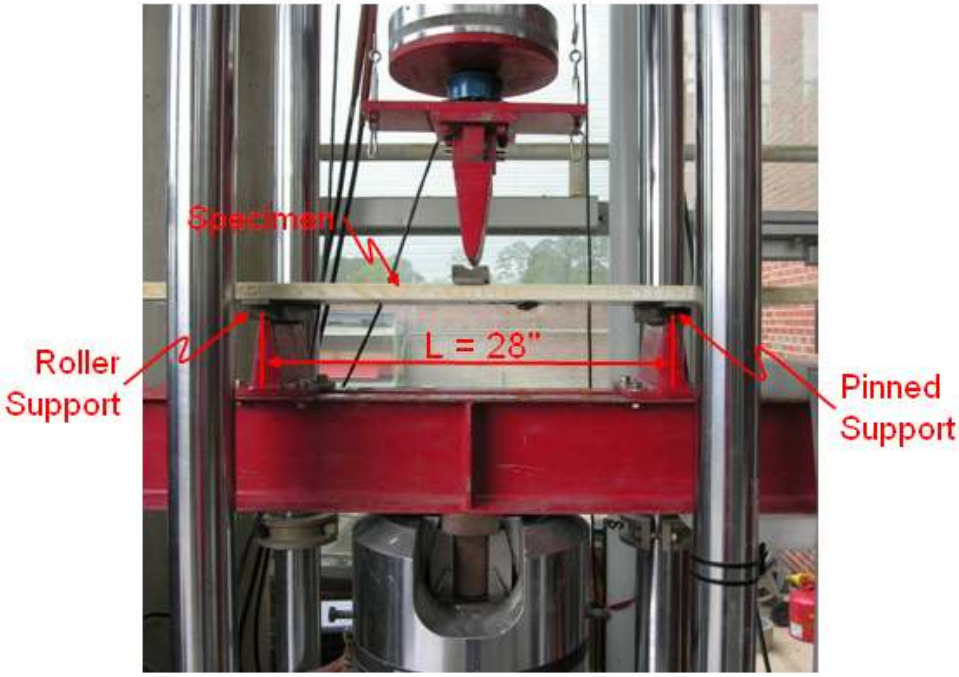

Figure 3.11 Fatigue Test Setup 28" Span

Figure 3.12 Fatigue Test Load Cell Setup

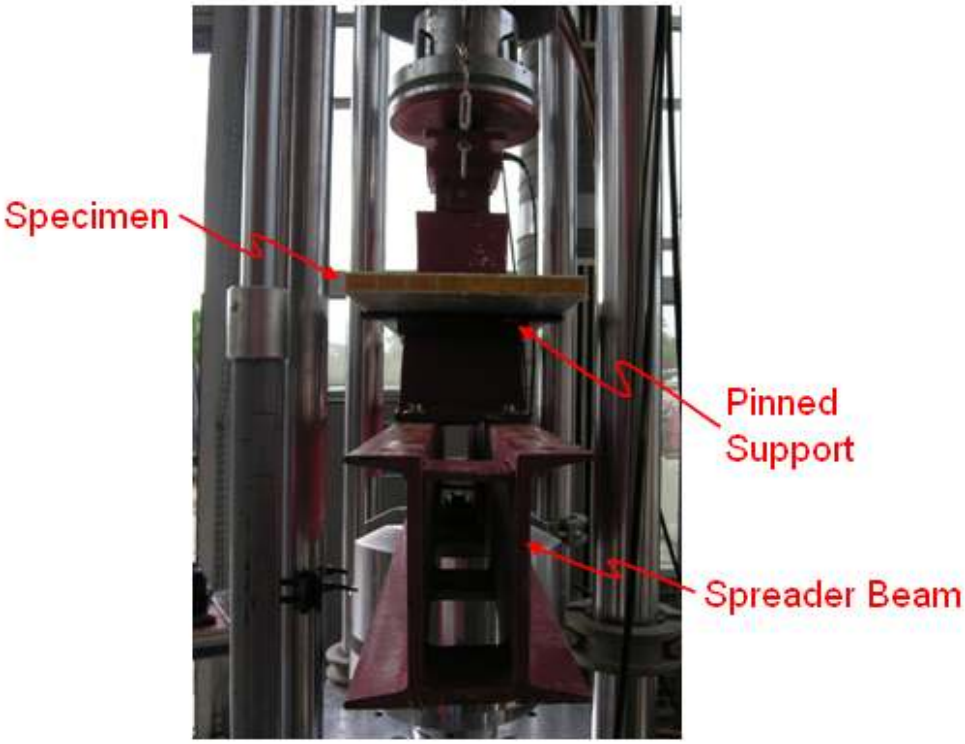

Figure 3.13 Fatigue Test Profile View

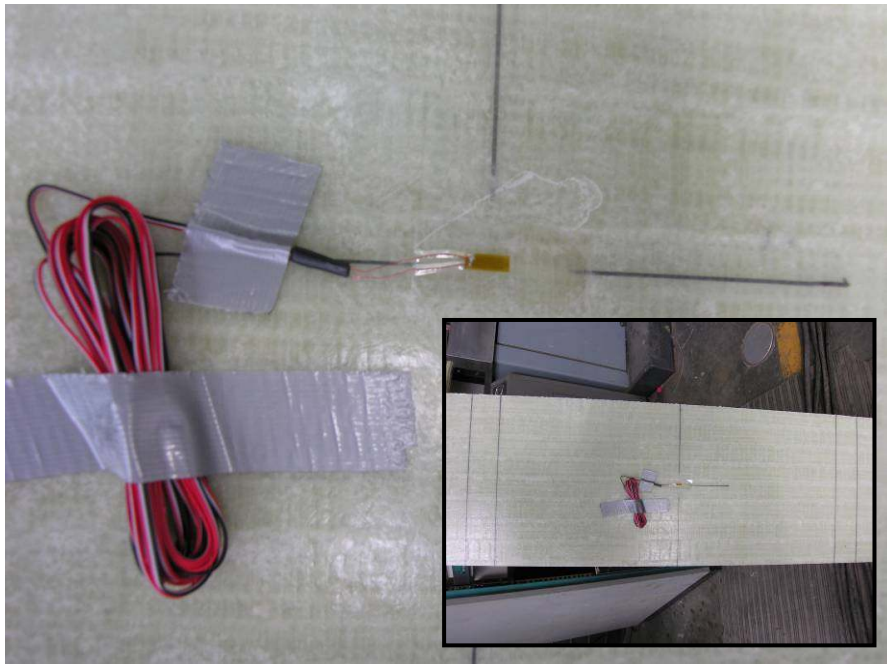

Figure 3.14 Fatigue Test Strain Gage

Chapter 4

4 Two-Way Behavior of 3-D GFRP Sandwich Panels

4.1 Introduction

This Chapter presents test results of the experimental program, described in Chapter 3, for the two-way bending tests performed on the 3-D GFRP sandwich panels. The chapter describes also the Finite Element Analysis (FEA) modeling that was utilized to model the behavior of the panels subjected to two-way bending. The accuracy of the model was evaluated by the measured data. The calibrated model was used to study different parameters believed to affect the two-way behavior. The chapter also describes a rational model which has been developed to describe the nonlinear behavior of these sandwich panels and was used to provide design considerations for the 3-D GFRP sandwich panels.

4.2 Two-Way Behavior of the 3-D Sandwich Panels

As described in Chapter 3, six individual panels were tested under a concentrated quasi-static load until failure. The panels spanned 40 in. in each direction and were simply supported by all four sides. Deflection and the strain were measured at the top and bottom of the panels at quarter-span and on the bottom surface at mid-span. The measured load-deflection and load-strain at the specified locations are shown in Figure 4.1 and Figure 4.2, respectively. The behavior indicates in general an increase of the panel stiffness by increasing the applied load. This behavior has been observed by the measured deflection and strain data. The increase in the stiffness is due to the effect of membrane action which is caused by the geometric nonlinearity of the panel's deflected shape; which will be discussed

in more detail later in this chapter. It was observed also that the stiffness of the panels tends to increase mainly when the deflection becomes approximately equal to the thickness of the panel. The measured tension strain of the top and bottom skins, shown in Figure 4.2, also shows evidence of membrane action. During the initial loading, when deflections were small, the measured strain at the top of the panel was compressive which indicates that the behavior was dominated by flexure. However, as the deflections increased the measured strain at the top and bottom surfaces became tensile. This behavior suggests development of membrane forces within the panel which was simply supported along all four edges.

Failure of all tested panels was due to buckling of the panel at the support, as shown in Figure 4.3. Figure 4.4 shows also delamination occurred between the foam and skin layers of the panel due to buckling of the panels edges at the support. Reasons for the buckling failure will be discussed in the following section in this chapter. Following buckling of the panel edges, tension rupture of the panel's bottom skin at mid span was observed as shown in Figure 4.5.

The measured ultimate load and deflection values for each of the two-way bending specimen are given in Table 4-1. The table indicates that panels with array insertion patterns and fiber insertion densities of 8 fipsi generally exhibited approximately 67% increase in ultimate load when compared to the 4 fipsi panels with identical thickness, skin plies, and foam type. This increase in strength can be attributed to the increased resistance to shear deformation of the panel with higher fipsi, which increases the composite action mechanism of the sandwich panel. For the 2 inch thick panels with 4 fipsi and different foam type the

panels failed at the same ultimate load and the deflection was within a 10% range. Use of the alternate foam type may have caused the debonding behavior shown in Figure 4.4, between layers during failure which could be a concern in some applications.

The observed behavior, up to ultimate load, for the 1 inch thick panels with wall insertion patterns spaced at 1.5 and 2 in. was comparable. The measured buckling load of the panel with walls spaced at 1.5 in. was within 10% of the ultimate load of the panel with walls spaced at 2 in. Also, the panel with walls spaced at 1.5 inch exhibited some residual strength after buckling occurred. Post buckling the panel was capable to continuously carry the applied load and the maximum load was increased by 14% beyond the buckling load. The panel failed due to tension rupture at the center of the panel's bottom skin.

Detailed information of the experimental results for the two-way bending behavior can be found in Appendix A, including the load versus deflection and load vs. strain graphs for each tested two-way bending specimen.

4.3 Finite Element Modeling of Two-Way Behavior

There are several ways to model composite sandwich panels using the finite element method. The different modeling techniques differ mainly in the level of detail used to represent the core of the panel. In the first modeling technique, the skin, foam core, and fiber insertions are each modeled independently. The skin is modeled using plate elements, the foam core is modeled using solid elements, and the fiber insertions are modeled using uniaxial elements. This technique provides the greatest level of detail related to the behavior of the fiber insertions since they are modeled explicitly. Alternatively, the core properties

can be modeled using smeared material properties. In this case, the skins are modeled using shell elements while the core is modeled using orthotropic solid elements. Using this approach the effect of the fiber insertions is captured by increasing the stiffness of the core in the through thickness direction of the panel. In this way the insertions are smeared within the foam core. In the final technique, the skins and the core are modeled together using layered shell elements with different material properties assigned to each layer. In this approach the stiffness of each element represents the smeared stiffness characteristics of the entire panel including the skins, foam core, and fiber insertions.

Since the main focus of the modeling was to study the two-way overall behavior of the panel rather than on the behavior of the individual parts of the panel, the first model was not considered. By inspection it was found that, combining each layer of the panels into one element could introduce some inaccuracy without consideration of the material of each layer. Based on the above, it was determined to use the model in which the skins and core (foam and insertions) are modeled separately. This method provides a simpler model that can accurately depict the panel's two-way behavior which was measured experimentally. Modeling the core of the panel by smearing the effect of the fiber insertions is also acceptable in this case since the panels are large enough that the repeating pattern of the fibers can be considered using the density of fiber insertions only. The material properties of the panel's GFRP skins and each core pattern were previously determined through an experimental study conducted at the Constructed Facilities Lab at NC State University during

the last five years. The elastic modulus of the GFRP skins, as well as, the core shear modulus for each panel type are given in Table 4-2 (Patrick, 2006).

The analysis was conducted using the ANSYS finite element program. Details of the elements used in the analysis are shown in Figure 4.6. The thin skins of the panel were modeled using the built-in SHELL281 element. The element has 8 nodes with 6 degrees of freedom at each node: translations in the X, Y, and Z axes, and rotations about the X, Y, and Z-axes. The SHELL281 element is recommended in ANSYS for modeling laminated composite shells or sandwich construction. The accuracy in modeling composite shells is governed by the first order shear deformation theory. Also, the model uses SOLID186 elements for the foam core and smeared fiber insertions. The SOLID186 element is defined by 20 nodes having 3 degrees of freedom per node, translations in the nodal x, y, and z direction. It should be noted that the solid elements used to model the core do not have rotational degrees of freedom at the nodes as do the SHELL281 elements used to model the skins. This could possibly result in an incompatibility between the rotations of the skin and core. However, the model translations of the skin and core were equal. Therefore, the effect of the incompatible rotations would be localized to a very small region close to the loading point. Comparison of the FE results to the measured behavior of the tested panels demonstrated good correlation further indicating that the effect is negligible.

The four foot square tested panels were simply supported on each edge resting on 4" wide neoprene pads. The support conditions allowed uplift of the panels but resisted penetration. The support conditions were simulated in the FE model by using compression

only link elements, as shown in Figure 4.7. These elements allowed rotation and vertical translation of the panel at the supports. Further, the compression only link elements allowed uplift of the panels near the supports to simulate buckling of the edge of the panels which was observed experimentally. The concentrated load at the center of the panel on a 4 inch square area was modeled by applying equal loads to each node within that area to resemble the test set up.

Initially, a linear analysis was performed using the material properties previously determined from tests conducted at the CFL. Results of the linear analysis showed that the linear model could only capture the initial stiffness of the panels for small deflections as shown in Figure 4.8. In this Figure, the stiffness is accurately modeled up to a maximum deflection of 0.4 in. The measured load-deflection curve shows also significant increase of the stiffness as discussed previously. However, the linear model could not accurately predict this stiffening behavior within large deflection range which was due mainly to geometric nonlinearity of the panel.

Based on the above, a nonlinear analysis was performed to accurately model the response of the panel for large deflections. Using the geometric nonlinear solution of the ANSYS program, a load step is applied and the program iteratively checks the stiffness matrix and equilibrium based on the deformed structure. Once equilibrium is reached the next load step is executed and the process repeats until the final load step. Figure 4.8 indicates good correlation between the nonlinear FEA results and the measured deflection for a 1 inch thick panel with wall pattern fiber insertions. The model is able to account for the

increase in the stiffness due to membrane action caused by the large deflections exhibited by the panel. The deflection profile along the center line and the diagonal line of the panel, shown in Figure 4.9, indicate a ponding effect at the center of the panel near the concentrated loading. The deflection profile along the diagonal line shows also regions of high stiffness at the corners of the panel indicated by the change in curvature of the deflected shape. Figure 4.10 shows the normal stress contours and profiles of the top skin fibers. The figure shows the large normal compressive stresses at the edges of the panel in the X direction. Also, pockets of small tensile stresses develop near the area of applied load. The stress contours and profile of the normal stress in the X direction of the bottom fibers is shown in Figure 4.11. The figure shows that regions of outer normal compressive and inner tensile forces have developed in the panel's bottom skin. The large compressive stresses near the panel's edges cause the tested panels to buckle along its edge. Analytical Results for the other experimentally tested panels subjected to two-way bending are shown in Appendix A.

The ANSYS model however, was unable to predict buckling at the edge of the panel. Since buckling of the panel causes a sudden dramatic reduction in the resisted load, which was observed experimentally, the ANSYS model cannot converge on the next load increment and solution terminates. However, the analysis detected some pre-buckling behavior at higher load levels. This is evident by the profile of the reactions at the support, shown in Figure 4.12, which is similar in shape to the buckled panel. The reduction in the reaction at the center of the panel edge indicates that the panel started to lift from the support.

Overall the FEA model provides an accurate prediction of the two-way bending behavior of the panels in question. The good correlation between the model and the experimental results indicates that the model can be used to study various parameters believed to affect the performance of the panel under two-way action. The effect of the various parameters is discussed in detail in the following section.

4.4 Parameters Affecting Two-Way Behavior

Since the number of tested panels was limited in comparison to the many parameters affecting the two-way behavior, the FEA model was used to extend the scope of the current study to include two-way bending panels with different parameters. Confidence in the model which was calibrated using the experimental results, satisfying equilibrium, compatibility, and continuity, allows use of parameters outside the bounds of the experimental testing.

The various parameters that were studied in the parametric study of the two-way bending response of the panels were:

a. Total Panel Thickness (h)
b. Fiber Insertions per Square Inch (fipsi)
c. Elastic Modulus of the Panel Skins (E_{skin})
d. Aspect Ratio of the panel (L/W)

The pattern type of the insertions was not considered since the FEA model smears the effect of the fibers across the entire area of the panel. Therefore, it is more appropriate to study the effect of the fipsi since both wall and array patterns have comparable core shear stiffness in each direction, respectively. All the parameters considered are shown in Table 4-3 through Table 4-6, along with the other properties of each panel to be studied. The parameters were

varied over a range of considerable values which represent the typical range which can be manufactured. The following discusses the effect of each parameter on the two-way bending behavior of the 3-D sandwich panels.

4.4.1 Thickness

The thickness of the panel has significant effect on the panel behavior. Table 4-3 provides details of the panel configuration used to study the effect of the panel thicknesses. By varying the thickness only, the panel's behavior significantly changes as shown in Figure 4.13. The effect was examined for two different fiber insertion densities to examine the effect of varying thickness may change with a different fiber insertion pattern.

The load-deflection relationship for panels with 4 fipsi and varying thicknesses is shown in Figure 4.13. The figure shows that increasing the total thickness of the panel from 1 inch to 4 in. reduces the deflection by 25%. This phenomenon is due to the increase of the overall stiffness of the panel. The trend of the load-deflection behavior for all the thicknesses considered was similar in nature, indicating an increase of stiffness with increasing deflection due to the effect of membrane action. Theories of two-way solid plates subjected to large deflection suggest that the load deflection relationship is linear while the maximum deflection is less than half the thickness of the plate (Boresi, 2003). However, the predicted load-deflection behavior for the panels with 3 and 4 inch thicknesses were found to be nonlinear even when the deflections were less than half the thickness of the sandwich panel. The total deflection in this case is sufficiently large to activate the membrane forces since the sandwich panels undergo significant shear deformation.

The relationship between deflection and total panel thickness is shown in Figure 4.14, for three different load levels. The results indicate in general that the reduction of deflection is linearly proportional to the increase of the thickness for a given load level. Increasing the thickness consequently increases the flexural rigidity, and therefore, decreases the deflection. The figure indicates that increasing the panel thickness by 1 inch can reduce the total deformation between 0.15 to 0.18 in. only. These results indicate also that the behavior is independent of the level of applied load. Therefore, the percent increase of the thickness of the panel is not equally proportional to the percent decrease of the deflection.

The load deflection behavior for panels with 8 fispi, shown in Figure 4.15, shows the effect of varying thicknesses within the range from 1 to 4 in. Because of the increase in the insertion density the results are different from the previous panels with 4 fipsi. The results suggest for thin panels that increasing the insertion density decreases the total deflection of the panel by decreasing the amount of shear deformation. However, the total deflection is still large enough to activate the membrane forces. When the thickness of the panels is large, greater than 2 in., increasing the fipsi more drastically decreases the total deflection. The effect of increasing the insertion density has a greater effect on the thicker panels since the percentage of shear deflection in the total deflection is significantly greater. Consequently, the nonlinear effect of membrane forces is also reduced because of the decreased total deflection, reflected by the linear load-deflection relationship of the 3 and 4 inch thick panels.

In general, the results for panels with 8 fipsi indicate that increasing the thickness reduces the deflection as shown in the deflection versus panel thickness graph in Figure 4.16. The results suggest for lower load levels the deflection is nonlinearly related to the total thickness of the panel. The relationship is nonlinear due to the coupled effect of the increased shear deformation and reduced membrane action of thicker panels. However, the relationship can be considered to be linear at high load levels as indicated by the figure. Results for panels with 4 fipsi and 8 fipsi indicate that increasing the thickness of a panel with 8 fipsi has double the effect on the total deflection compared to panels with only 4 fipsi.

Therefore, panel thickness is linearly related to the total deflection of the sandwich panels at high load levels. The effect of the thickness can be increased by enhancing the composite action through increased levels of fipsi. Also, the nonlinear behavior due to membrane forces can be decreased by providing the panel with sufficient flexural and shear rigidity.

4.4.2 Fiber Insertions Density

One of the main parameters that have a major effect on the overall performance of a 3-D sandwich panel is the density of the fiber insertion pattern. Increasing the amount of fipsi increases the shear rigidity of the core as well as increases the out of plane compressive stiffness of the panel. Also, the 3-D sandwich panels rely on the insertions to transfer the shear forces between the layers of the panel, in order to achieve composite action. To study the effect that the density of the fiber insertions has on the two-way behavior different fiber

insertion densities were considered, as described in Table 4-4. Two different thicknesses were utilized to allow for consideration of their effect on the fiber insertion density.

As expected, increasing the fipsi for a panel increases the shear stiffness of the panel. However, it does not increase the flexural rigidity evident by the negligible effect of changing the insertion density from 4 fipsi to 10 fipsi on the load-deflection relationships of 1 inch thick panels shown in Figure 4.17. This effect is negligible since the overall behavior is governed by membrane action due to large deflections evident by the highly nonlinear behavior of the panels. The results suggest for thin panels that the membrane forces resist the majority of the applied load; therefore, the bending component of the resistance is small compared to the membrane resistance. The thin panels are typically governed by flexure and membrane action since the shear contribution is small. Therefore, increasing the shear stiffness does not significantly affect the behavior. The negligible effect on the deflection from increasing the density of fiber insertions for 1 inch thick panels is shown in Figure 4.18. Changing the insertion density from 4 to 10 fipsi caused only a 4% decrease in the total deflection. The results suggest also that the maximum deflection is linearly related to the insertion density. However, the effect is very small and can be considered constant, evident by the flat slope of the fipsi-deflection relationship. Therefore, the increase in fipsi has an insignificant affect on the two-way behavior of thin 3-D GFRP sandwich panels since the behavior is primarily affected by membrane action.

Load-displacement relationships for 2 inch thick panels with varying fipsi are shown in Figure 4.19. The results suggest the presence of membrane forces indicated by the

nonlinear behavior. The effect of increased insertion density for the 2 inch thick panels is more pronounced than the effect on the 1 inch panels. As discussed in Section 4.4.1, increasing the thickness of the panel consequentially increases the relative contribution of the shear deflection to the overall deflection of the panel. The higher percentage of shear deflection in the 2 inch thick panels causes the effect of changing the fipsi to be much more significant. The fipsi-deflection relationship is more noticeable and still linear for the 2 inch thick panels at various load levels, as shown in Figure 4.20. For the 2 inch thick panels increasing the insertion density from 4 to 10 fipsi causes a 13% reduction in the total deflection, more than 3 times larger than the reduction for 1 inch thick panels.

Therefore, increasing the amount of fipsi will increase the shear stiffness of the panel. However, the effect is negligible for thin panels since the behavior of the panel is governed by flexural and membrane action with little contribution from the shear behavior. As the panel thickness is increased, the relative contribution of the shear deformation increases. Therefore, increasing the core shear modulus by increasing the fiber insertion density has a more pronounced effect on the overall panel behavior. The results indicate also that the behavior is independent of the level of applied load.

4.4.3 Elastic Modulus of Skins

The elastic modulus of the FRP skin is dependent on the material from which the sheets are made. The different elastic moduli that were considered in the study are given in Table 4-5. The modulus of elasticity ranges from 2700 ksi, the elastic modulus previously determined for the GFRP skins, to 20,000 ksi, a typical value for carbon FRP sheets. The

modulus for a given material can also fluctuate based on the percent fiber content. Through examination of the tested panel's skins it was found that doubling the number of skin plies did not double the thickness of the composite skins, indicating a change in the percent fiber content of the skins. This is due to the crushed strand mat and excess adhesive used to manufacture the skins. Again, the study examines the effect of the skin stiffness using two fiber insertion densities to determine their effect on the stiffness of the FRP skins.

Increasing the elastic modulus of the panel's skins will increase the flexural rigidity of the panel as evident by the increased initial stiffness of the load-deflection relationships, shown Figure 4.21, for panels with 4 fipsi. The results suggest also a higher degree of nonlinearity of the load-deflection relationship for panels with stronger skins. Increasing the elastic modulus increases the panel's resistance to bending which decreases the total deflection. The reduced deflection should decrease the effect of the membrane forces. However, the increase of the elastic modulus is also directly related to the magnitude of the membrane forces. Therefore, increasing the elastic modulus of the skins also increases the nonlinearity of the load-deflection relationship. The relationship between the maximum deflection and the skin modulus for panels with 4 fipsi is nonlinear at various load levels, as shown in Figure 4.22. This is due to the coupled effect that changing the skin stiffness has on the flexural and membrane behavior of the sandwich panels. The figure shows that the effect on the membrane behavior is more significantly affected by the elastic modulus than the total deflection for deflections greater than 1 inch at the 10 kip load level. When the deflection is less than 1 inch the effect on the membrane behavior due to the elastic modulus

and the total deflection are almost equal evident by the almost constant relationship between the total deflection and skin modulus. The load-deflection relationships for panels with 8 fipsi and varying elastic moduli of the skin are shown in Figure 4.23. The effect of increasing the insertion density results in decreased total deflection by decreasing the amount of shear deformation in the panel. Comparing Figure 4.21 and Figure 4.23 indicates that a similar trend of the behavior regardless of the fiber insertion density. The relationship between the skin strength and total deflection is shown in Figure 4.24 at various load levels. Similar to the 4 fipsi panels, the relationship is nonlinear due to the coupled effect of the skin modulus on the flexural and membrane behaviors. The figure shows also that the relationship is dependent on the level of applied load. At low load levels the membrane forces are not fully developed and the majority of the deflection is due to flexural and shear deflection. As the load is increased the membrane forces start to develop and the effect of the skin stiffness on the deflection is more pronounced.

Therefore, increasing the elastic modulus of the panel's skins can greatly affect the two-way bending behavior of the 3-D sandwich panels by increasing the flexural rigidity and effect of membrane action. The relationship between the skin stiffness and the total deflection is dependent on the applied load level. Also, the effect of the elastic modulus on the membrane behavior can be reduced by increasing the level of fipsi.

4.4.4 Aspect Ratio

This section will study the effect on the behavior of 3-D sandwich panels of aspect ratios applicable to two-way bending. The configurations of the panels with aspect ratios to

be studied are given in Table 4-6. Aspect ratios ranging between 1 and 2 were considered as this represents the typical range for two way behavior. The aspect ratios were analyzed with two different fiber insertion densities to determine their effect on the overall two-way behavior of the panels.

Since the panel dimensions have changed in order to examine the desired aspect ratios, the load versus deflection curves can not directly be compared for the different panels under consideration. Therefore, the load versus deflection per unit width for the three aspect ratios was compared. Figure 4.25 shows the load-deflection behavior of the 4 fipsi panels subjected to two-way bending with varying aspect ratios between 1 and 2. The results suggest that by increasing the aspect ratio, from 1 to 2, the nonlinear behavior due to membrane forces is reduced. The membrane forces are reduced since the supports on the short side of the panel are less effective in transferring the load. Although, membrane action is still present for aspect ratios up to 2 evident by the nonlinear behavior of the load-deflection relationship. Also, the figure shows the results for two other panels simply supported on all four sides with aspect ratios of 5 and 10. While the degree of nonlinearity is reduced the overall behavior is still nonlinear. This is due to the localization of the point load to the center of the panel. The deflection/width vs. aspect ratio graph for the panels with 4 fipsi is shown in Figure 4.26. For aspect ratios between 1 and 2 the results suggest a linear deflection-aspect ratio relationship. The linear behavior of each load level suggests that the behavior is the same regardless of the load level. Panels with 8 fipsi behaved in a similar fashion, with linearly increasing deflection/span values for increased aspect ratios.

Increasing the level of fipsi had no effect on the behavior of the panels besides decreasing the degree of shear deflection.

The aspect ratio of 3-D sandwich panels subjected to two-way bending is related to the panel's membrane behavior. As the aspect ratio of a panel is increased the stiffening effect due to membrane action is reduced since the behavior of the panels shifts toward one-way bending. Panels with aspect ratios between 1 and 2 may develop the membrane force mechanism dependent on the other parameters of the panels.

4.5 Two-Way Behavior of the 3-D GFRP Sandwich Panels

The behavior of the tested simply supported panels subjected to two-way action was governed by different mechanisms throughout the various stages of loading. Initially, when the deflections were small with respect to the panel thickness the panel behavior is governed by the plate bending mechanism. As the deflection increases and the deflections become large, on the order of magnitude of the panel thickness, the relationship between load and displacement becomes nonlinear with an obvious increase of the stiffness due to the effect of membrane action. This behavior is quite different than the typical flexural behavior due to the development of internal tensile forces in the skins of the panel caused by the geometric nonlinearity of the panels. Large deflection of the center portion of the sandwich plate also causes high compressive forces to be developed near the edge of the plate. This behavior is evident in the tested sandwich panels by the effect of the developed compressive forces causing the panels to buckle along their edge.

The solution for the flexural and shear deflections of a square simply supported sandwich plate was given by Yen in 1951. Consider a square sandwich plate simply supported on each edge of length ($L_x = L_y$) and loaded by a concentrated load (P) at the center of the panel on a small square area of length (a) as shown in Figure 4.27. Based on the double Fourier sine series the maximum deflection (w_{max}) of the sandwich plate can be expressed in the following nondimensional form (Yen, 1951):

$$\frac{w_{\max}}{B_c} = 4k \sum_{m=1,3,\cdots}^{\infty} \sum_{n=1,3,\cdots}^{\infty} C_{mn} \tag{4.1}$$

where C_{mn} is defined by: $C_{mn} = \frac{1}{2\pi^4 K_{mn}^o} \left\{ \left[\frac{6(1+r)^2}{rR} \right] (m^2 + n^2 k^2) + 1 \right\}$

and K_{mn}^o is given by: $K_{mn}^o = \frac{6(1+r)^2}{rR}(m^2 + n^2 k^2)^3 + [3(1+r)^2 + 1](m^2 + n^2 k^2)^2$

where B_c is deflection factor for a sandwich plate subjected to a concentrated load, k is the aspect ratio of the sandwich plate, r is the ratio between the thickness of the sandwich panels core (c) and the thickness of the skin (t), and R is the stiffness factor of the sandwich plate. The above factors are given by the subsequent equations as follows:

$$B_c = \frac{PL_x^2}{D} \tag{4.2}$$

$$k = \frac{L_x}{L_y} \tag{4.3}$$

$$r = \frac{c}{t} \tag{4.4}$$

$$R = \frac{G_c t L_x^2}{\pi^2 D} \tag{4.5}$$

Where G_c is the core shear modulus and D is the flexural rigidity of the sandwich panel's skins about their neutral axis per unit width, as follows:

$$D = \frac{Et^3}{12(1-\nu^2)} \tag{4.6}$$

where E is the elastic modulus of the panel's skins and ν is Poisson's ratio of the panel's skins. Equation 4.1 can be solved directly using typical spreadsheet software and converges relatively quickly.

When the deflections are small with respect to the thickness of the plate the stiffness of the plate can be accurately determined by plate bending behavior. However, when the deflections become large internal membrane forces develop which can drastically change the behavior of the plate, as described by Ugural (1999). The internal membrane forces are due to stretching of the membrane's middle surface. Timoshenko uses the energy method to obtain an approximate solution for the deflection of a flexible membrane subjected to a uniformly distributed load. Following this method, the maximum deflection of a square membrane under a concentrated load (P) was derived and is given as follows:

$$w_o = 0.438\sqrt[3]{\frac{L_x^2 P}{Et}} \tag{4.7}$$

where w_o is the maximum deflection of the membrane at it's center, L_x is the span length, E is the elastic modulus of the membrane, and t is the thickness of the membrane.

Combining Yen's linear solution for the flexural and shear deflections of a square sandwich plate subjected to a centrally located concentrated load, from Equation 4.1, and Timoshenko's nonlinear solution for the maximum deflection of a membrane subjected to a concentrated load, Equation 4.7, the overall behavior of the tested sandwich panels was modeled. A graphical representation of the sandwich plate bending and membrane contributions of a typical tested sandwich panel is shown in Figure 4.28. In this case, the model uses the experimentally tested properties of the RDPS3-6 panel to model the two-way behavior and accounts for the additional stiffening effect due to the membrane action of the two skins. The figure shows that the model substantially overestimates the observed stiffening effect due to membrane action. This indicates that the membrane forces were not fully developed in the tested sandwich panels. The reduced effect of the membrane forces can be attributed to the stiffness of the sandwich panels and the difference between the boundary conditions of the model and the experimental setup. The model assumes that the skins of the panel are behaving as a totally flexible membrane, as shown in Figure 4.29A, and neglects the flexural rigidity when calculating the membrane contribution. The experimentally tested panels, however, are not flexible. The rigidity of the skins decreases the effect of the membrane forces since a portion of the load is carried by the stiffness of the panel, as shown in Figure 4.29B. The support conditions, shown in Figure 4.30, of the theoretical model and the experimental setup also contribute to the stiffness of the panel. The experimental setup allowed for upward deflection at the panel's edges. However, the model

of the simply supported membrane does not allow for uplift at the corners of the panel inducing downward reactions which increase the stiffening effect of the membrane forces.

Therefore, accounting for the complete membrane action of the skins resulted in an over prediction of the stiffness of the panel. An alternative approach, which is based on the measured results and the linear solution for the deflection of a sandwich plate given by Yen et al. was developed to account for the effective membrane action of the panel's skins. Using the experimental results and Yen's model for the flexural and shear behavior, the percentage of the total applied load resisted by membrane action was determined as shown in Figure 4.28. The percentage of the applied load resisted by membrane action for four of the tested panel is given in Figure 4.31. Two panels were omitted since the measured loads not completely reliable. It was found that the 4 curves for the tested panels closely matched each other. This is due to the similar initial stiffness and the overall nonlinear behavior of the four tested panels, as shown in Figure 4.32. The initial stiffness for each of these panels ranged between 1920 lb/in to 2500 lb/in based on the calculated linear behavior from Yen. The percentage of the applied load resisted by membrane action has a wider range of values initially since the sensitivity is much greater for the low load levels which coincide with the small deflections.

The membrane action curves were verified using the nonlinear finite element model and Yen's linear model for the flexural and shear behavior. The two membrane action curves for the RDPS3-6 panel are shown in Figure 4.33. The figure shows the good correlation between the nonlinear FE model and the experimental results. Thus, the overall panel

behavior can be determined from the results of the nonlinear FE analysis and the linear model described by Yen et al. Since the serviceability of the panel is critical to the overall panel behavior, the design procedure is based on the selected deflection level. For a given level of deflection, the force resisted by the plate bending mechanism can be calculated using Equations 4.1 – 4.6. For the same deflection level, the percentage of the total force resisted by membrane action can be determined from the curve in Figure 4.33 using the results of the FE analysis. Similar curves were developed for different panel configurations as described below. The total load required to achieve a given level of deflection can be calculated as:

$$P_{total} = \frac{1}{1 - \%P_{mem}} P_{bend} \tag{4.8}$$

where P_{total} is the predicted load due to plate bending and membrane action, $\%P_{mem}$ is the percentage of the total load resisted by membrane action for a given deflection from the membrane action curve, and P_{bend} is the load resisted by the flexural and shear rigidity of the sandwich panel calculated from Equation 4.1 for the given deflection. The proposed model was used to predict the behavior of the tested panels. Comparison of the predicted and measured load-deflection behavior is given in Figure 4.34A-F for all the tested panels. The figures indicate good correlation between the proposed model and the experimental results. The effect of membrane forces obviously has a large effect on the overall behavior of the panels in question.

The effect of the span length was investigated using this approach based on results from the nonlinear FE model. The membrane action curves, shown in Figure 4.35, were

calculated for three span lengths of 24, 44, and 88 in. using the proposed model. The figure indicates that the overall span of the panel does not have a significant effect on the membrane behavior with respect to the deflection to span ratio. Therefore, only one design curve can be used for a panel configuration with various span lengths.

To account for the effect of various aspect ratios, membrane action curves were obtained for two types of panels. The membrane action curves for a 1 inch thick panel with relatively stiff skins and various aspect ratios are shown in Figure 4.36. The figure shows how increasing the aspect ratio of the panel decreases the effect of membrane action. As the aspect ratio of the panel is increased the panel behavior is governed by one-way bending rather than by two-way bending. Therefore, the effect of membrane action is reduced as the aspect ratio is increased.

For comparison, another panel configuration was used to verify the effect of the panel's parameters. The four membrane action curves, shown in Figure 4.37, were derived based on the nonlinear FE results and Yen's linear approximation for the bending and shear behavior. The figure shows the membrane action curves for 2 in. thick panel with reduced skin stiffness, relative to the total stiffness of the panel, and aspect ratios ranging from 1 to 10. A 2 inch thick panel with flexible skins was chosen based on the results of the parametric study. This panel represents a stiff panel with relatively flexible face skins. Therefore, the effect of membrane action for this panel configuration is expected to be reduced compared to the more flexible panel with stiffer face skins. This trend can be observed by comparing the membrane action curves for the 1:1 aspect ratio of the two panel

configurations considered. Again, the figure shows that increasing the aspect ratio of the panel reduced the percentage of the applied load resisted by membrane action. The curve for the 10:1 aspect ratio panel lies on the X-axis since the Yen model overestimated the initial stiffness of the panel.

Therefore, membrane forces should be considered in any design applications that have deflections larger than half the thickness of the panel. Neglecting the stiffening effect could possibly result in an overly stiff design which may increase the cost and weight of the structure to achieve an acceptable level of deflection.

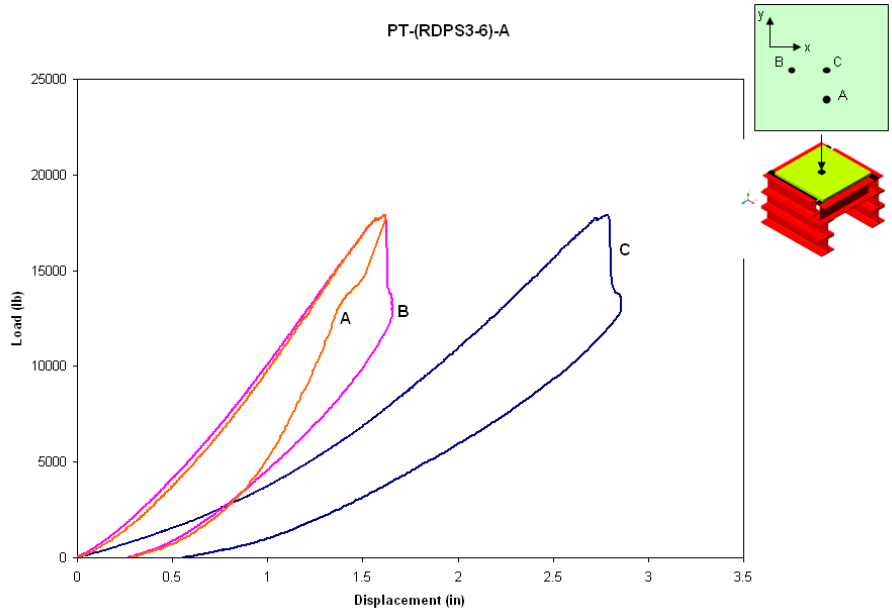

Figure 4.1 Load vs. Displacement Typical

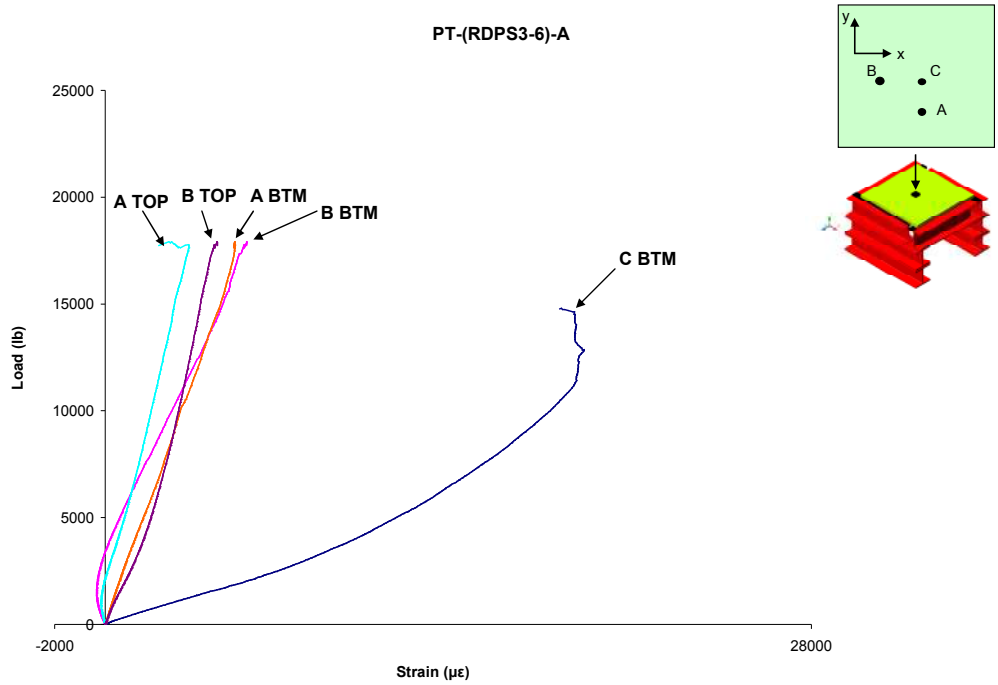

Figure 4.2 Load vs. Strain Typical

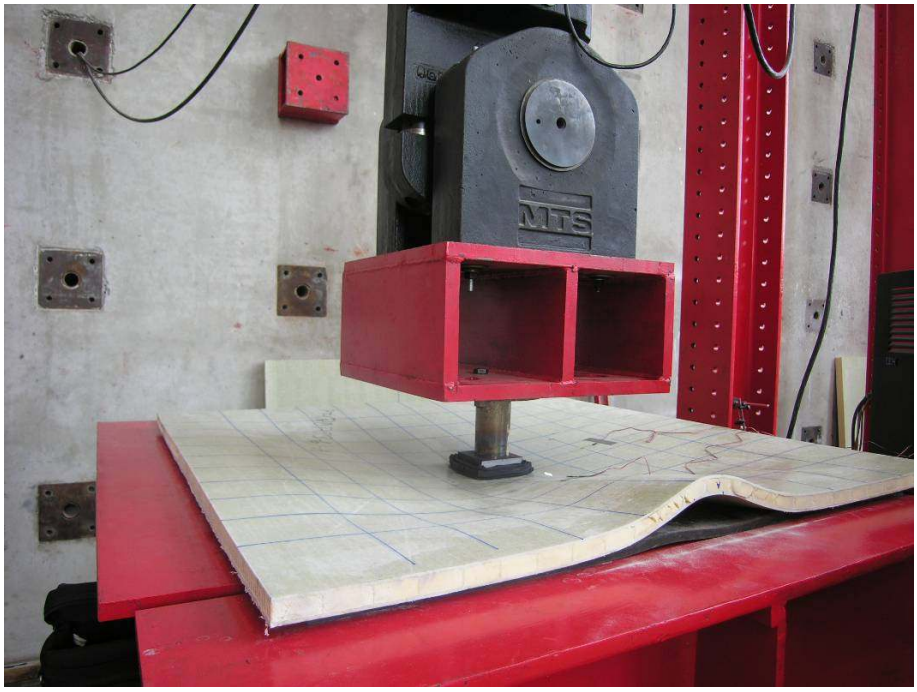

Figure 4.3 Typical Failure Mode

Figure 4.4 Delamination between foam and skin layers

Figure 4.5 Tension Rupture of Skin

Table 4-1 Experimental Results for the Two-Way Sandwich Panels

Panel Type	Insertion Pattern	Skin Plies	Foam Type	Panel Height (in)	Ultimate Load (kips)	Ultimate Deflection (in)
RDPS2-2-1	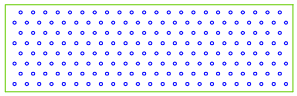 4 fipsi	2	1	1.5	14.0	2.95
RDPS4-1		4	1	2	13.3	2.72
RDPS4-7		4	2	2	13.3	2.4
RDPS4-2	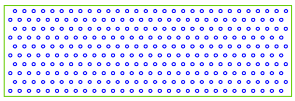 8 fipsi	4	1	2	22.3	2.99
RDPS3-5	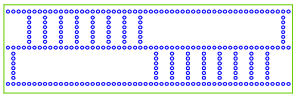 1.5” Wall Spacing	4	1	1	16.5	2.54
RDPS3-6	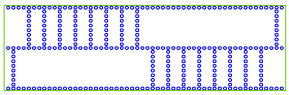 2” Wall Spacing	4	1	1	17.9	2.77

Table 4-2 3-D GFRP Sandwich Panels Material Properties

Panel Type	Insertion Pattern	Skin Plies	Foam Type	Panel Height (in)	E_{skin} (ksi)	Core Shear Modulus, G (psi)
RDPS2-2-1	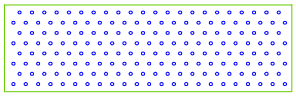 4 fipsi	2	1	1.5	2700	400
RDPS4-1		4	1	2		
RDPS4-7		4	2	2		
RDPS4-2	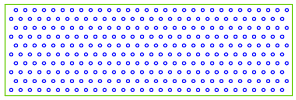 8 fipsi	4	1	2	2700	600
RDPS3-5	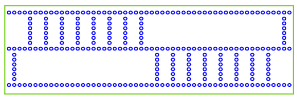 1.5” Wall Spacing	4	1	1	2700	1310
RDPS3-6	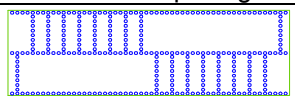 2” Wall Spacing	4	1	1	2700	1120

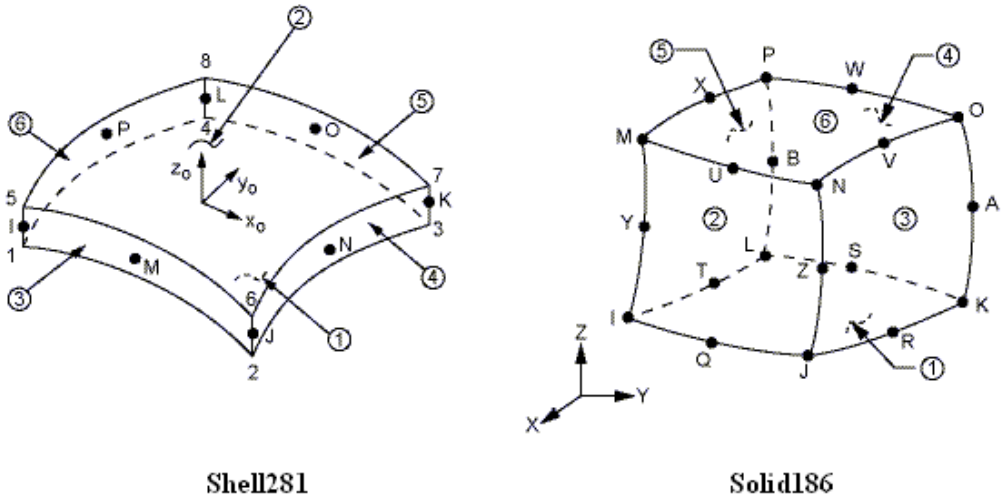

Figure 4.6 Element Types used in Sandwich Panels

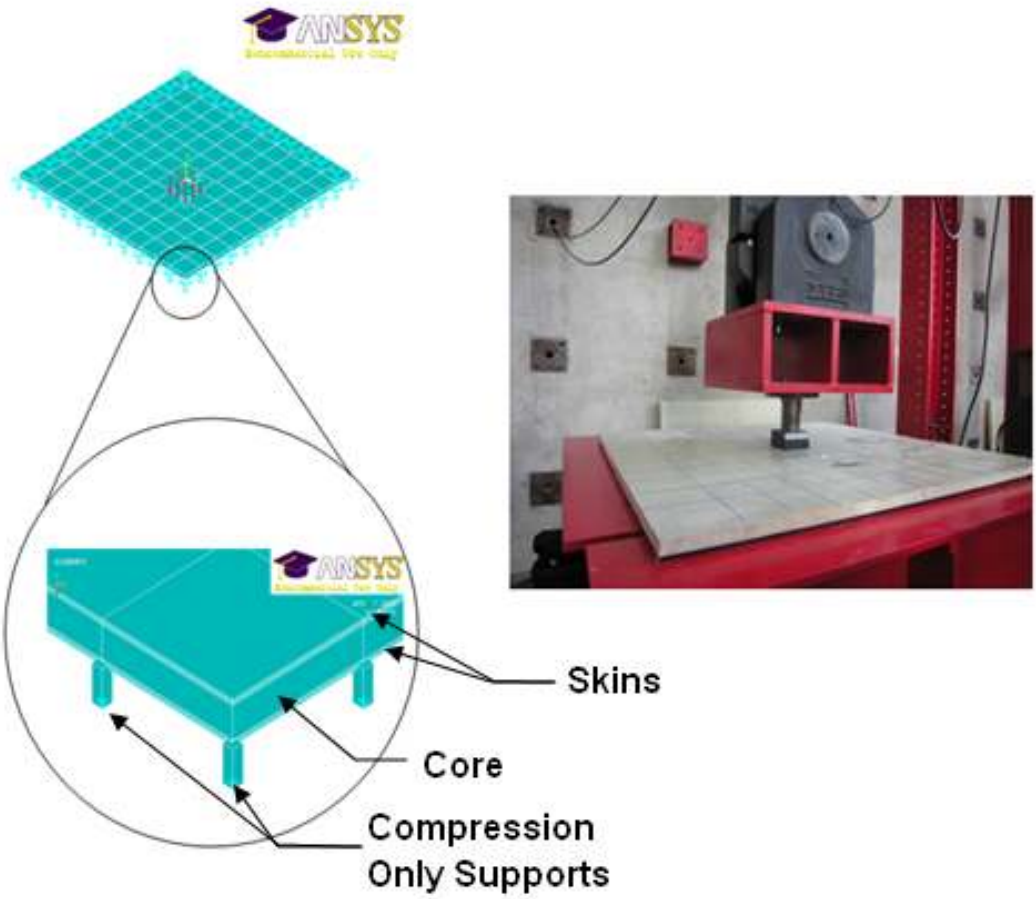

Figure 4.7 Model Support Conditions

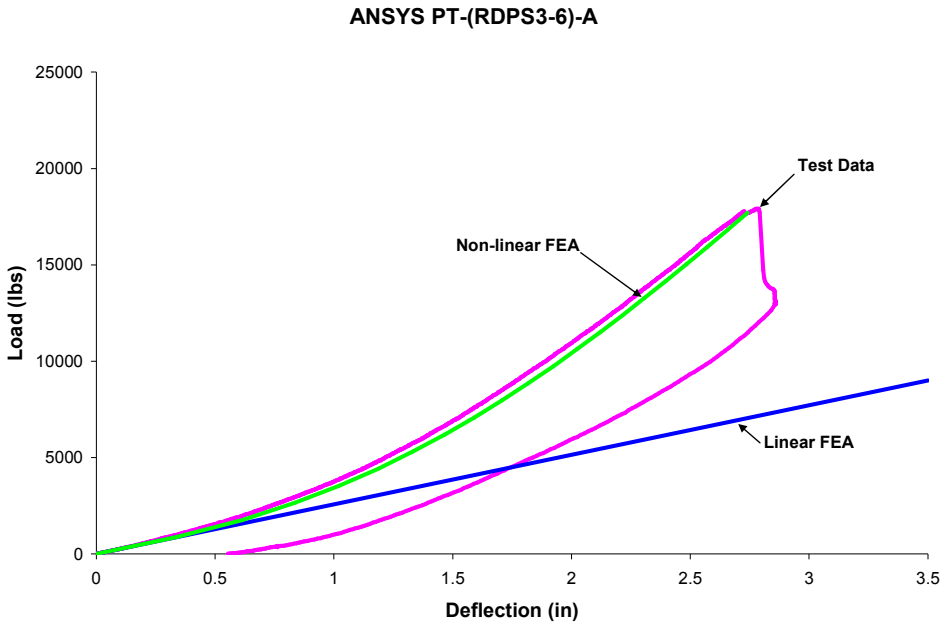

Figure 4.8 Typical ANSYS Results

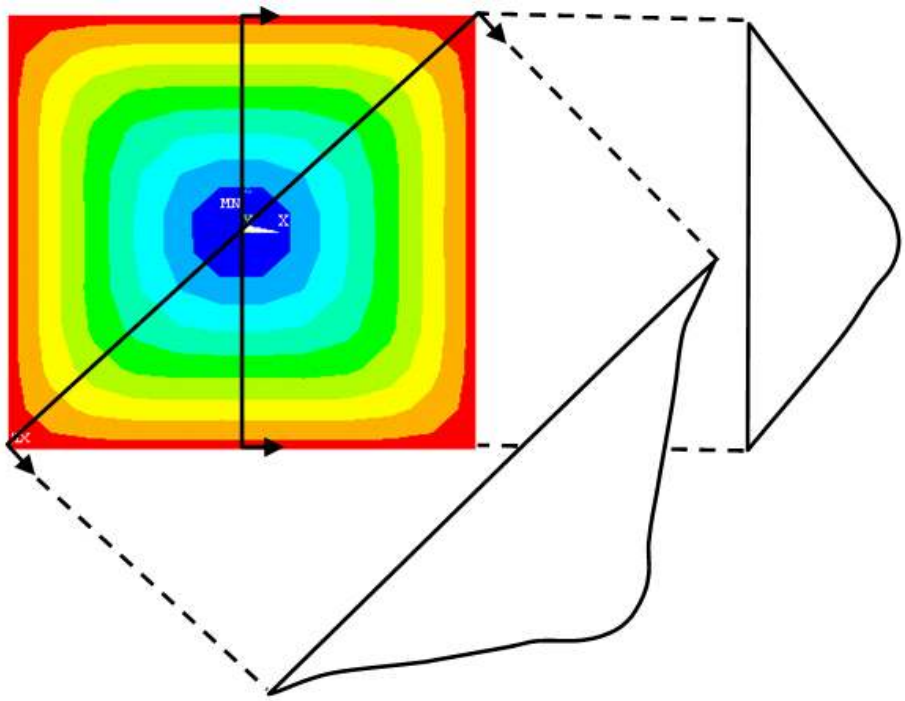

Figure 4.9 Deflection Contours and Profiles

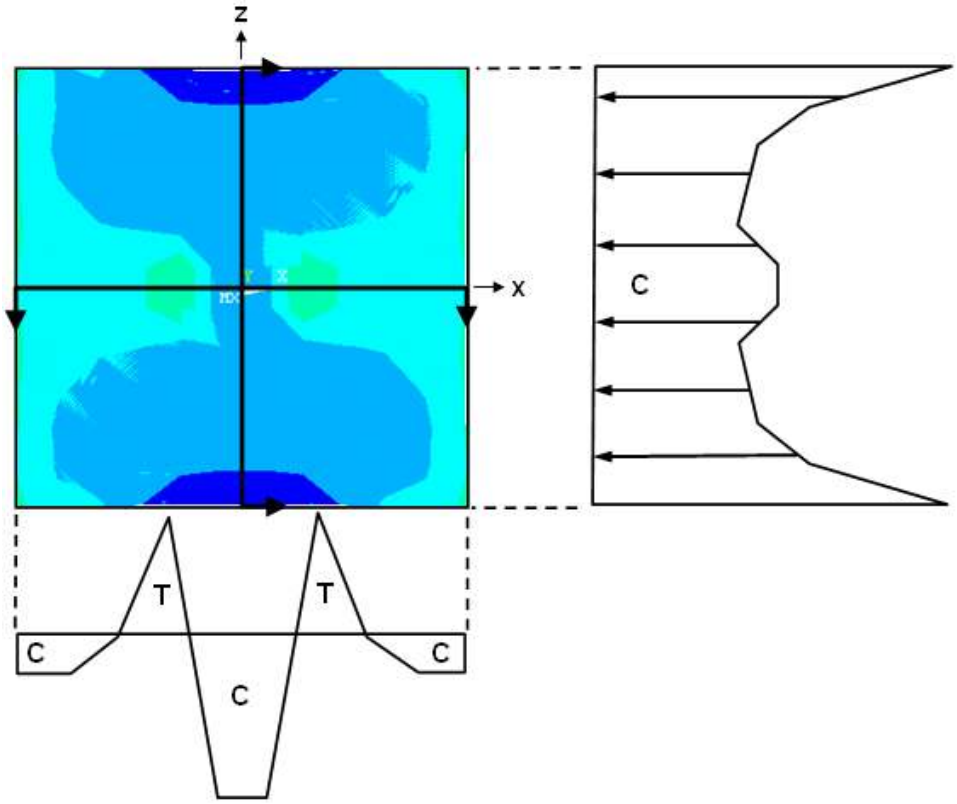

Figure 4.10 Normal Stress Distribution in the X Direction of the Top Fibers

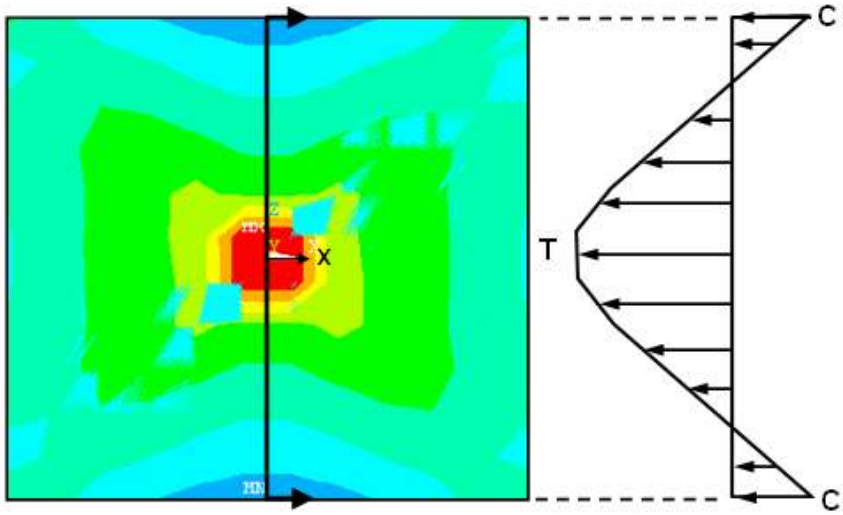

Figure 4.11 Normal Stress Distribution in the X direction of Bottom Fibers

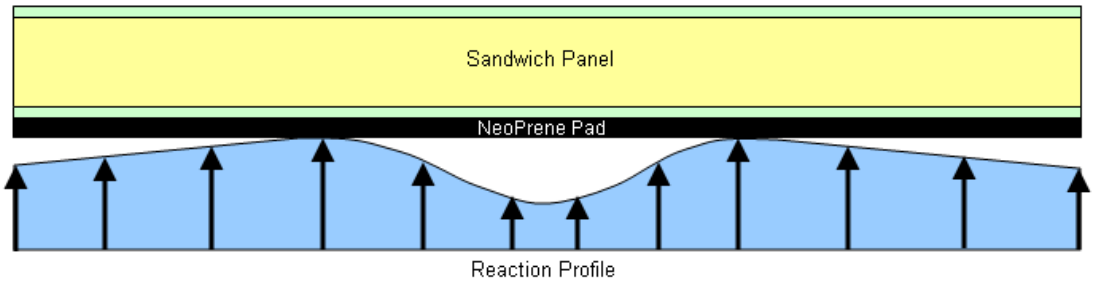

Figure 4.12 Reaction Profile

Table 4-3 Thickness (h)

fipsi	Length (in)	Width (in)	Aspect Ratio (L/W)	E_{skin} (ksi)	Thickness (in)
4	44	44	1x1	2700	1
					1.5
					2
					3
					4
8	44	44	1x1	2700	1
					1.5
					2
					3
					4

Table 4-4 Fiber Insertions per Square Inch (fipsi)

Thickness (in)	Length (in)	Width (in)	E_{skin} (ksi)	Shear Modulus (psi)	fipsi
1	44	44	2700	400	4
				500	6
				600	8
				700	10
2	44	44	2700	400	4
				500	6
				600	8
				700	10

Table 4-5 Elastic Modulus of the Skins (E_{skin})

fipsi	Length (in)	Width (in)	Aspect Ratio (L/W)	Thickness (in)	E_{skin} (ksi)
4	44	44	1x1	2	2700
					8000
					14000
					20000
8	44	44	1x1	2	2700
					8000
					14000
					20000

Table 4-6 Aspect Ratio (L/W)

fipsi	E_{skin} (ksi)	Thickness (in)	Length (in)	Width (in)	Aspect Ratio (L/W)
4	2700	1	44	44	1:1
				28	3:2
				22	2:1
8	2700	1	44	44	1:1
				28	3:2
				22	2:1

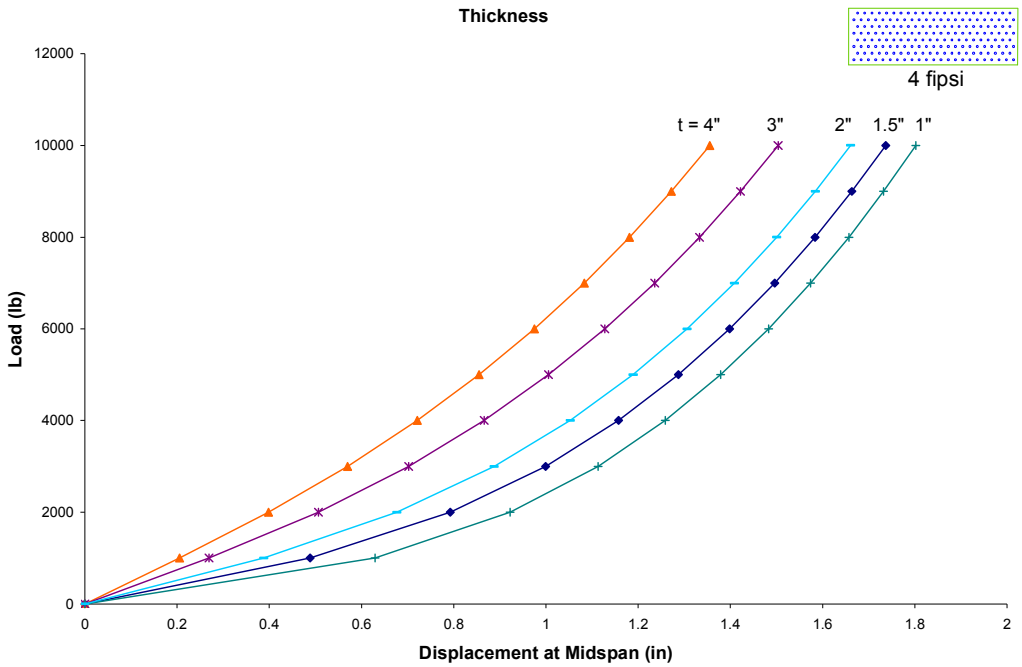

Figure 4.13 Effect of Panel Thickness with 4 fipsi

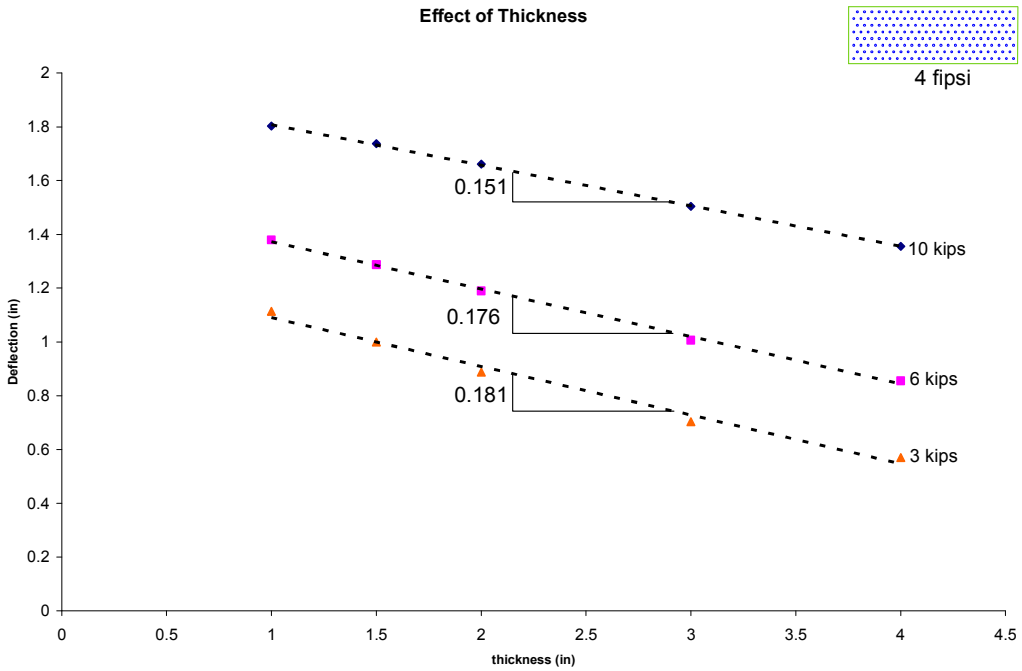

Figure 4.14 Defection vs. Thickness 4 fipsi

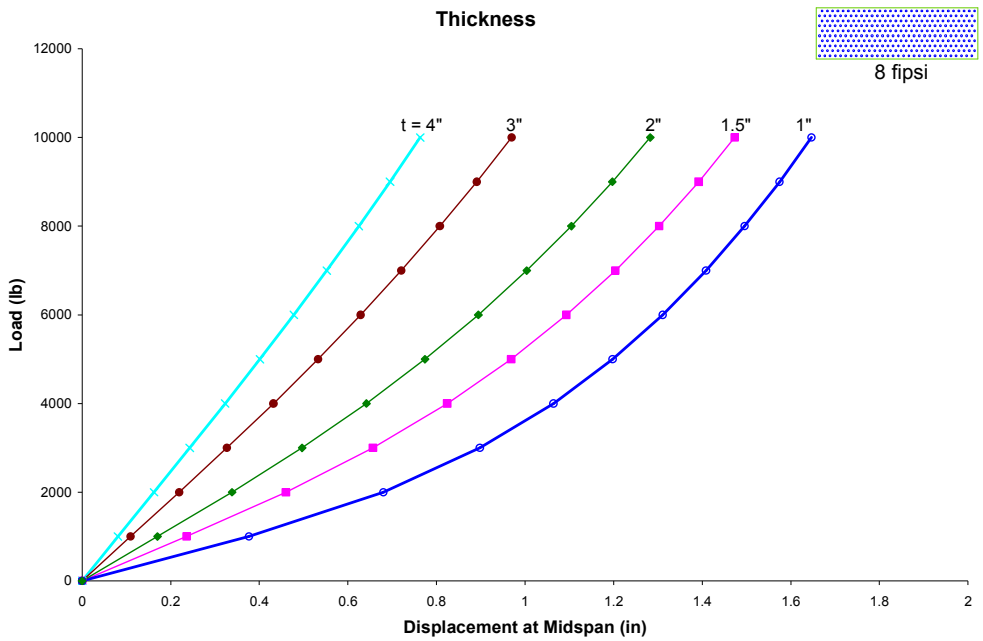

Figure 4.15 Effect of Thickness with 8 fipsi

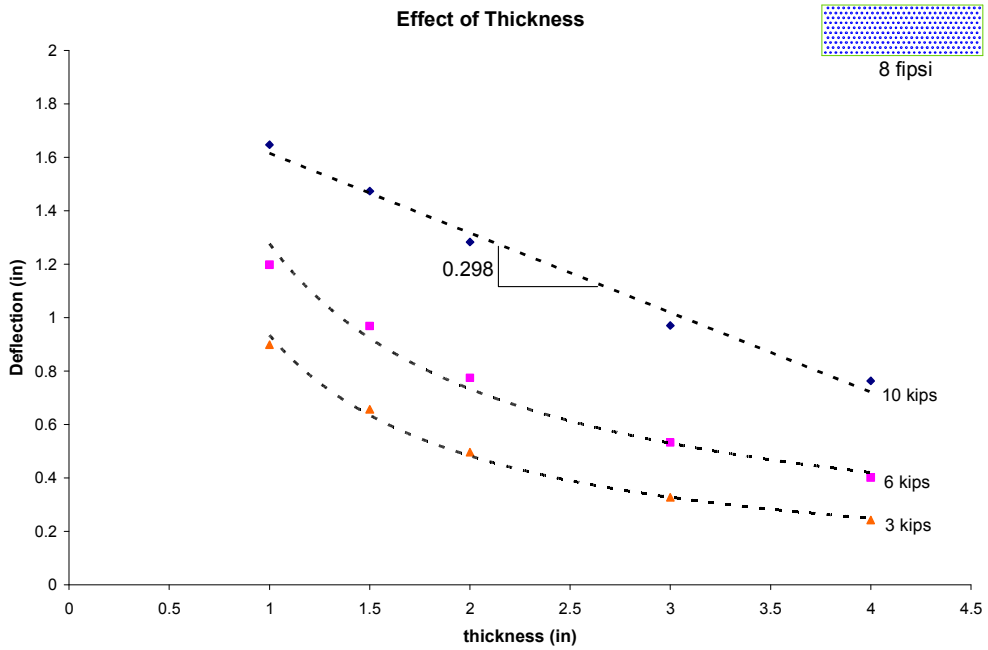

Figure 4.16 Deflection vs. Thickness 8 fispi

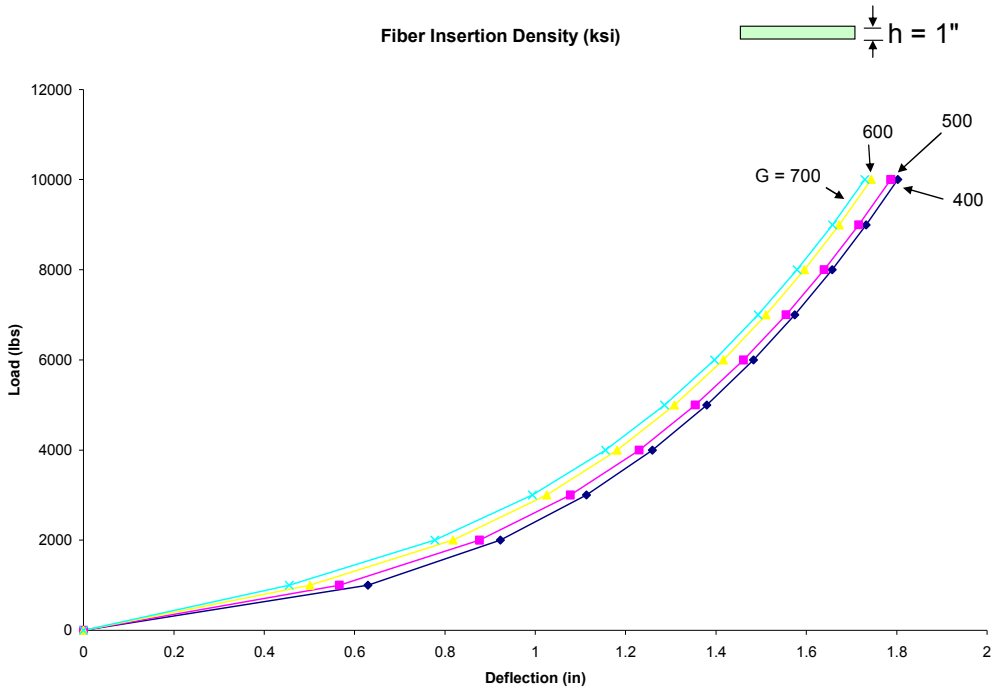

Figure 4.17 Effect of fipsi for a 1 inch panel

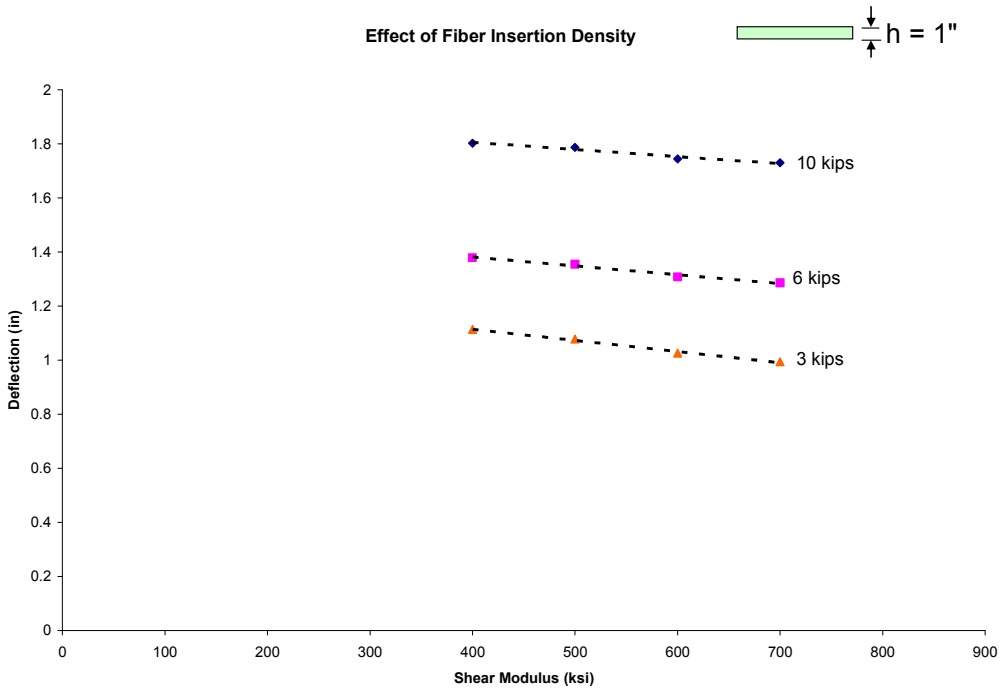

Figure 4.18 Deflection vs. Shear Modulus 1" thick

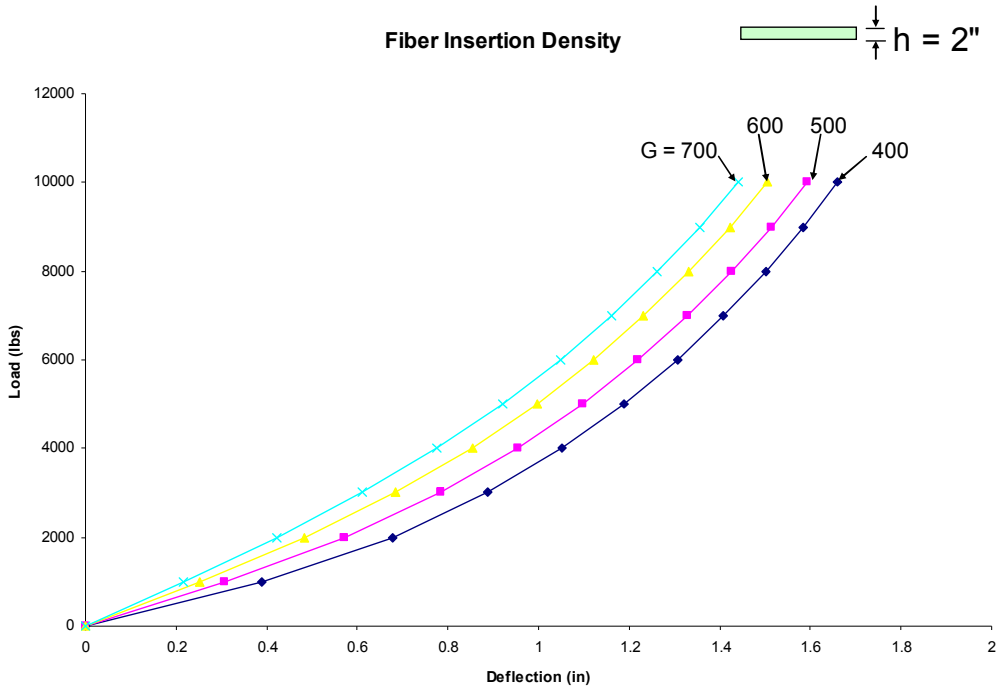

Figure 4.19 Effect of fipsi for a 2" panel

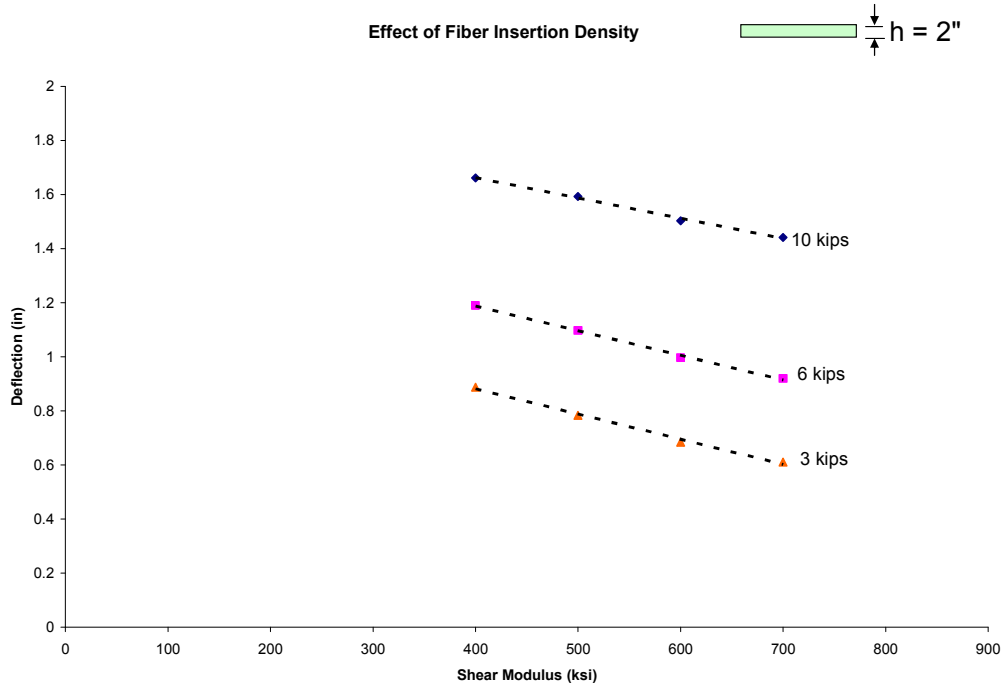

Figure 4.20 Deflection vs. Shear Modulus 2" thick

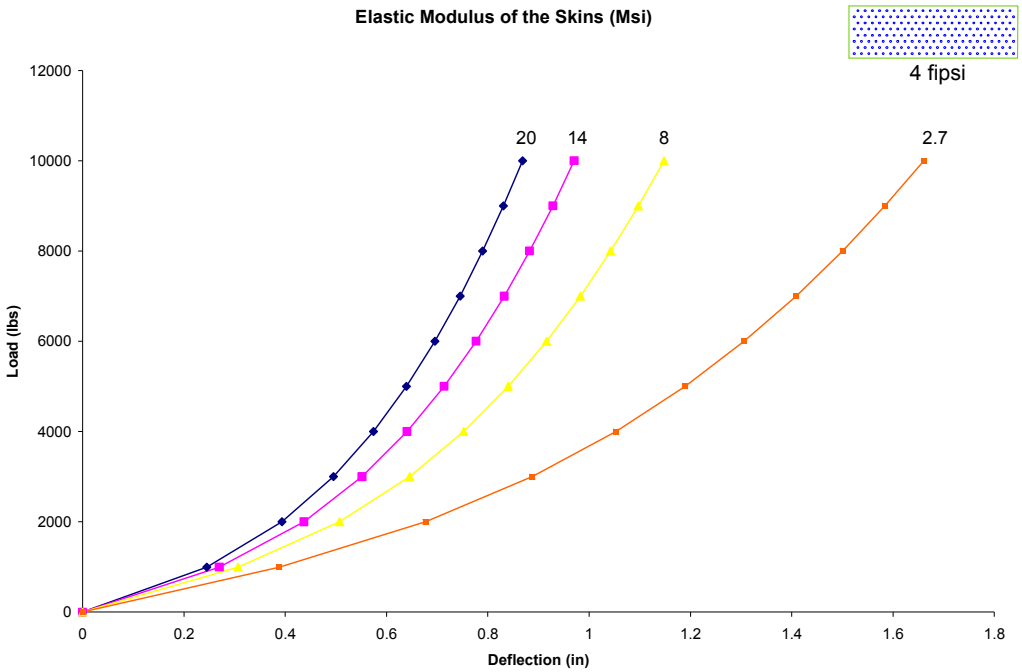

Figure 4.21 Effect of Skin's Elastic Modulus 4 fipsi

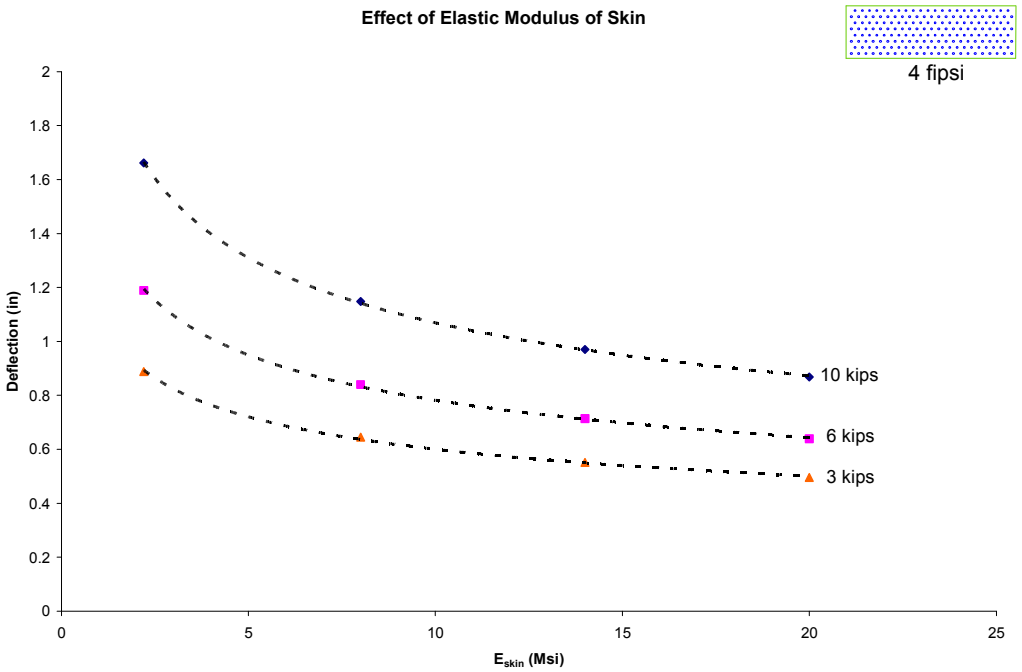

Figure 4.22 Deflection vs. E_{skin} 4 fipsi

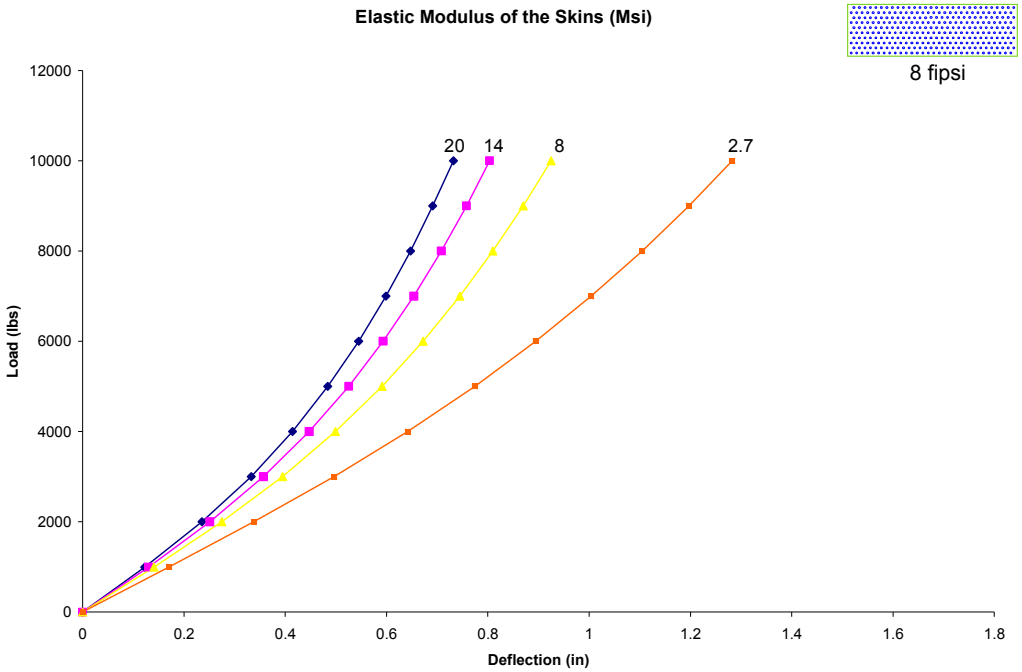

Figure 4.23 Effect of Skin's Elastic Modulus 8 fipsi

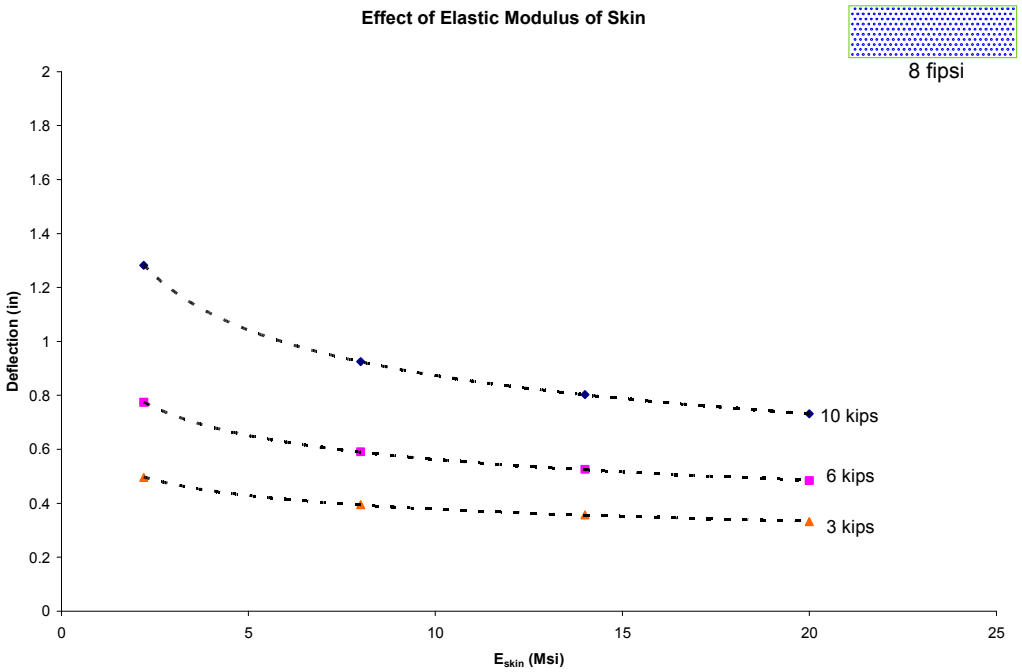

Figure 4.24 Deflection vs. E_{skin} 8 fipsi

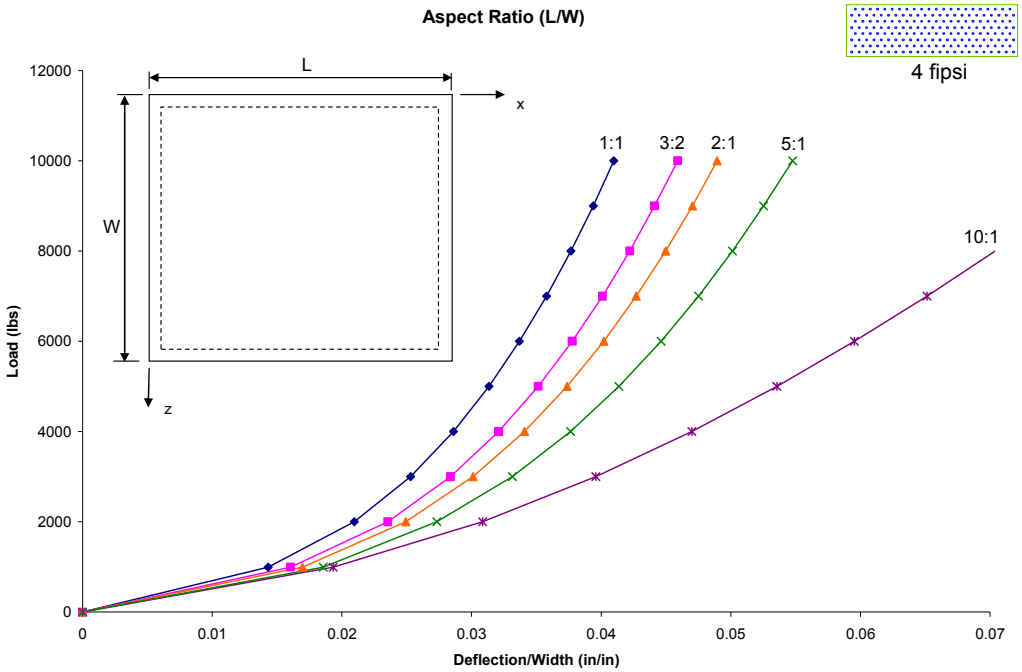

Figure 4.25 Effect of the Panel's Aspect Ratio with 4 fipsi

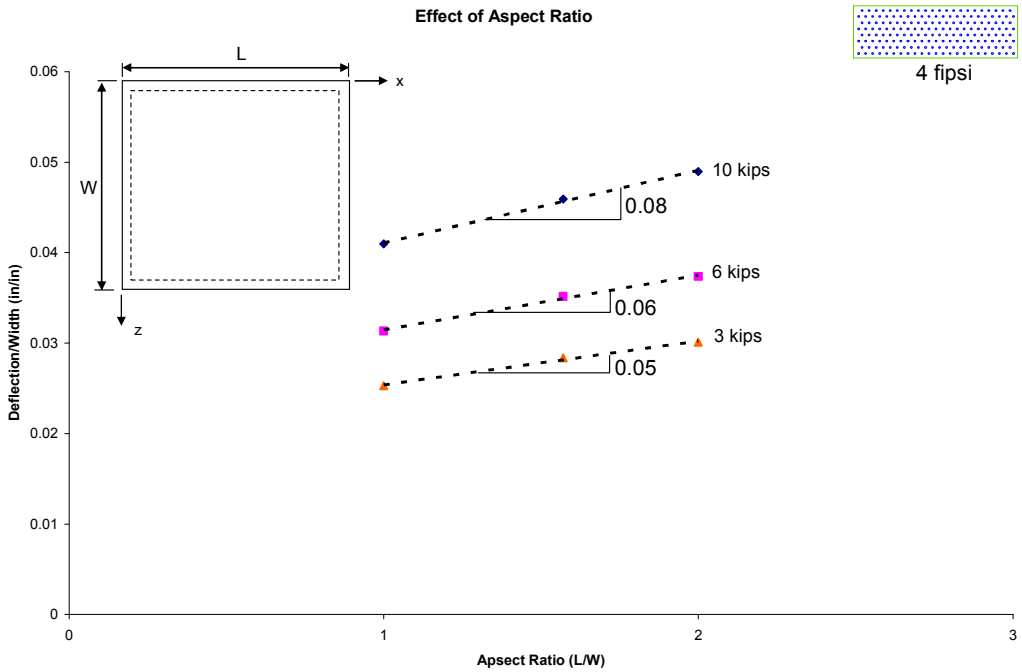

Figure 4.26 Deflection/Short Span vs. Aspect Ratio 4 fipsi

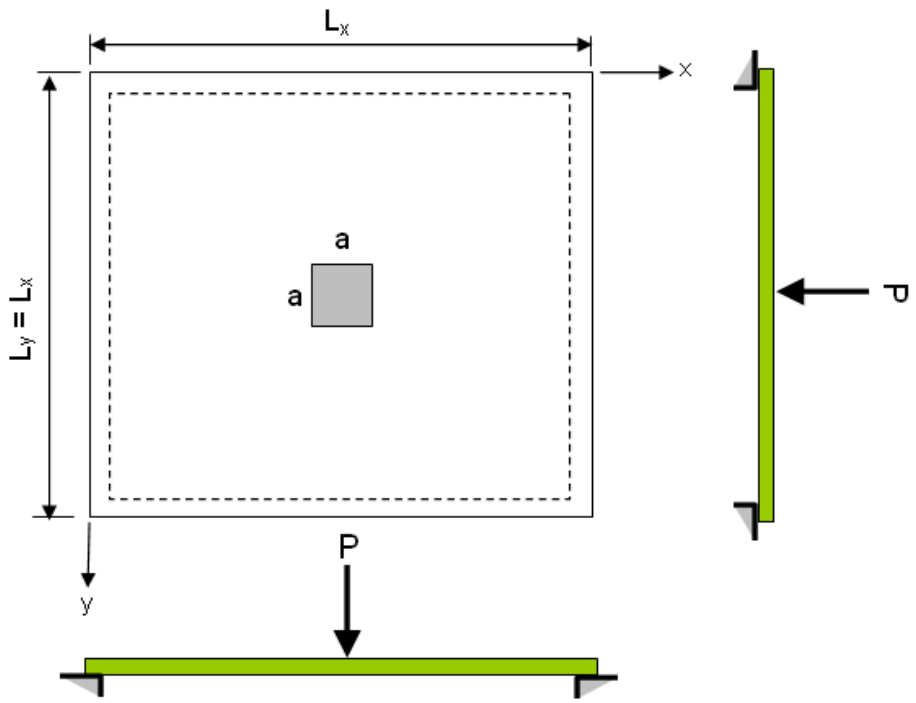

Figure 4.27 Rectangular Simply Supported Sandwich Panel Subjected to Concentrated Load (P)

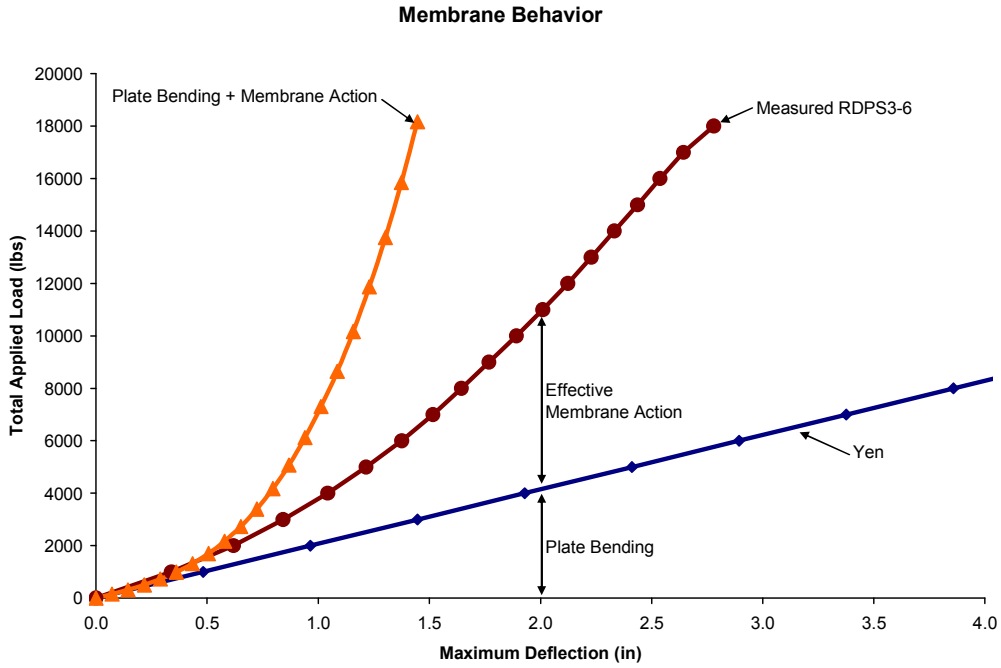

Figure 4.28 Load-Displacement Behavior of Two-Way Sandwich Panel

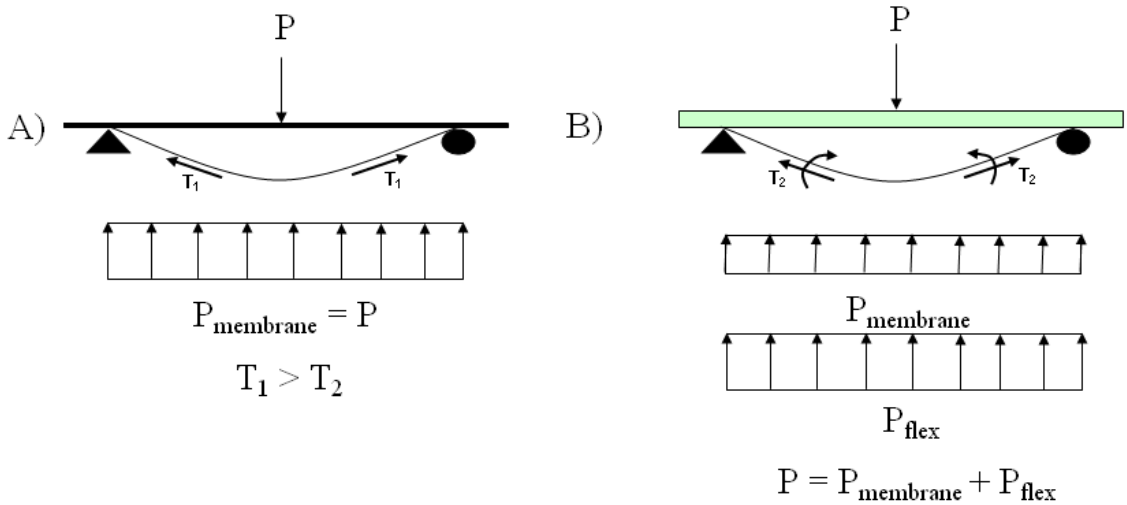

Figure 4.29 Effect of Panel Rigidity

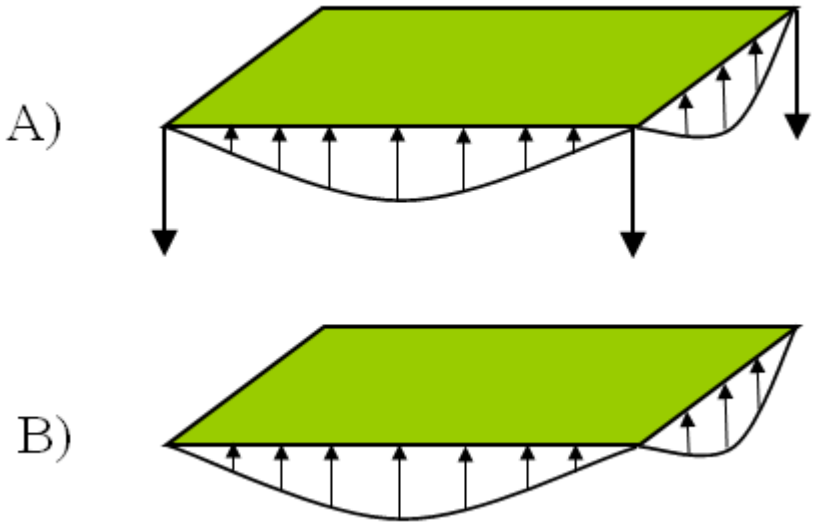

Figure 4.30 Theoretical (A) and Experimental (B) Support Conditions

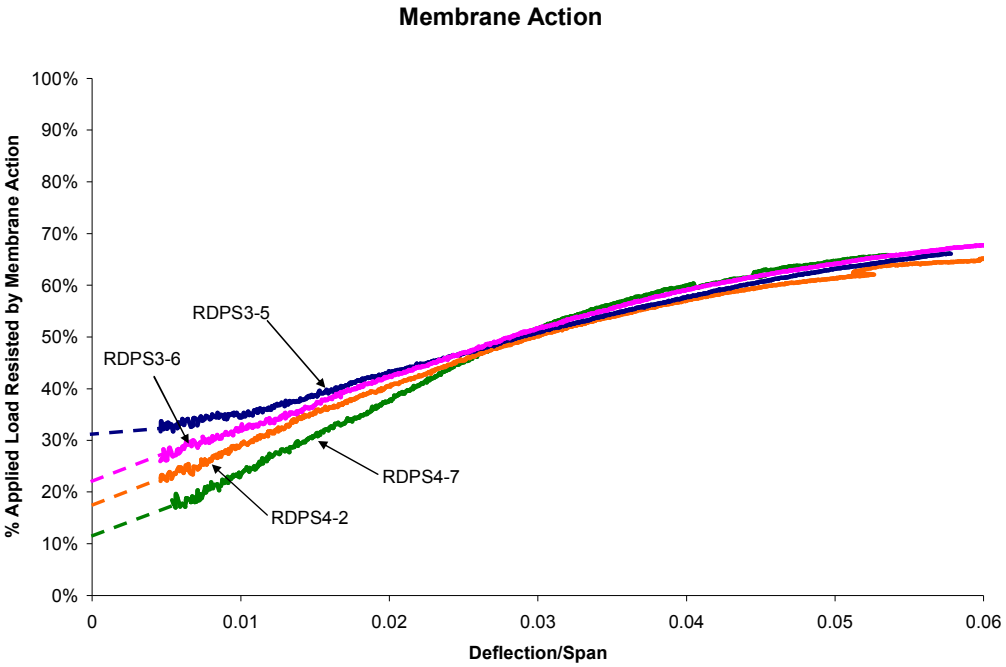

Figure 4.31 Experimental % Applied Load Resisted by Membrane Action

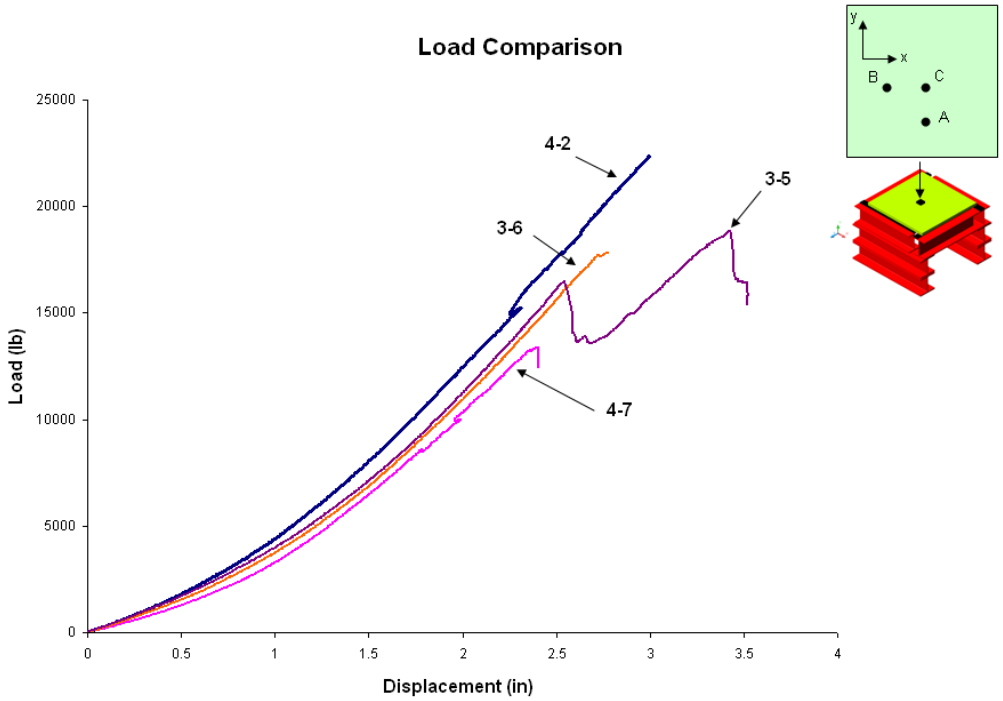

Figure 4.32 Nonlinear Behavior of the Tested Panels

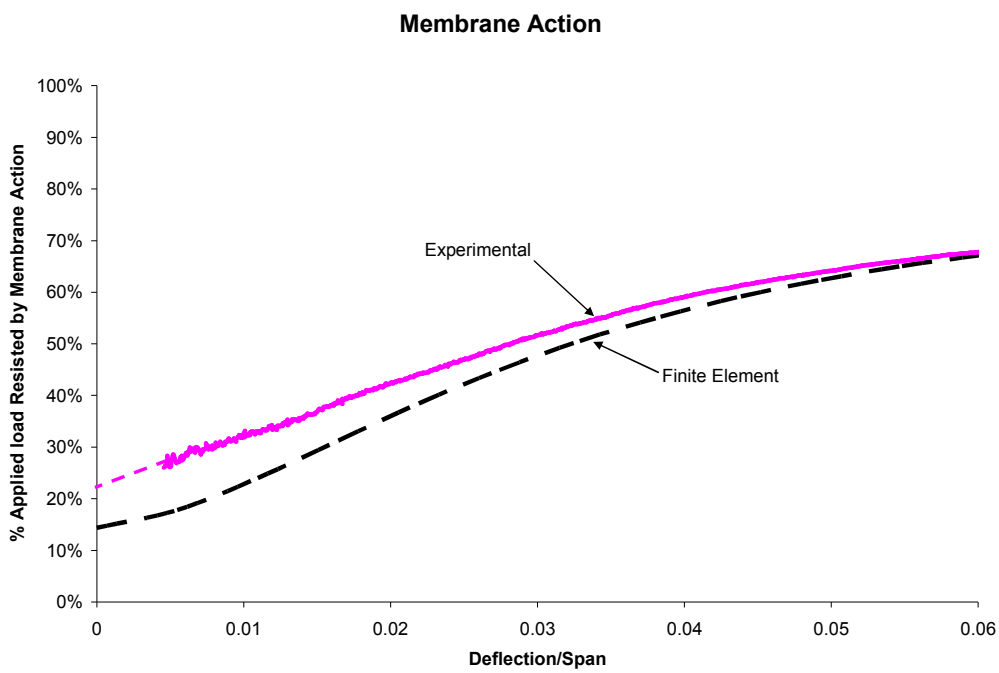

Figure 4.33 Membrane Action Experimental vs. FEA

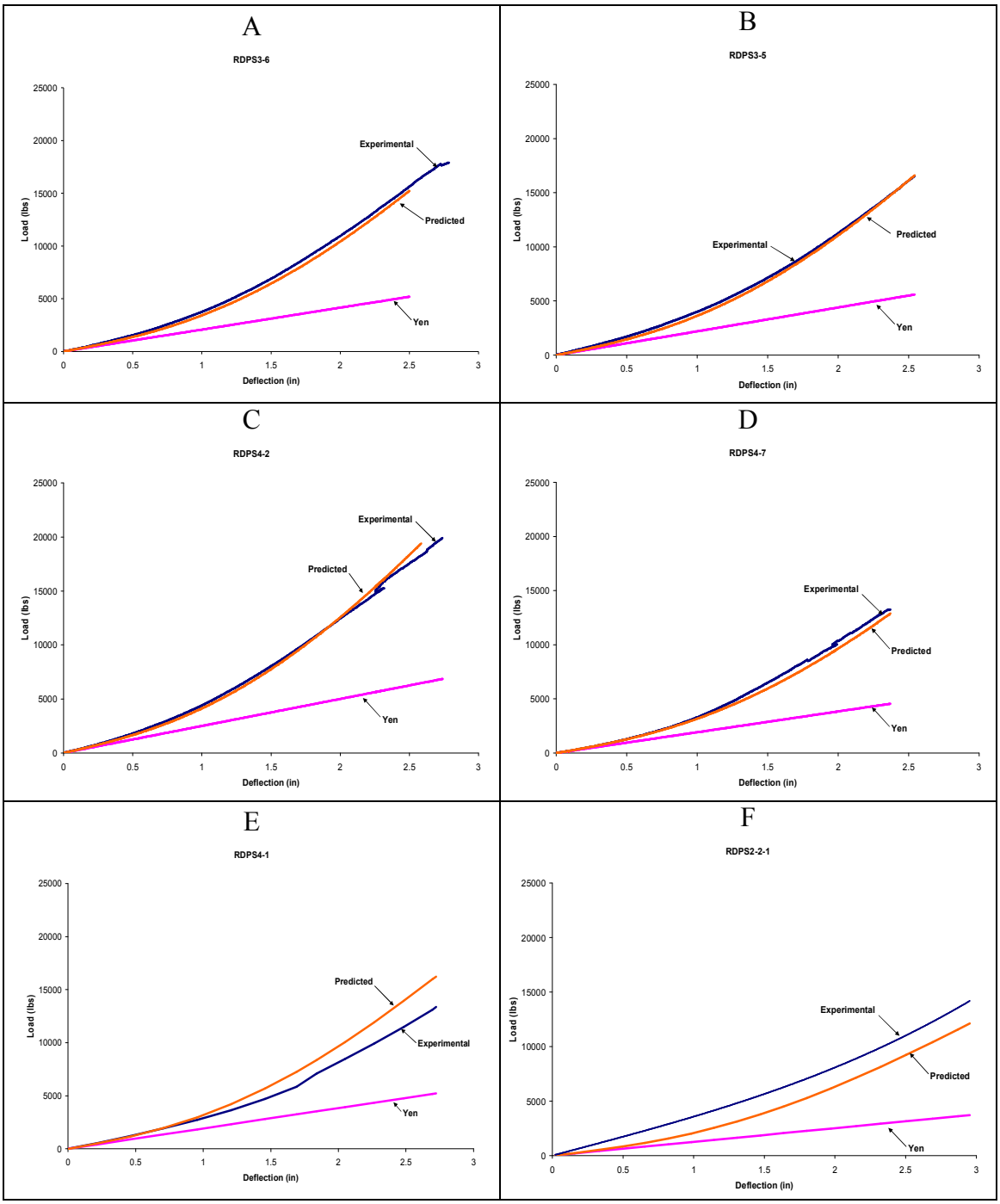

Figure 4.34 Predicted Two-Way Behavior of Tested Panels

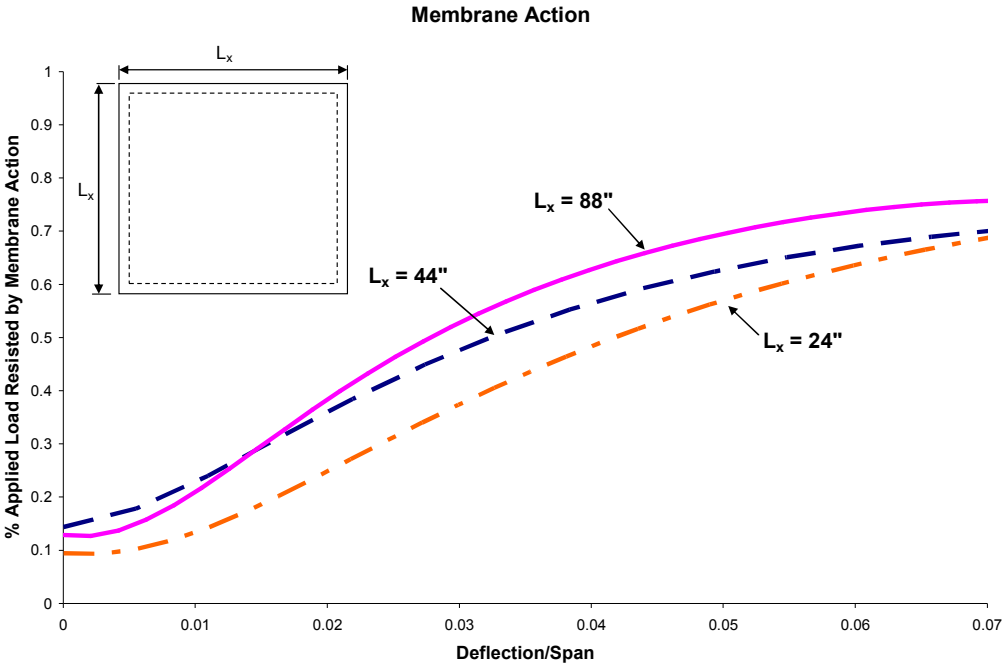

Figure 4.35 Effect of Span Length

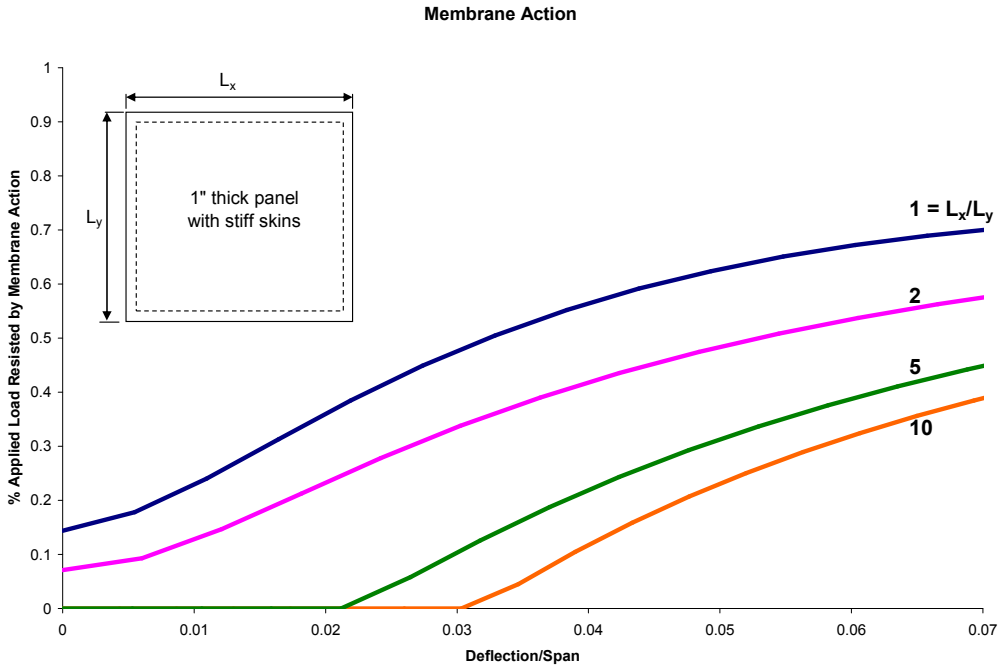

Figure 4.36 Membrane Action Curves for 1" Thick Panels with Stiff Skins

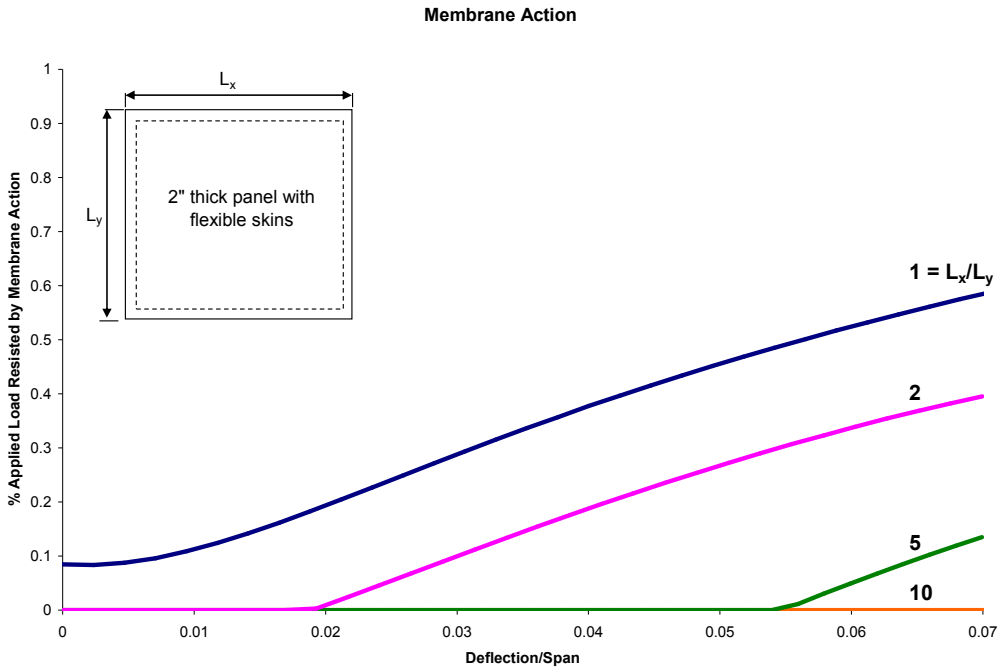

Figure 4.37 Membrane Action Curves for 2" Thick Panels with Flexible Skins

Chapter 5

5 Fatigue Performance of 3-D GFRP Sandwich Panels

5.1 Introduction

To study the fatigue performance of the proposed sandwich panels the panels were subjected to two different loading patterns and two different spans. The load patterns and spans were selected to study the effect of the applied shear stress and the span lengths under typical service life conditions. The experimental program considers also, the effect of the density and pattern of the through thickness fibers. Several panels were subjected to the 1,000,000 cycle limit which was selected to represent the typical life span of the use of these sandwich panels. Test results of these panels indicated that the behavior could be determined using only 600,000 cycles. The experimental results of the fatigue testing were analyzed to examine the overall fatigue performance of the sandwich panels, including: the effect of core shear stress, flexural stresses in the GFRP skins, and fiber insertion density of regular array patterns. The results of the fatigue study including the failure mode, degradation of deflection, and degradation of strain are presented and discussed in this chapter. The results for several of the test specimen are presented in detail. The results of the remaining tests are presented in a similar format in Appendix A.

5.2 Fatigue Performance

Typical measured maximum deflection versus number of cycles for the fatigue specimens is given in Figure 5.1. The test results indicate that the measured deflections reflect significant degradation within the first 10,000 cycles followed by relatively lower

degradations up to 100,000 cycles. After the completion of 100,000 cycles the maximum deflection tends to become constant or slightly increase linearly with the number of cycles, as shown in Figure 5.2 for the applied shear strain of 2%. The fatigue behavior was found to be largely dependent on the applied shear strain level. The behavior is also dependent on the span to depth ratio which affects the flexural and shear behavior of the sandwich panels. The maximum normal strain induced in the skin versus number of cycles graph is shown in Figure 5.3, indicates a similar behavior; a large deterioration over the first 10,000 cycles followed by a relatively constant strain after 100,000 cycles.

The maximum deflection versus number of cycles graph for panels with array fiber insertion patterns and 8 fipsi subjected to the 1% core shear strain condition is given in Figure 5.4. For these panels, failure occurred prior to completion of the 600,000 cycle limit. Failure was caused by the rupture of the fiber insertions which lead to delamination between the bottom skin and foam core. The panels exhibited shear cracks in the foam core within the first 6,000 cycles, as shown in Figure 5.5. As the number of cycles increases more shear cracks were developed on each side of the panel. After completion of the first 150,000 cycles, significant increase in the number of shear cracks was observed subsequently causing them to combine as shown in Figure 5.6. Some shear cracks propagated along the locations of the fiber insertions after 240,000 cycles, as shown in Figure 5.7. Finally, failure due to debonding of the foam and bottom skin layers occurred after 300,000 cycles. By careful examination it was found that the horizontal debonding crack, shown in Figure 5.8, was

caused after to the rupture of the fiber insertions as shown in Figure 5.9. The picture in this figure was taken using the magnified lenses of a high performance Olympus Camera.

5.3 Discussion of the Test Results

Degradation of the panels is believed to be caused by softening of the fiber insertion connections to the sandwich panel's skins. The fatigue degradation mechanism is similar to the failure mechanism of the direct shear test specimens under static loading conditions, previously reported by Patrick (2006). While the fiber insertions can still contribute to the overall strength of the panel their contribution is decreased. Originally the fiber connections can be considered to be totally fixed, however, as the number of cycles increases the local matrix surrounding the connections starts to soften. The softened connections start to behave more like pined than fixed connections; Figure 5.10 illustrates this described concept. Softening of the fiber insertion connections is thought to be attributable to the initiation and propagation of microcracks in the fiber insertions at their connection to the sandwich panel's skins. Cracking between the skin and insertion fibers may also lead to softening of the fiber insertion connections. The various types of cracking are shown in Figure 5.11. The microcracks in the fiber insertions are caused by the crimped nature of the insertions at their connection. The crimped shape is due to the brittle nature of the glass fibers, since the fibers cannot be bent into the skin layers at 90 degrees without causing rupture of the glass fibers. As the panels are loaded, the fibers engage and begin to straighten. The repeated bending and straightening of the fiber insertions allows the microcracks to propagate which can lead to rupture of the insertions.

In many cases, most of the panel's degradation, due to connection softening, was observed over the first 100,000 cycles. This indicates that the majority of connection softening occurs over this range. The increase in the maximum deflection and strain is caused by the degradation of the connection between the panel's skins reducing the effect of composite action. As the composite action effect is reduced the moment of inertia and shear rigidity of the panels were decreased; thus, increasing the amount of total deflection as well as the magnitude of normal stresses in the sandwich panel's skins.

The measured initial maximum deflections for all of the tested panels are given in Table 5-1. Examination of the table indicates that on average, doubling the magnitude of the maximum applied load also doubled the measured initial deflection. This reflects the elastic behavior of the panels in this range. After 600,000 fatigue loading cycles, panels subjected to the overloading stress condition had final deflections that were typically 120% to 150% greater than the final deflections of the panels subjected to the service stress level. This indicates that the intensity of the applied shear stress had a discernable effect on the fatigue performance of the panel.

The results indicate that fiber insertion densities have a definite effect on the one-way bending behavior of the panels. Panels with array patterns of 8 fipsi were initially much stiffer than their 4 fipsi counterparts. The 8 fipsi panels subjected to a large number of cycles rely on the insertions to resist the induced shear strain and provide composite action between the layers of the sandwich panel. Once the insertion connections start to degrade or rupture, the panel acts effectively as a panel with fewer fipsi and damaged connections and therefore

exhibits a higher shear strain than 2% under the same loading conditions. Thus, the panels are unable to sustain the repeated loading required to achieve a core shear strain of 2% for a panel with 8 fipsi. Similarly, degradation of the fiber insertions results in a lower degree of composite action between the core and the skins of the panel. This consequently leads to an increase in the total deflection of the panel under the effect of repeated loading and could lead to fatigue failure of the panel due to softening of the insertion connection.

5.4 Analysis of Fatigue Performance

This section presents analysis of the experimental results of twenty four one-way panels that were tested, to determine the panel's overall fatigue performance. The analysis includes a study of the effect of the internal shear stresses, bending stresses, and fiber insertion densities on the fatigue behavior of the 3-D sandwich panels. Since the types of panels tested were limited, the analysis compares panels with the same configuration and different loading levels, span lengths, and insertion patterns. This exploratory study was used to determine the overall fatigue behavior of the 3-D GFRP sandwich panels throughout their service life.

As discussed in Section 5.3, softening of the fiber insertion connections leads to some degradation of the panels which is believed to be caused by the initiation and propagation of microcracks at the connection of the insertions to the top and bottom GFRP skin layers. Observation of the failure surface indicated that cracking between the skin and insertion fibers may also lead to softening of the fiber insertion connections. Behavior of the panels indicate that the connection of the fibers may act in a "fixed" fashion, however, by loading

the panel the connections become softened and act as "pinned" connections as shown in Figure 5.10 and Figure 5.11. While the fiber insertions can still contribute to the overall stiffness of the panel their contribution is decreased by the softening effect.

The following analysis is based on the experimental data measured from the fatigue testing program described in Chapter 3. For each test the degradation was determined based on comparing the behavior after the repeated loading to the initial static deflection exhibited by the panel. The measured displacement over the first 100,000 cycles for a 2 inch thick panel with 4 fipsi and loaded to 2% core shear strain on a 40 inch span is shown in Figure 5.12. The incremental degradation in terms of the change in the deflection every 10,000 cycles ($\Delta\delta$), as a percentage of the initial static displacement (δ_o), was evaluated from the measured response as follows:

$$\Delta\delta = \frac{\delta_i - \delta_{i-10k}}{\delta_0} \tag{5.1}$$

Where δ_i is the maximum deflection after completion of the ith cycle and δ_{i-10k} is the maximum deflection after completion of the previous $10{,}000^{th}$ cycle.

The incremental degradation versus number of cycles graph for the same test configuration is shown in Figure 5.13. The behavior is characterized by a high initial rate of degradation over the first 10,000 cycles followed by a low and almost constant rate of degradation after 100,000 cycles. The incremental degradation can be used to determine the total degradation of the panel, as the sum of the incremental degradations, as follows:

$$Degradation = \sum \frac{\delta_i - \delta_{i-10k}}{\delta_0} \tag{5.2}$$

and, $$Degradation = \frac{(\delta_i - \delta_{i-10k}) + (\delta_{i-10k} - \delta_{i-20k}) + \cdots + (\delta_{10k} - \delta_0)}{\delta_0}$$

which simplifies to: $$Degradation = \frac{\delta_i - \delta_0}{\delta_0} \tag{5.3}$$

The degradation curve for the same panel is shown in Figure 5.14. The degradation curve shows also the panel's high rate of degradation over the first 100,000 cycles followed by a fairly constant rate of degradation throughout the remainder of testing.

Shenoi et al. (1997) demonstrated that a nonlinear power law model could be used to represent the creep-fatigue interaction of sandwich beams for short term tests as an empirical model, instead of the more commonly used linear Bürger model. Although, the Bürger model has more of a physical basis than the power law, additional terms must be verified through testing. Since, the time and number of specimens were limited; the empirical power law model was used to extend the experimental data to a 1,000,000 cycle service life for each panel, as shown in Figure 5.15. The selection of one million cycles is a value typically used by the industry to evaluate the service life of buildings and bridges. This figure demonstrates that the power law can accurately predict the experimental results for repeated loadings up to 600,000 cycles. Based on the demonstrated fit of the results within the 600,000 cycle range, the power law was used to extrapolate the fatigue degradation to the typical 1,000,000 cycle service life of the sandwich panel. Degradation curves were fitted to the experimental data for each fatigue specimen using the power law of the form:

$$\frac{\delta_i - \delta_0}{\delta_0} = mi^n \tag{5.4}$$

Where i is the cycle number, and m and n are constants determined for the particular panel and testing configuration. For the panel considered in Figure 5.15, the maximum predicted degradation during the typical service life is 25%. Using sandwich theory to calculate the static displacement of the panel the engineers could then predict the increase in deflection that the panel may exhibit throughout its service life. In this case, the increase in deflection may be as much as 25% due to the deterioration of the fiber insertion connections. The remaining portion of this chapter will detail how the span and loading conditions can change the fatigue performance of the 3-D sandwich panels.

5.4.1 Effect of Shear Stresses

Test results indicate that increasing the maximum applied shear stress in the core has a significant effect on the degradation of the panel's properties. This section discusses the effect of the shear stress on the fatigue behavior of the panels and possible degradation due to softening of the fiber insertion connections. The shear stress in the core of the sandwich panels can be determined using Elementary Sandwich Theory (EST). EST uses the fundamental mechanics equation for shear stress (τ) produced by the internal shear force (V), given by:

$$\tau = \frac{VQ}{Ib} \tag{5.5}$$

Where Q is the first moment of the area, I is the moment of inertia of the cross section, and b is the width of the panel. The core shear stress in the sandwich panel can be assumed to be constant since the foam core is weak, compared to the GFRP skins, reducing the shear stress in the sandwich panel's core to:

$$\tau = \frac{V}{bd} \tag{5.6}$$

where d is the distance between the center of the panels skins. In this case, the panels are simply supported and loaded by a concentrated load (P) at midspan. Therefore, the shear force (V) in the panel is equal to half the applied load, giving an expression for the core shear stress in terms of the applied load (P):

$$\tau = \frac{P}{2bd} \tag{5.7}$$

Within the service load range, where the load-deflection behavior of the static 3-point bending testing was observed to be linear, increasing the applied stress, as approximately given in Equation 5.7, the shear strain will be increased linearly based on the constant shear modulus, G. However, test results of a previous study conducted by Jason Patrick (2006) indicated that the initial portion of the core shear stress-shear strain graph was observed to be nonlinear for shear strains greater than 1%, as shown in Figure 5.16. This nonlinear behavior indicates some degree of localized deterioration in the core materials, foam and GFRP insertion fibers, when subjected to core shear strains greater than 1%. Accumulation of the localized degradation in the core may lead to gradual fatigue of the sandwich panels when subjected to cyclic loading at shear strains greater than 1%.

The degradation curves for the two different levels of shear strain for 1 in. thick panel with wall fiber insertion patterns spaced at 1.5 in. are shown in Figure 5.17. This figure displays the typical effect of increasing the shear stress on the fatigue performance of the sandwich panels with wall fiber insertion patterns. The results of the fatigue tests indicate that the wall type patterns loaded up to 2% core shear strain exhibited degradations up to 35% of the initial static deflection after 1,000,000 cycles. Also, the results indicate that increasing the applied shear stress increased the amount of initial and long term degradation by up to 25%. The increased degradation due to the higher shear stress is caused by the significant shear deformation induced by doubling the applied shear stresses due to the nonlinear nature of the core. This means that the induced shear strain in the core is much higher than the 2% predicted, causing significantly more deterioration of the insertion connections. The total amount of degradation of the panels loaded to 1% shear strain was generally limited to 20% of the initial deflection, in this case. This represents a more acceptable level of degradation than the 35% for most typical applications.

The variability of results was greater for panels with array fiber insertion patterns. Similarly to the wall insertion patterns the test results indicate increasing the shear stress in the panel increased the amount of degradation. This effect is illustrated in Figure 5.18 for the 1.5 inch thick panels with 4 fipsi and 2 skin plies. These panels were loaded up to the two shear loads corresponding to 1% and 2% core shear strain. The results indicate similar levels of degradation for each panel over the first 200,000 cycles. As the number of cycles increased the rates of degradation of the two panels diverge. Degradations up to 45% of the

initial displacement are expected after the 1,000,000 cycle service life for the panel subjected to the higher shear stress range. The difference in the final degradation, due to the increased level of applied shear stress, is minimal, only 4% and 7% for span lengths of 40 and 28 in., respectively. This may be due to a reduced level of fixation of the insertion connections for panels with only 2 skin plies, compared to panels with 4 skin plies. Since the connection of the insertions to the skins made from two GFRP plies provide less fixation, the connections can degrade from a "fixed" connection to a "pinned" more easily.

The fatigue behavior of 2 inch thick panels with 4 fipsi and the alternate foam type is shown in Figure 5.19. The figure shows a much larger change and continuous degradation of the insertion connection over the service life under the effect of the 2% core shear strain loading compared to the 1% loading. The different foam type used in this panel, which is not commonly used for these sandwich panels, could have lead to the cause of the increased degradation. For panels with the same configuration but built with a different foam type, which is more commonly used, the results showed a much lower and almost no degradation increase by increasing the applied shear strain, as shown in Figure 5.20. The figure displays the effect of increasing load on these panels for a span of 40 in. In this case, for loadings up to 2% the degradation is limited to 25%. The change in degradation was only two percent due to increasing the applied shear strain from 1% to 2%. Therefore, for these types of panels increasing the shear stress in the core has a limited effect on the deterioration of the fiber insertion connections.

Doubling the applied shear stress for the 2 inch thick panels with 8 fipsi caused failure of the panel prior to the minimum 600,000 cycle testing limit. Failure of the panel was evident by the sudden increase in the rate of degradation occurred, as shown in Figure 5.21. This point coincides with the point in which the panel's degradation reaches 100%. The 8 fipsi panels subjected to the 2% core shear strain rely on the insertions to resist the applied shear force between the layers. Due to the nonlinear nature of the shear stress-shear strain behavior of the core, this high level of shear stress induces excessive shear strains between the sandwich layers, much greater than the 2% shear strain predicted. The induced shear strains lead to severe degradation of the insertion connections and the development of plastic hinges in the insertions at their connection to the panel's skins. Once the insertion connections start to degrade or rupture the panel effectively behaves similar to a panel with fewer fipsi and damaged connections subjected to a much higher shear strain. The effective panels in this case, were unable to sustain the repeated loading condition of the 8 fipsi panel, consequently leading to failure of these panels. Thus, the fatigue performance of the panels with 8 fipsi array patterns may fail because of the continuous softening of the insertions and their connections when loaded to 2% core shear strain.

In each case, increasing the core shear stress increases the percentage of degradation with respect to the initial deflection of the panel. The results also suggest, under the effect of 1% core shear strain loading the degradation is limited to 25% of the initial deflection. In most cases, doubling the applied load and consequently the applied shear stress can cause significant degradation ranging from 2 to 35 percent relative to the degradation under the 1%

core shear strain loading. Of all the panels loaded by shear strains equivalent to 2%, based on the assumption of linear behavior of the material, 75% exhibited degradations greater than 25% of their initial static displacement during their 1,000,000 cycle service life. The results showed also that the large amount of degradation of these panels is due to the higher level of the applied loading which induced excessive levels of core shear strain, which were greater than predicted, causing excessive deflection under the applied service load or even failure of the panel. Fatigue behavior of the panels also indicates clearly that the type of foam is critical when the panels were subjected to 2% core shear strain loading condition. For these reasons, the service load level should be limited to 1% core shear strain to avoid any excessive deflection under the applied service load which could lead to failure. Based on the power law model for each specimen loaded to 1% core shear strain the values of m and n range between 0.0028 to 0.0349 and 0.1367 to 0.3136, respectively. With an average degradation for all panels loaded to 1% core shear strain for up to 1,000,000 cycles, as follows:

$$\frac{\delta_{avg} - \delta_0}{\delta_0} = 0.0163 i^{0.1855} \tag{5.8}$$

Therefore, given the initial static displacement (δ_o), the average increased deflection (δ_{avg}) due to the degradation caused by the repeated service loading can be determined after the ith cycle based on Equation 5.8. The predicted degradation curve for the 1% shear strain loading condition is compared to the degradation curves for each fatigue specimen loaded to 1% predicted core shear strain in Figure 5.22. The predicted degradation curve represents the

average degradation of the tested panels that were loaded up to a predicted core shear strain of 1%. In some cases the predicted degradation is unconservative, however, the maximum under-prediction is within 4% relative to the initial static displacement of the panel. The figure shows also that the maximum degradation in each case was less than 25% except for the panel with 2 skin plies. Therefore, the minimum number of skin plies should be limited to 4 plies to avoid any excessive deterioration of the sandwich panels.

5.4.2 Effect of Span Length

The spans of the fatigue tests also have a significant effect on the displacement behavior of the panel. The span lengths of the panels considerably affect the bending behavior of the sandwich panels by changing the relative contribution of the bending and shear deflections. Figure 5.23, shows the relationship between the panel's span-depth ratio and the percentage of the predicted total deflection attributable to bending and shear deflections for panels subjected to 3-point bending with total panel thicknesses of 1, 1.5, and 2 in. The depth of the panel is the distance between the centers of the panel's skins. The figure shows that the percentage of the shear deflection ($\%\Delta_S$) to the total deflection decreases linearly for increasing span-depth ratios; consequently the percentage of the total deflection due to bending ($\%\Delta_B$) is increased linearly. Table 5-2 highlights the predicted shear and bending components of the total deflection for each panel thickness and span length tested. For the tested panels, the percentage of shear deflection range from 53% to 85% of the total deflection. This indicates that the one-way deflection behavior of the tested panels is primarily affected by the shear deflection.

The shear deformation of the panels is primarily resisted by the GFRP fiber insertions. As the panel deflects the insertions engage; since the insertions are crimped, due to the manufacturing process, at their connection to the skins they begin to straighten as they are engaged. The repeated loading may allow microcracks in the insertions to propagate and cause softening of the insertions at their connection. Therefore, the increased percentage of shear deformation, for panels with shorter spans, may also significantly increase the degradation that the panels experience over their service life.

The GFRP fiber insertions also significantly affect the flexural behavior of the sandwich panels by providing composite action of the panel's layers. As discussed in Section 5.3 the degradation of the panel's properties can also be caused by the deterioration of the connection of the insertion fibers to the panel's skins. The softened connection was found to be due to the development of cracking between the insertion and skin fibers. The deterioration of the connection reduces the effect of composite action which leads to some of the panel's degradation. Therefore, increasing the span length would increase the flexural deflection component and consequently increase the effect of the reduced composite action on the 3-D sandwich panels fatigue performance.

The degradation curves for each span length and shear strain level for the 1 inch thick panels with a wall type insertion pattern spaced at 2 in. are shown in Figure 5.24. The figure represents the typical observed effect on the fatigue performance of the sandwich panels due to varying the span length for each load level. Based on the test results and the predicted power law, panels loaded to a core shear strain of 1% exhibited an increase in the amount of

degradation due to decreasing the span length from 40 to 28 in. The figure shows also that the initial degradation is affected by the increased span length but the change is not significant. The results suggest that for panels with a service load equivalent to 1% core shear strain the fatigue performance is significantly affected by degradation of the insertion fibers. However, the deterioration due to softening of the insertion connection is small within the service load range.

Test results for the panels subjected to loads equivalent to 2% core shear strain are also shown in Figure 5.24. The results show small increase in the final amount of degradation due to increasing the span length of the panels, with the more commonly used foam, from 28 to 40 in. The figure shows also that the initial degradation is not significantly affected by the increased span length for the 2% strain loading condition. The results suggest that for panels loaded to high levels of shear stress the amount of degradation is significantly affected by the deterioration of the insertion connection. This is indicated by the small change in degradation relative to increasing the span length from 28 to 40 in. The deterioration of the connection reduces the degree of composite action between the sandwich panel's layers which causes the flexural deflection to increase. This effect on the fatigue performance is more pronounced for panels with longer spans since the flexural behavior is increased. Limiting the service load level to a maximum stress equivalent to 1% core shear strain would avoid any significant increase in deflection under the service loading condition caused by the deterioration of the insertion connections to the panel's skins.

In the case of the 1.5 inch thick panel with 4 fipsi and consisting of 2 skin plies, the degradation was more significantly affected by the percentage of shear deformation, which causes the deterioration of the fibers, for each load level, as shown in Figure 5.25. This is evident by the decreased amount of degradation for the panel loaded to 2% for a 40 inch span, compared to the 28 inch span, indicating little to no additional deterioration of the insertion connection. This behavior may be attributed to the number of skin plies. This supports the proposed concept, from Section 5.4.1, that panels with skins made from 2 skin plies provide less fixation of the insertion connection. Since the insertion connections are less rigid the effect on the fatigue performance is more substantially affected by the percentage of shear deformation, which causes the insertion fibers to degrade at their connection.

As indicated in Section 5.4.1, the foam type also affects the fatigue performance of the sandwich panels especially under high load levels equivalent to 2% core shear strain. This effect was also noticed when comparing the degradation curves for panels with the alternate foam type on various span lengths as shown in Figure 5.26. The figure shows a large increase in the final degradation for the panels loaded to 2% for span length of 28 and 40 in. compared to the small change for the panels subjected to a service load condition within the range of load equivalent to 1% core shear strain. The increased degradation for the panels with the longer span, indicates that the degree of composite action may more significantly affect the fatigue performance of the panels with the alternate foam compared to the panels with the more commonly used foam. Again, doubling the service load

significantly increases the degradation of the connection between the insertions and the skin plies of the panel. In this case, this reduced the degree of composite action of the panel resulted in a degradation of up to 60%. Therefore, the service load should be limited, such that the induced core shear strain is no more than 1% in order to limit the degradation to 25% of the initial deflection.

The effect of the span length on the fatigue performance of the 3-D sandwich panels has a coupled effect on the deterioration of the insertion fibers and their connection to the GFRP skins. Restricting the maximum applied service load such that the core shear strain is limited to 1% controls the deterioration of the insertion connections, as well as, limits the total amount of degradation to 25% of the initial static displacement. At the 1% core shear strain service load level the percentage of shear deflection can affect the fatigue performance, however, the effect is not significant. Panels whose behavior is more influenced by shear typically experience higher amounts of degradation than the other panels but the amount of degradation is limited to 25% for the 1% service load condition.

5.4.3 Effect of Fiber Insertion Density

The amount of fiber insertions can have dramatic effects on the flexural and shear rigidity of the panel. Panels with more fipsi have a larger shear modulus; the stronger shear connection achieves more composite action of the sandwich layers. This analysis investigates the effect of the fiber insertion density for array type patterns on the fatigue performance of the 3-D sandwich panels by comparing the experimental and analytical results for the 2 inch thick panels with 4 fipsi and 8 fipsi.

The results suggest for panels loaded to 1% core shear strain that increasing the insertion density can decrease the amount of degradation as shown in Figure 5.27. The decrease in degradation due to increased insertion density was observed to be similar for the 28 and 40 inch span lengths. Panels with 4 fipsi experienced an additional 10% degradation when compared to panels with 8 fipsi. The reduced degradation for the panels loaded to 1% core shear strain is due to the enhanced shear connection of the 8 fipsi panels between the sandwich layers which enhances the composite action of the panel's skins. The improved shear connection reduces the percentage of shear deflection between the panel's skins thus reducing the amount of degradation due to the applied shear stress, since the behavior of the panels with 8 fipsi is less affected by shear than the panels with 4 fipsi. On average the result of doubling the amount of insertions, from 4 fipsi to 8 fipsi, reduced the final degradation by 35%.

For the same panels loaded by an equivalent load corresponding to 2% core shear strain, the results suggest that the increased insertion density may cause premature failure of the panel as evident by the two degradation curves shown in Figure 5.28. In this figure the panel with 4 fipsi stays within the reasonable fatigue range, of 25%, while, the 8 fipsi panels rapidly degrades and reaches failure at 100% degradation around 240,000 cycles. The 8 fipsi panels subjected to the 2% core shear strain rely on the insertions to achieve composite action between the layers. Once the insertion connections start to degrade or rupture the specimen effectively behaves as a panel with fewer fipsi and damaged connections between the insertion and the skins subjected to a much higher shear strain. Consequently, the panels

are unable to sustain the repeated loading and the panels eventually fail due to significant softening of the insertion connection.

Therefore, increasing the fipsi for a panel can decrease the degradation of the panel due to the improved shear connection of the sandwich layers. However, increasing the amount of fipsi may lead to premature failure if the applied load is large enough to cause significant softening of the insertion connections during the panel's service life. In each case in which failure occurred, core shear cracks developed within the first 10,000 cycles. Limiting the applied service load such that the core shear strain is less than 1% would prevent any cracking in the foam core and limit the final degradation to 25%, avoiding any significant increase in the service load deflection throughout the panel's service life.

5.4.4 Summary of the Sandwich Panels Fatigue Performance

Based on the fatigue results and predicted power law model, it was found that the fatigue performance of the 3-D GFRP sandwich panels is primarily affected by the intensity of the applied shear stress and the panel's shear behavior. A summary of the final degradation, after 1,000,000 cycles, is given for each panel testing configuration in Figure 5.29 and Figure 5.30 for spans of 40 in. and 28 in., respectively. The figures show that the panels loaded by a load equivalent to 2% core shear strain experienced an unpredictable and much wider range of final degradation. While, the degradation of panels under the effect of the 1% core shear strain loading was typically is limited to 25% of the initial deflection. Increasing the applied shear beyond the load equivalent to 1% core shear strain significantly increased the percentage of degradation with respect to the initial deflection of the panel.

This effect is caused by nonlinear nature of the core shear behavior for core shear strains greater than 1%. Fatigue behavior of the panels also indicates clearly that the type of foam is critical when the panels are subjected to 2% core shear strain. For these reasons, the service load level should be limited to 1% core shear strain to prevent excessive deflection under the applied service load which could lead to failure. Based on the power law model for each specimen an equation for the average degradation for all panels loaded to 1% core shear strain, was formulated as follows:

$$\frac{\delta_{avg} - \delta_0}{\delta_0} = 0.0163 i^{0.1855}$$

Therefore, given the initial static displacement (δ_o), the average increased deflection (δ_{avg}) due to the degradation caused by the repeated service loading can be determined after any number of cycles (i) up to 1,000,000 cycles as demonstrated by the experimental results.

Degradation of the panels is caused by softening of the fiber insertion connections to the sandwich panel's skins. Originally the fiber connections can be considered to act as "fixed" connections; however, as the number of cycles increases the local matrix surrounding the connections starts to soften. The softened connections start to behave more like "pined" than "fixed" connections. Softening of the fiber insertion connections is caused by the initiation and propagation of microcracks in the fiber insertions at their connection to the sandwich panel's skins. The microcracks in the fiber insertions are caused by the crimped nature of the insertions at their connection. As the panels are loaded, the fibers engage and begin to straighten. The repeated bending and straightening of the fiber insertions allows the

microcracks to propagate and lead to rupture of the insertions. Cracking between the skin and insertion fibers may also lead to softening of the fiber insertion connections. It was found that panels constructed using 2 skin plies provided less "fixation" of the insertion connection causing a higher amount of degradation, over 25%, when subjected to the recommended 1% core shear strain service load maximum. To avoid any degradation greater than 25% for panels loaded a service load of 1% core shear strain the panels should have a minimum of 4 skin plies to provide proper connection between the skins. Also, it was determined that increasing the number of fipsi would enhance the composite action between the sandwich layers and reduce the amount of degradation.

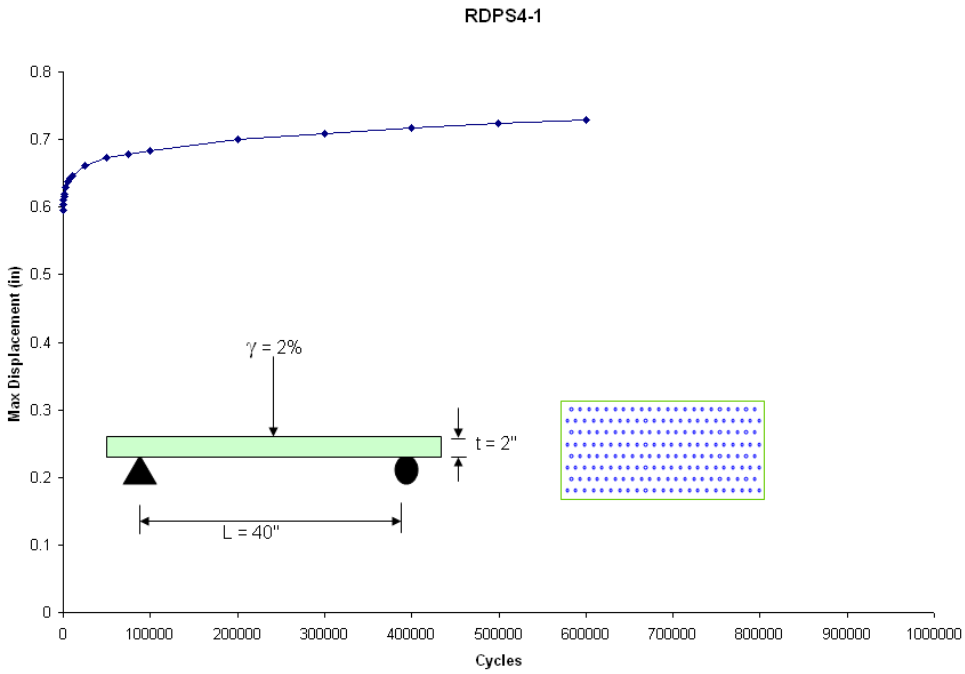

Figure 5.1 Maximum Displacement vs. Number of Cycles Typical

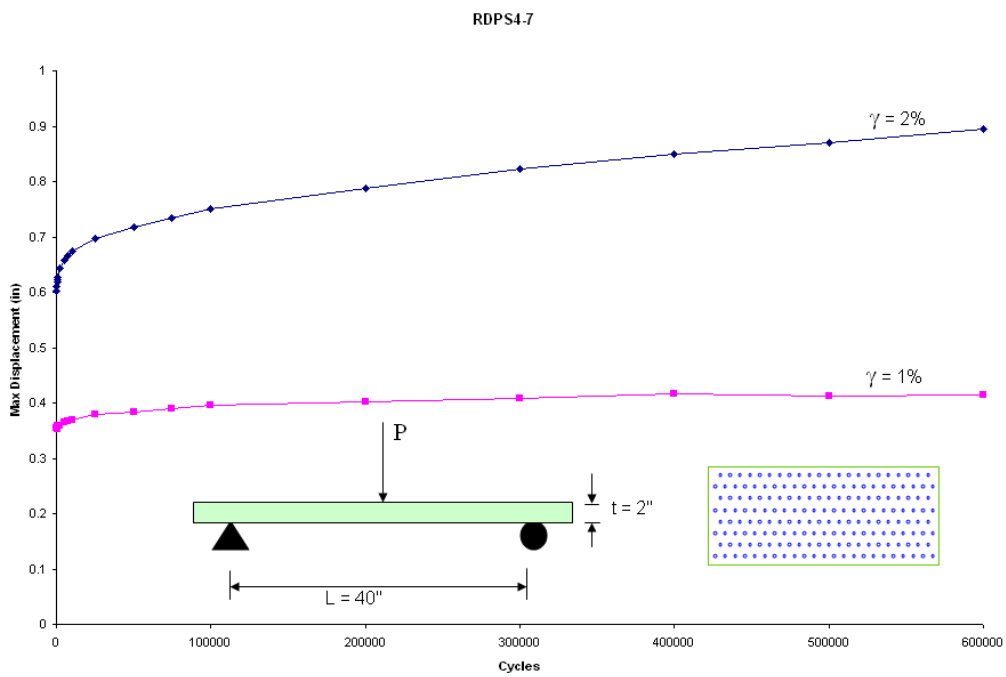

Figure 5.2 Constant Long-term Degradation

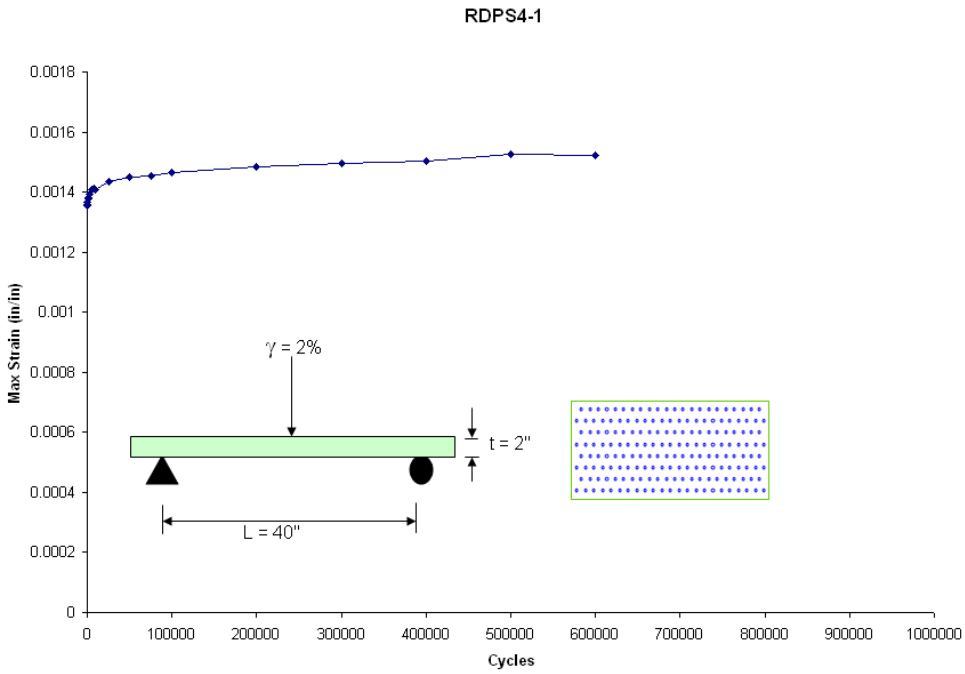

Figure 5.3 Maximum Strain vs. Number of Cycles Typical

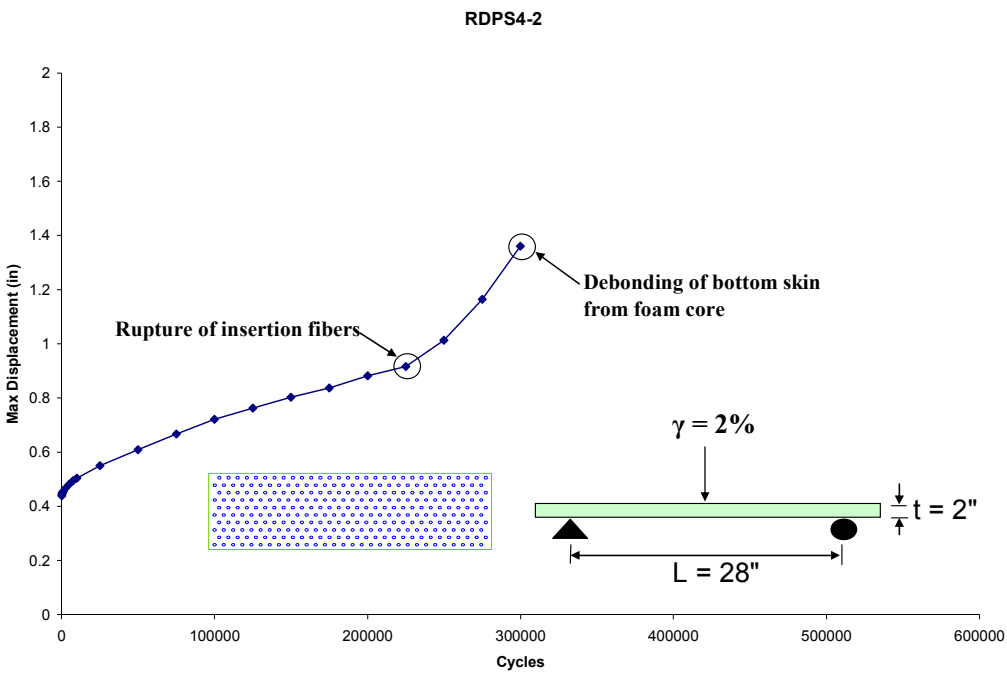

Figure 5.4 Maximum Displacement vs. # of Cycles Failure Specimen

Figure 5.5 Cracking first noticed at 6000 cycles

Figure 5.6 Cracking at 150,000 cycles

Figure 5.7 Cracking at 240,000 cycles

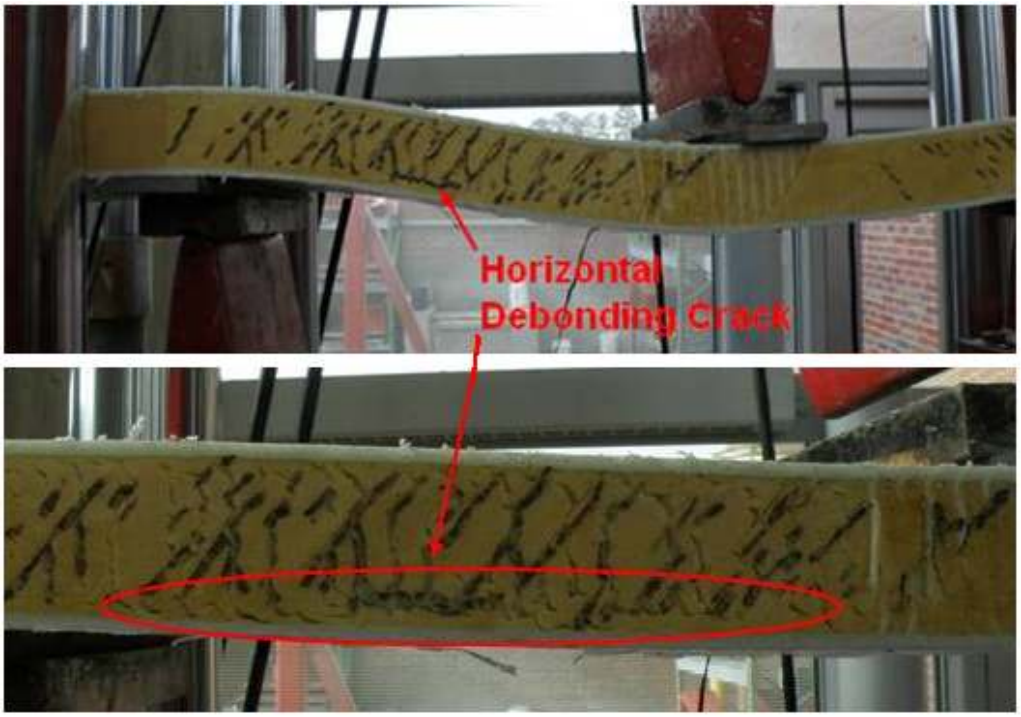

Figure 5.8 Cracking at 300,000 cycles

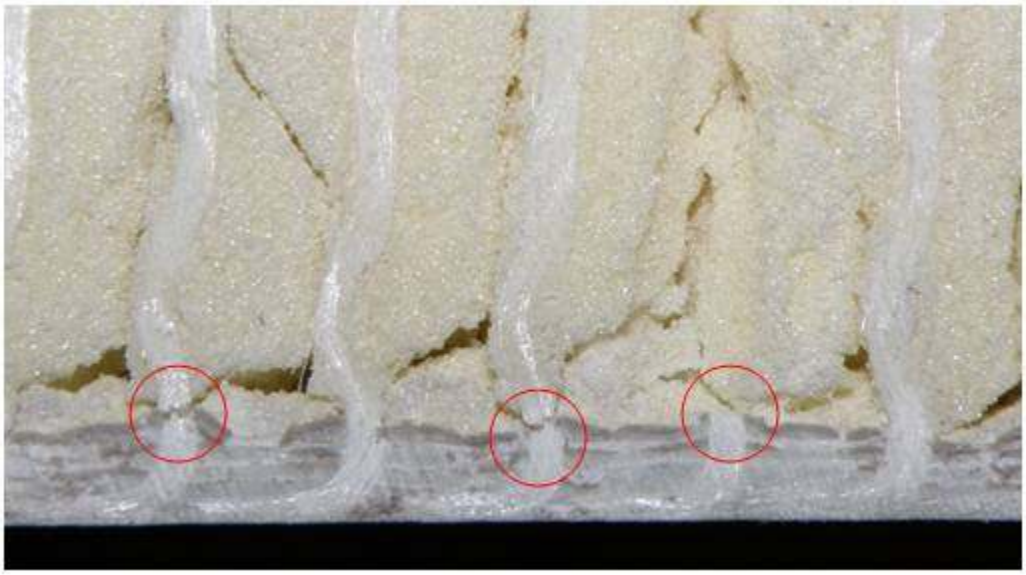

Figure 5.9 Rupture of Fiber Insertions at Connection

Table 5-1 Experimental Results for One-way Fatigue Testing

Loading	Span (in)	Pattern	Density (fipsi)	Specimen	Initial Max Deflection (in)	Final Max Deflection (in)
γ = 1%	28	Wall	8.53	FT-RDPS(3-5)-C	0.139	0.171
			7.59	FT-RDPS(3-6)-C	0.137	0.164
		Array	4	FT-RDPS(2-2-1)-C	0.174	0.237
				FT-RDPS(4-1)-C	0.178	0.226
				FT-RDPS(4-7)-C	0.201	0.232
			8	FT-RDPS(4-2)-C	0.195	0.222
	40	Wall	8.53	FT-RDPS(3-5)-B	0.353	0.402
			7.59	FT-RDPS(3-6)-B	0.337	0.377
		Array	4	FT-RDPS(2-2-1)-B	0.309	0.354
				FT-RDPS(4-1)-B	0.257	0.313
				FT-RDPS(4-7)-B	0.355	0.415
			8	FT-RDPS(4-2)-B	0.402	0.444
γ = 2%	28	Wall	8.53	FT-RDPS(3-5)-E	0.309	0.396
			7.59	FT-RDPS(3-6)-E	0.315	0.409
		Array	4	FT-RDPS(2-2-1)-E	0.373	0.527
				FT-RDPS(4-1)-E	0.346	0.409
				FT-RDPS(4-7)-E	0.436	0.570
			8	FT-RDPS(4-2)-E	0.439	1.360*
	40	Wall	8.53	FT-RDPS(3-5)-D	0.229**	0.246**
			7.59	FT-RDPS(3-6)-D	0.622	0.826
		Array	4	FT-RDPS(2-2-1)-D	0.639	0.829
				FT-RDPS(4-1)-D	0.596	0.729
				FT-RDPS(4-7)-D	0.601	0.910
			8	FT-RDPS(4-2)-D	0.631	1.827*

*** All final maximum deflections are for the 600,000th cycle, except specimen FT-(RDPS4-2)-D and FT-(RDPS4-2)-D which both failed around 300,000 cycles.**

**** Specimen FT-(RDPS3-5)-D was tested for a predicted core shear strain of 0.5% per the original testing program.**

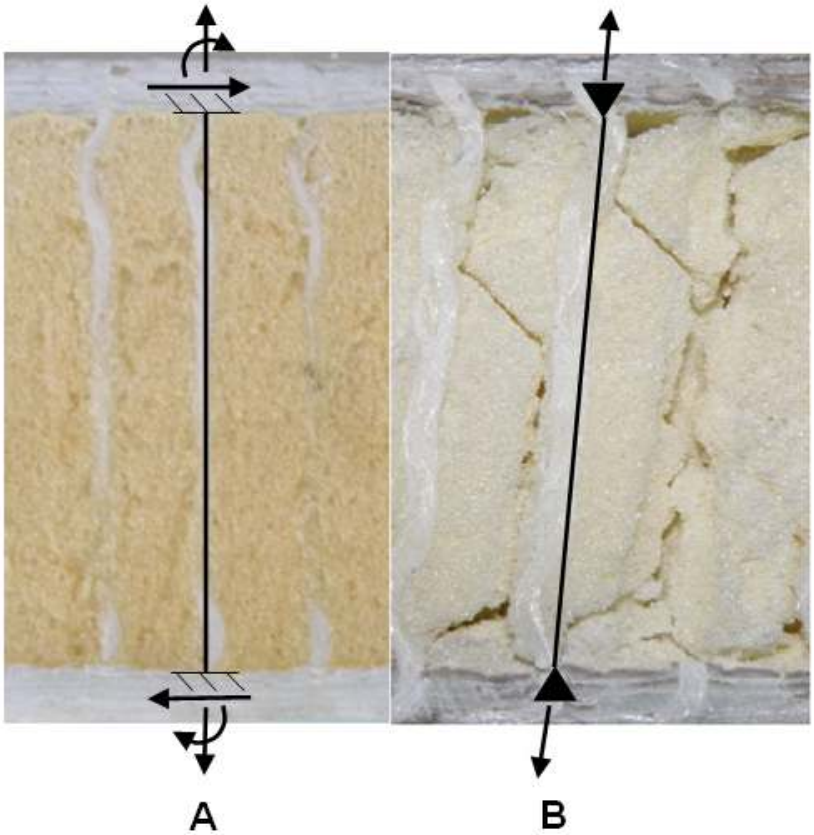

Figure 5.10 A) Original Insertion Connection B) Fatigued Insertion Connection

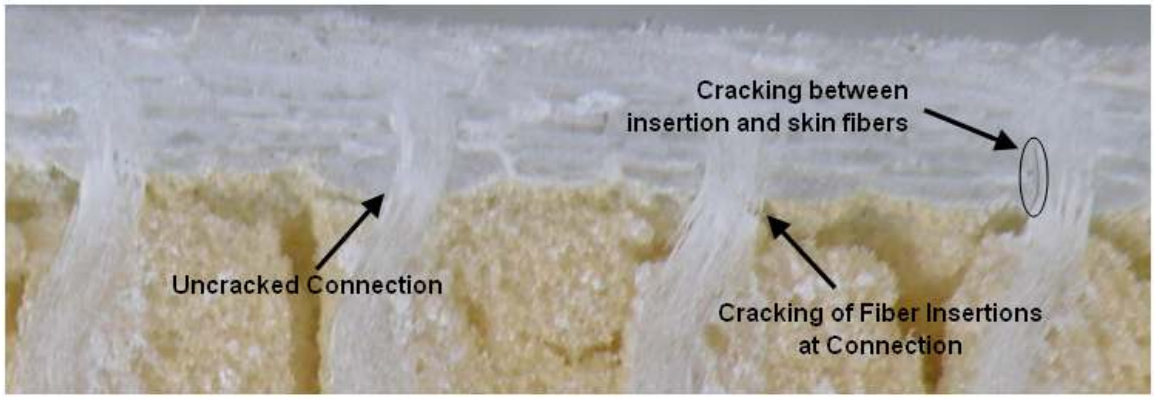

Figure 5.11 Cracking of fiber insertions at connection and

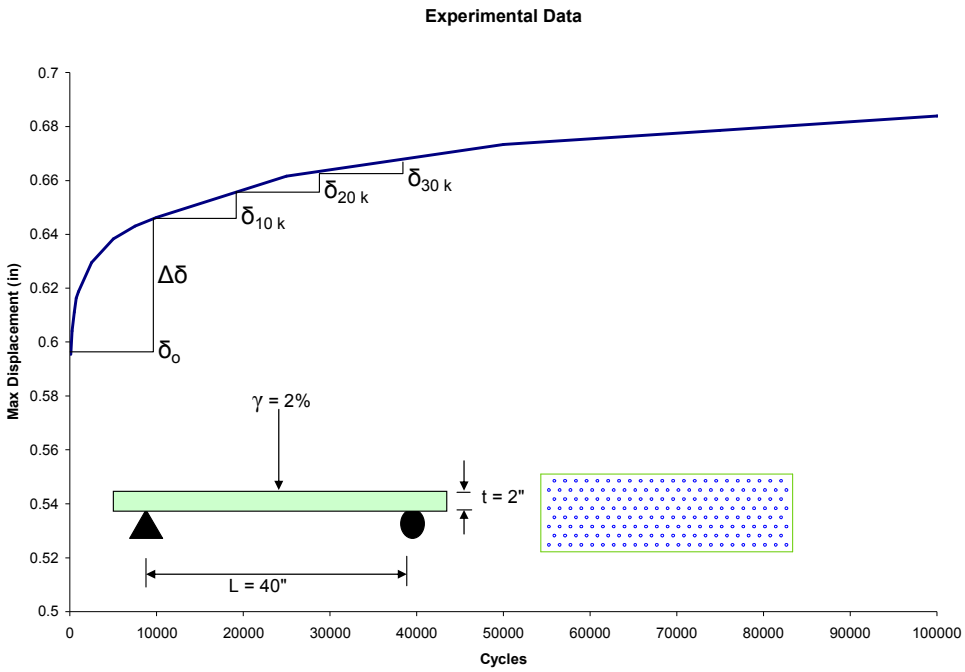

Figure 5.12 Initial Experimental Data

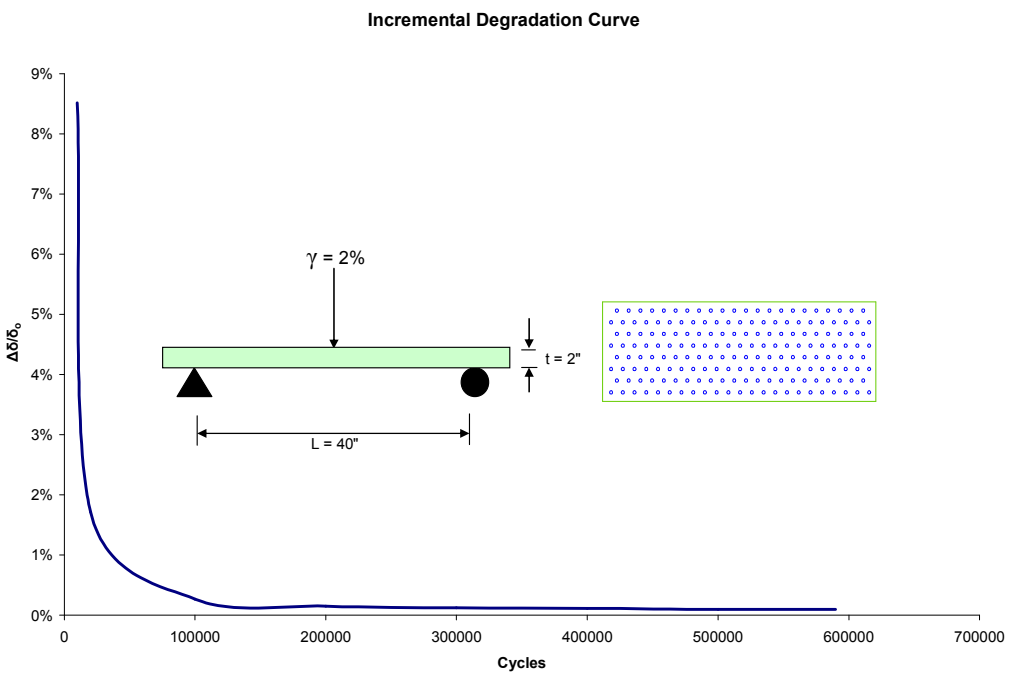

Figure 5.13 Incremental Degradation

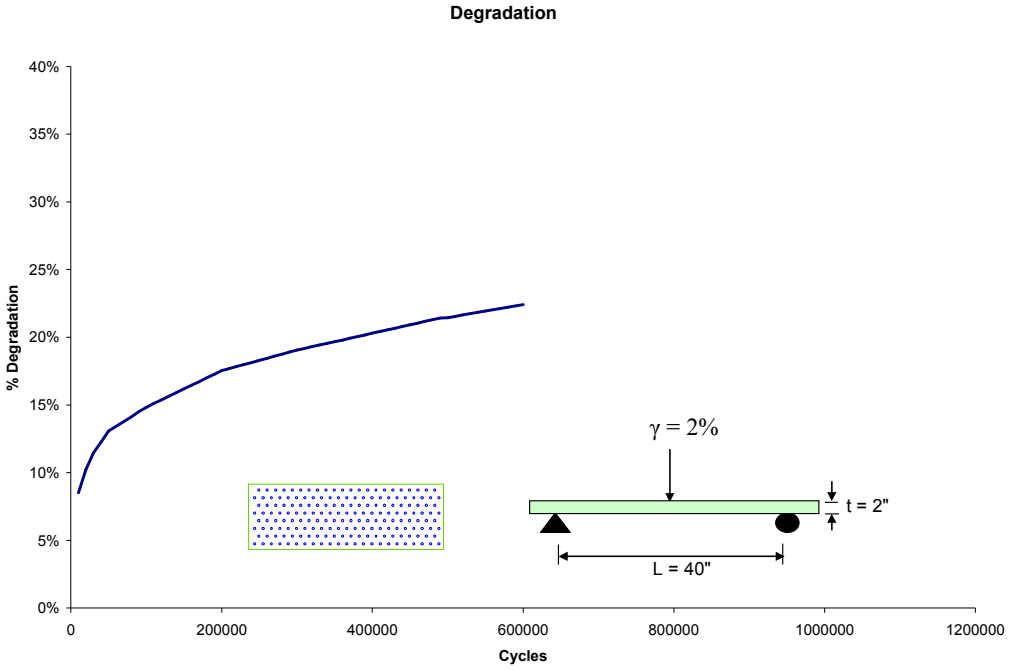

Figure 5.14 Degradation Data RDPS4-1

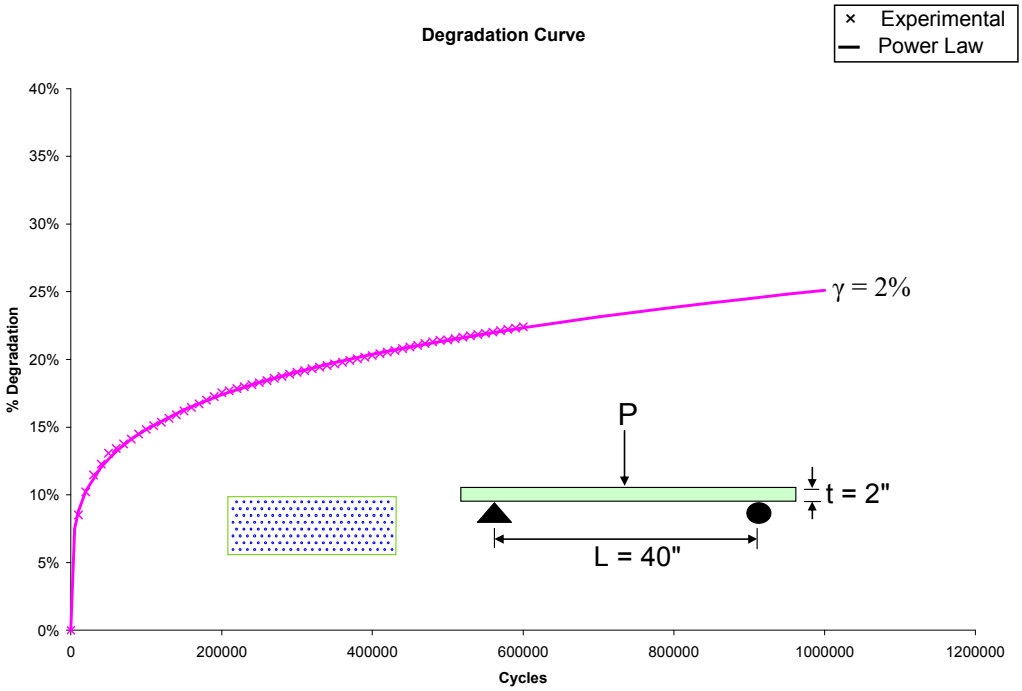

Figure 5.15 Degradation data extended to 1,000,000 cycle service life

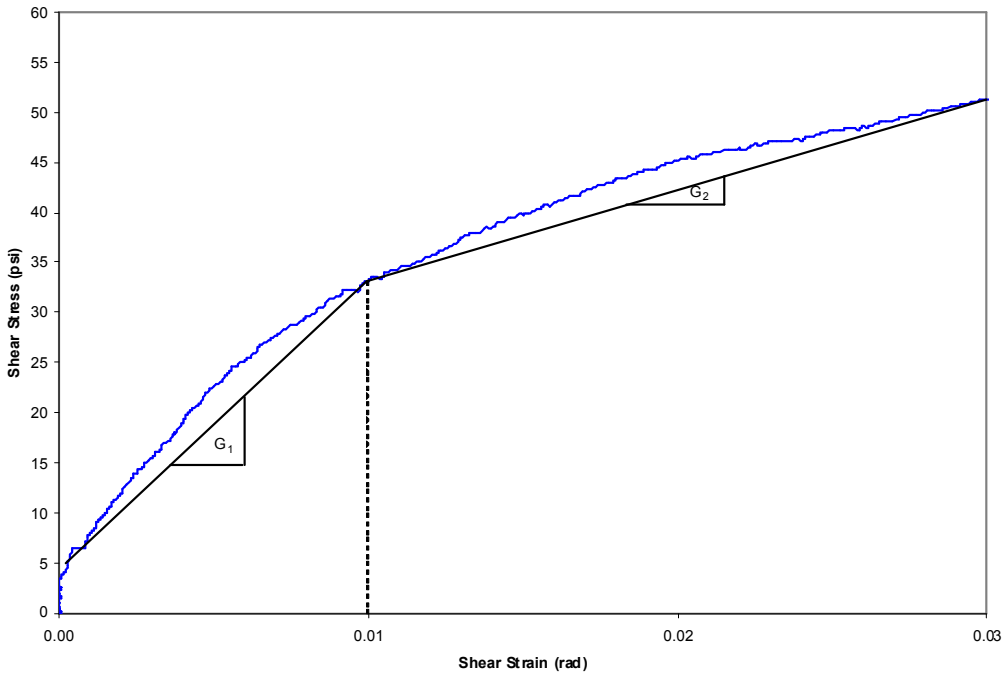

Figure 5.16 Initial Nonlinearity of Shear Behavior (Patrick, 2006)

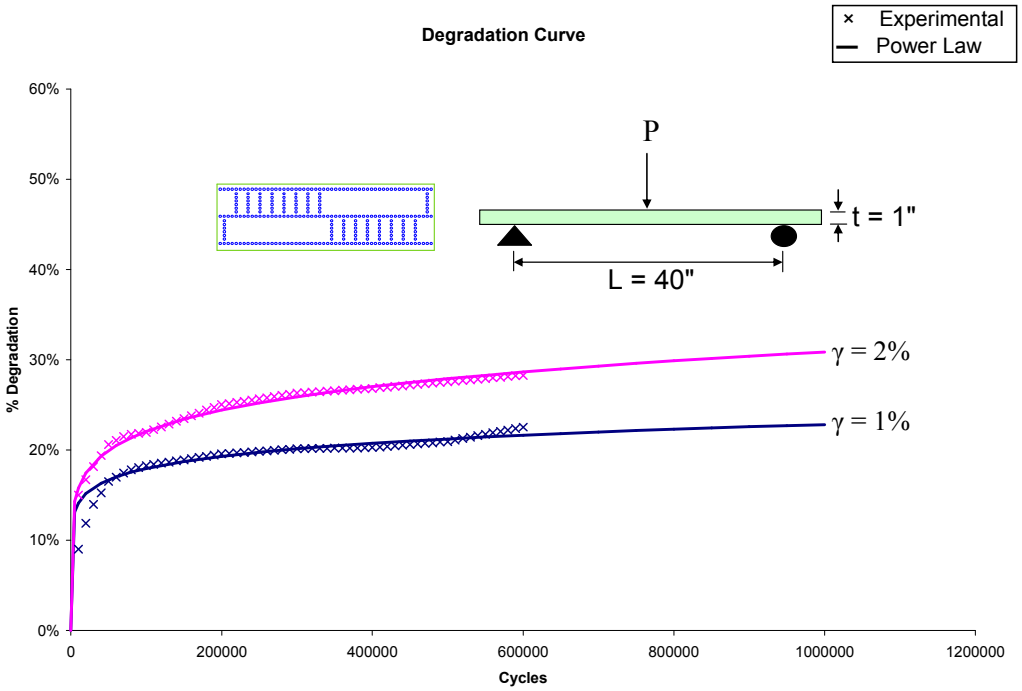

Figure 5.17 Degradation Loading Effect for RDPS3-5 Panels on 28" Span

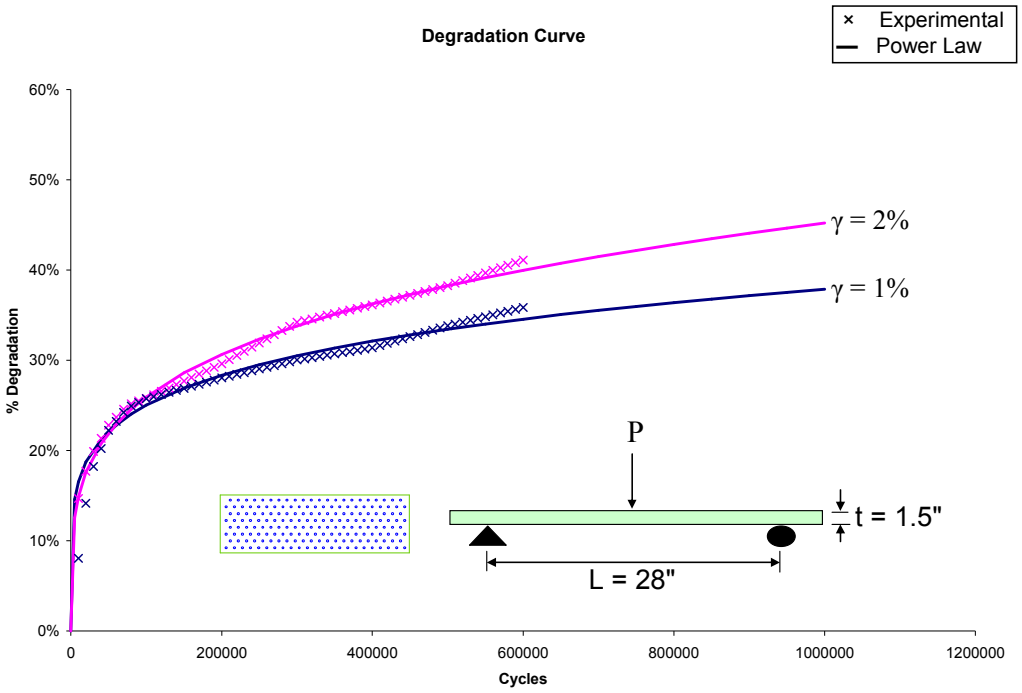

Figure 5.18 Degradation Loading Effect for RDPS2-2-1 Panels with 28" Span

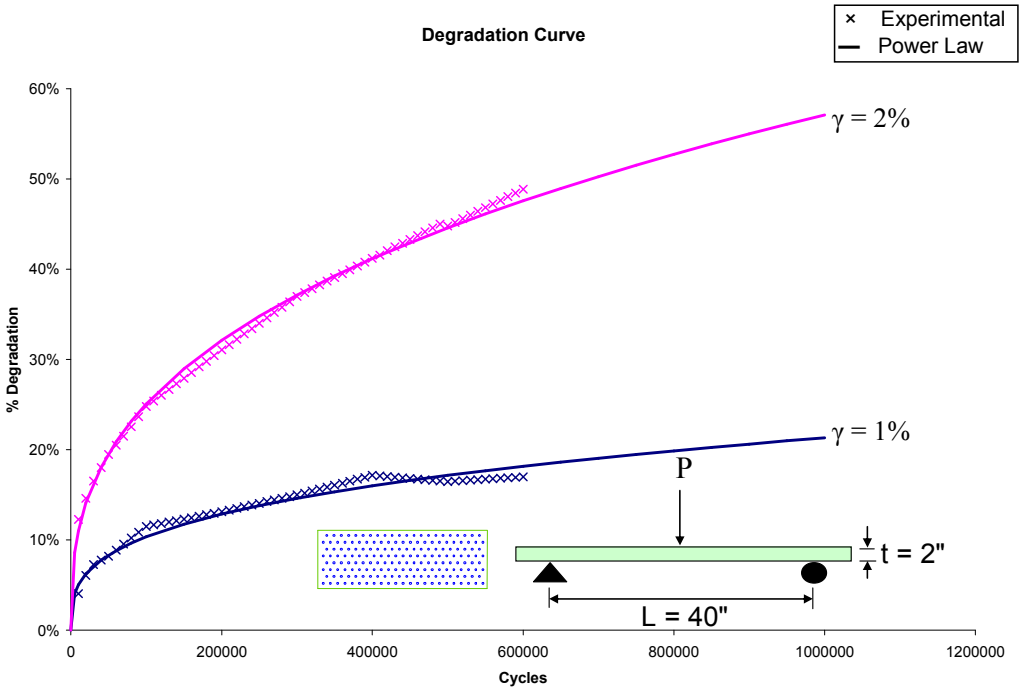

Figure 5.19 Degradation Loading Effect for RDPS4-7 with 40" Span

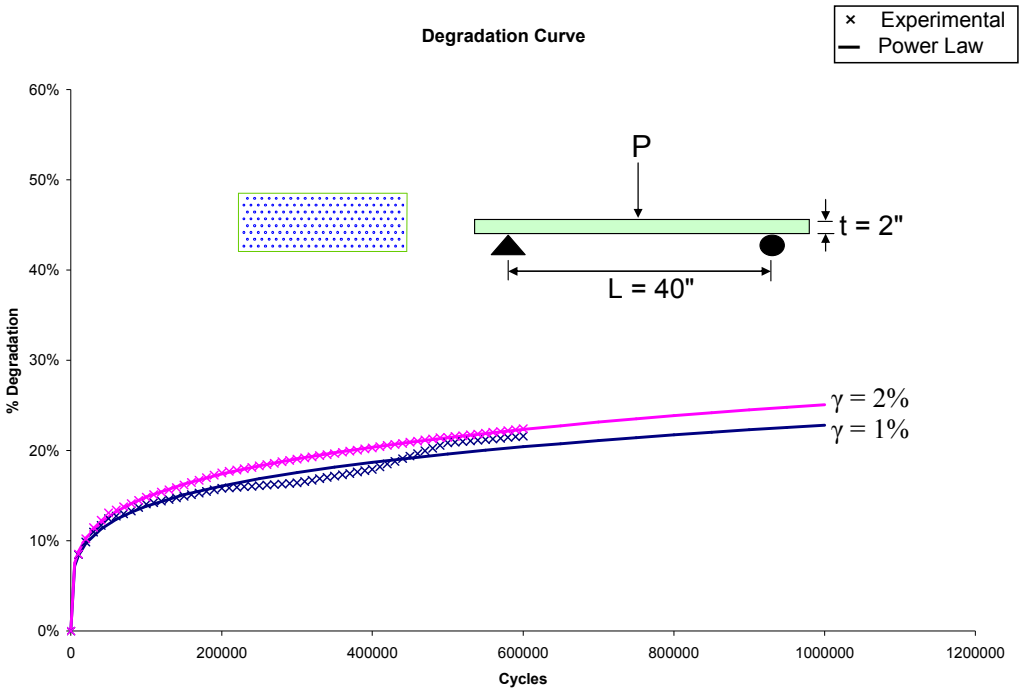

Figure 5.20 Degradation Loading Effect for RDPS4-1 with 40" Span

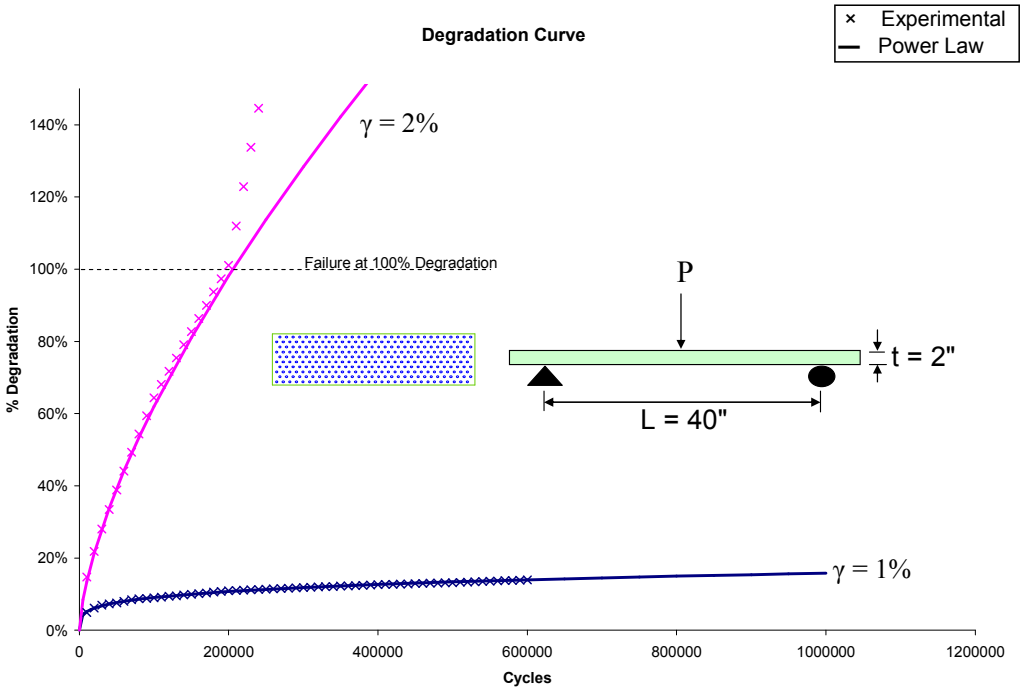

Figure 5.21 Degradation Loading Effect for RDPS4-2 with 28" Span

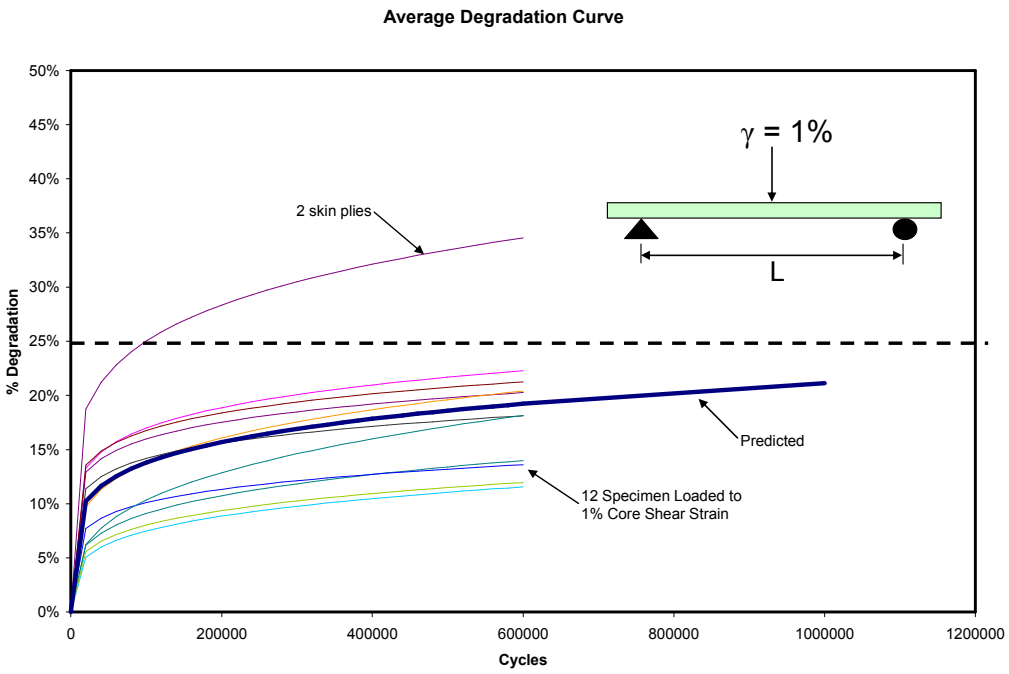

Figure 5.22 Predicted vs. Measured Degradation of 1% Shear Strain Loading

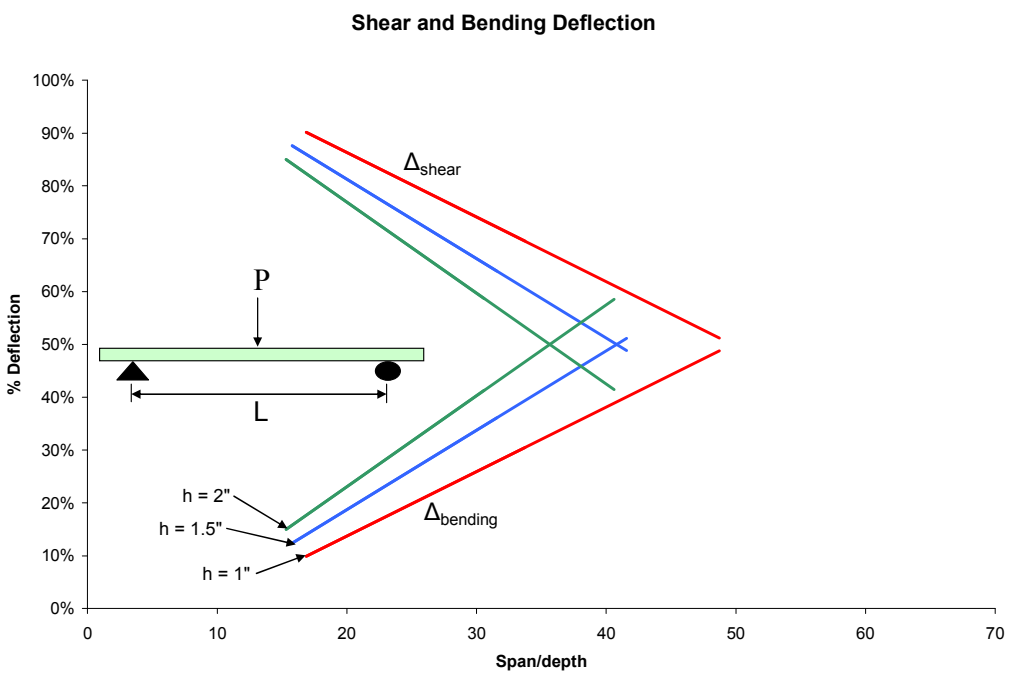

Figure 5.23 Theoretical Percentage of Bending and Shear Deflections

Table 5-2 Theoretical Percentage of Bending and Shear Deflections

Thickness	Span/Depth	$\%\Delta_B$	$\%\Delta_s$
1”	33.7	30%	70%
	48.2	47%	53%
1.5”	20.3	20%	80%
	29.0	34%	66%
2”	15.3	15%	85%
	21.9	26%	74%

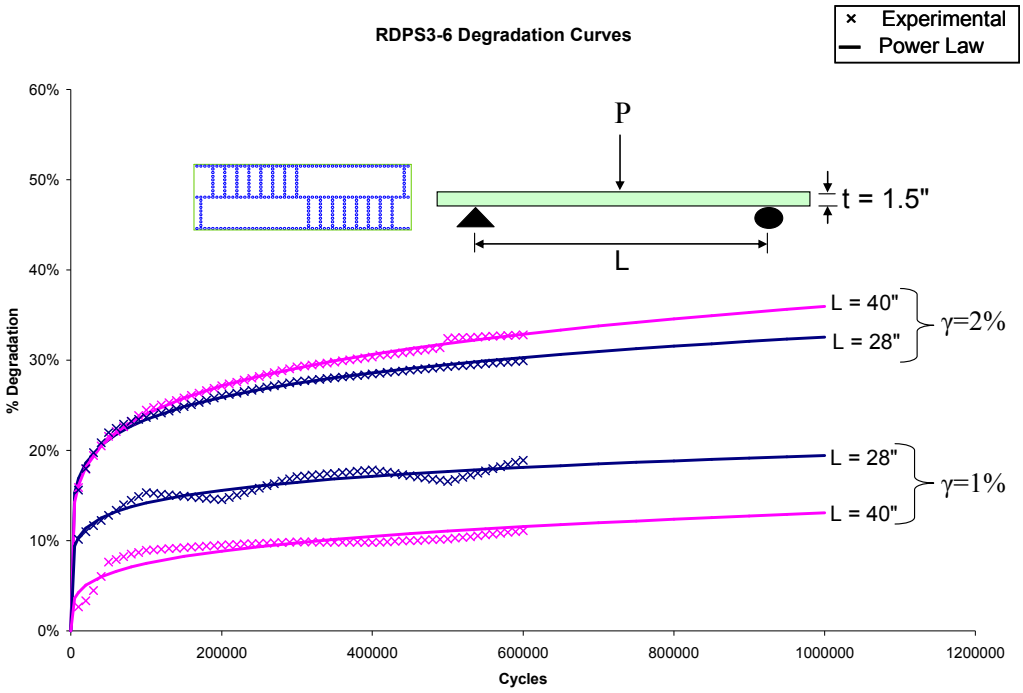

Figure 5.24 Degradation Span Effect for RDPS3-6 Panel

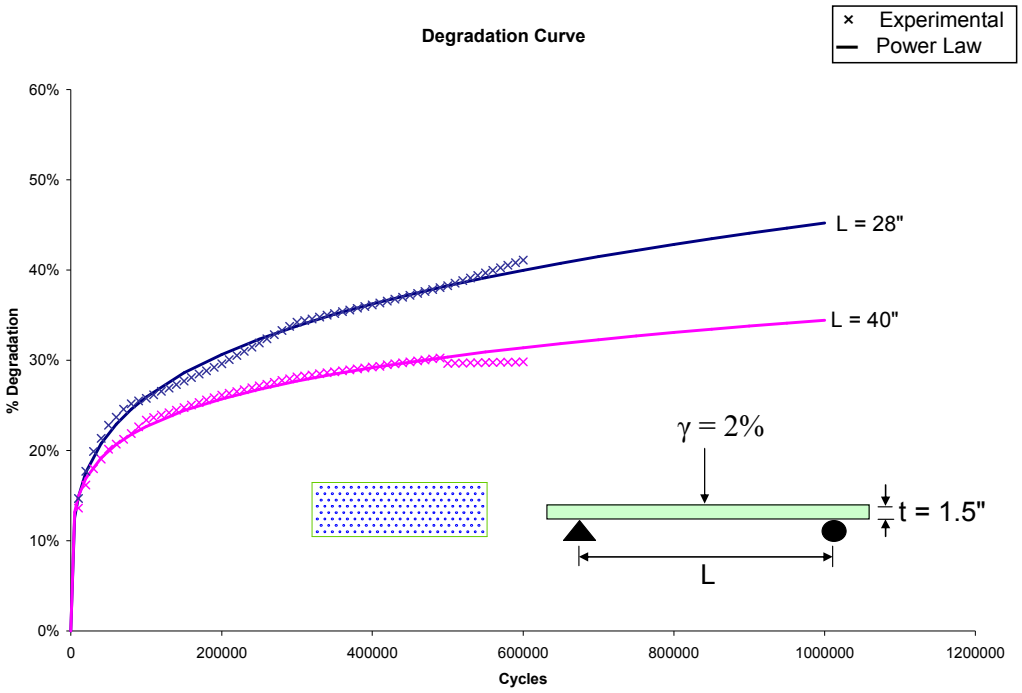

Figure 5.25 Degradation Span Effect for RDPS2-2-1 Panel γ_{core} = 2%

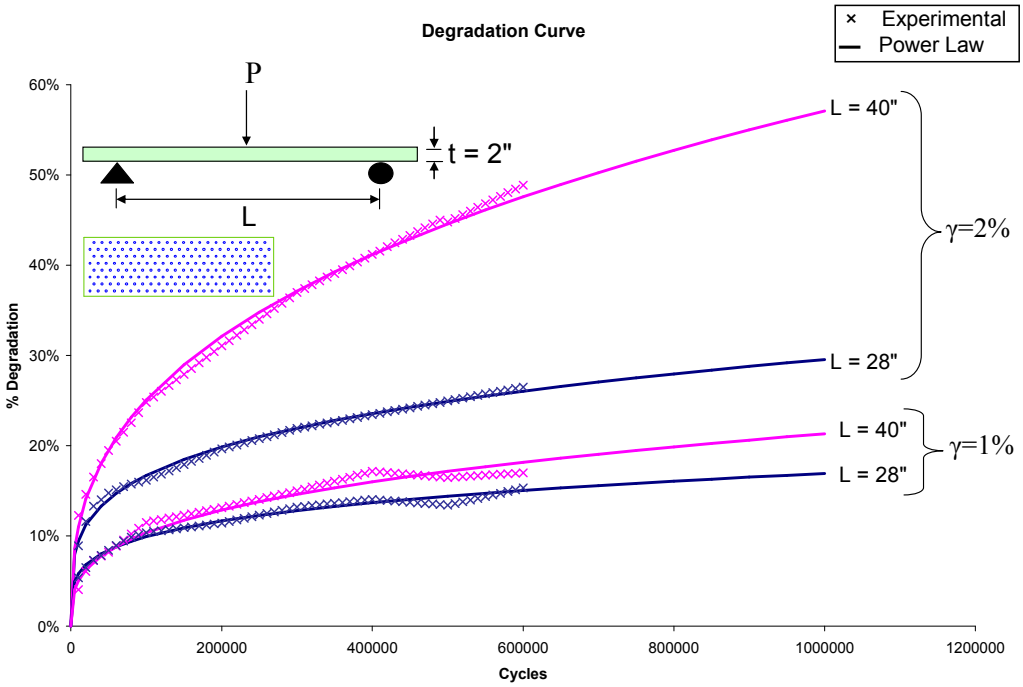

Figure 5.26 Degradation Span Effect for RDPS4-7 Panel

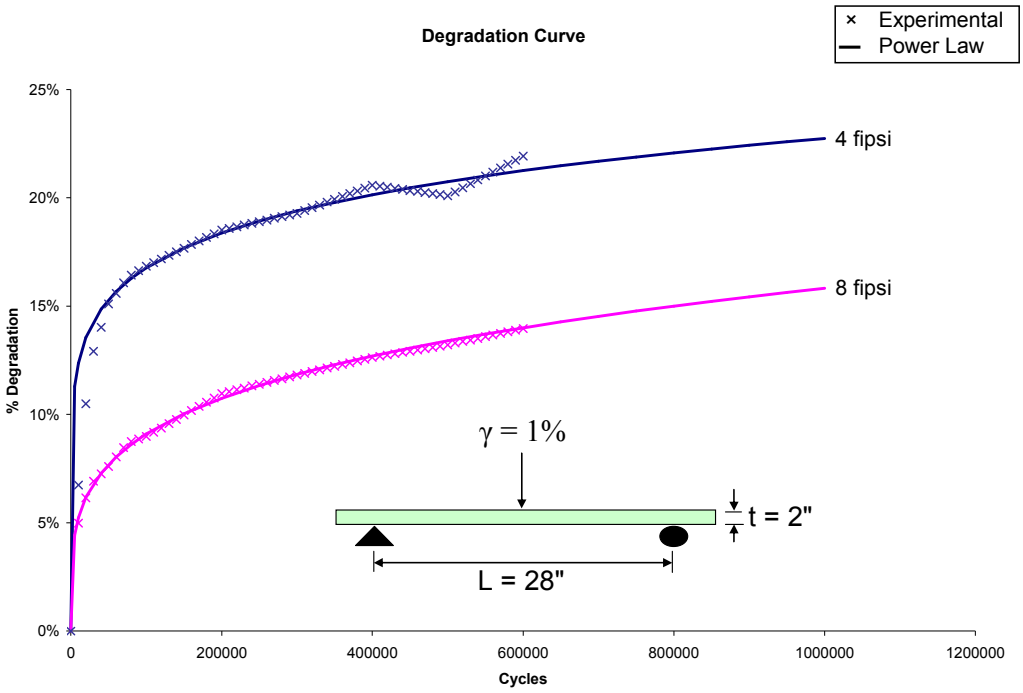

Figure 5.27 Degradation FIPSI Effect γ_{core} = 1%, L=28"

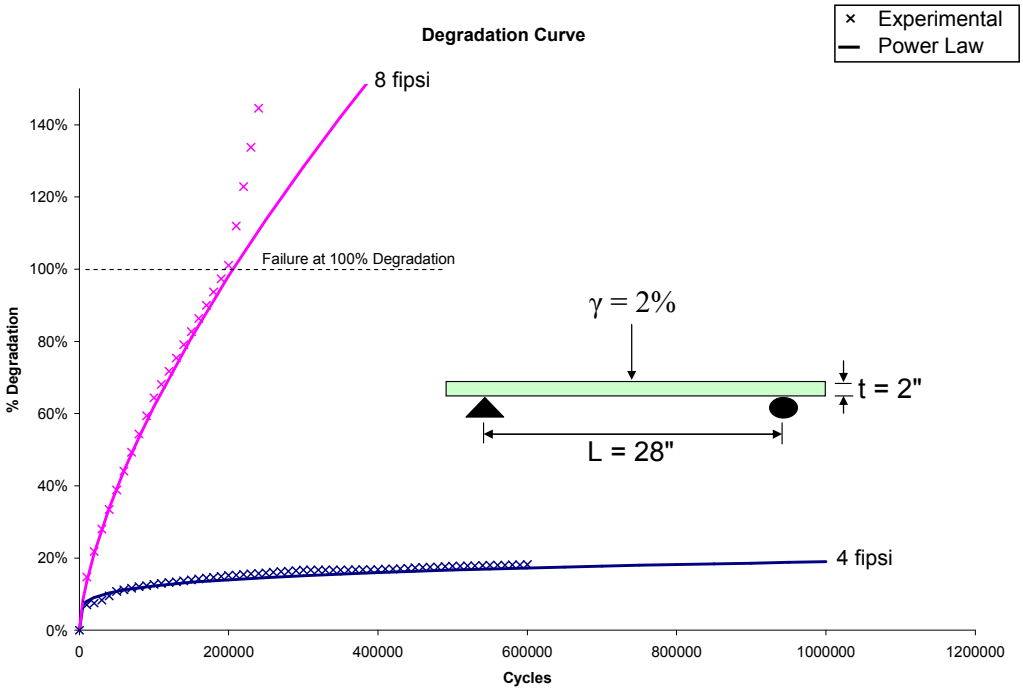

Figure 5.28 Degradation FIPSI Effect γ_{core} = 2%, L=28"

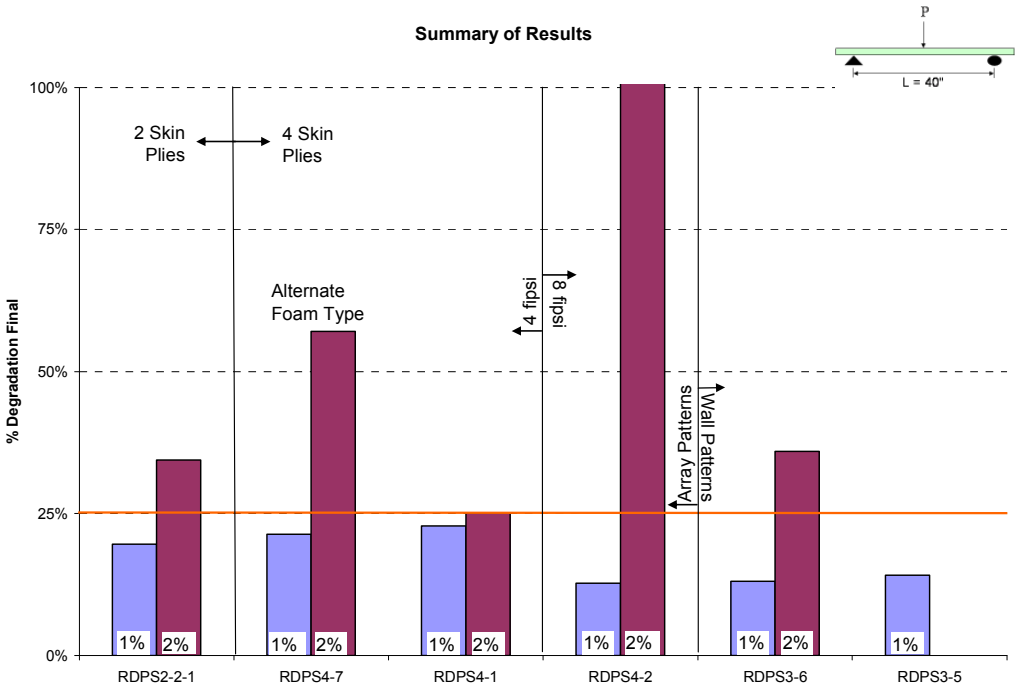

Figure 5.29 Summary of Fatigue Results L=40"

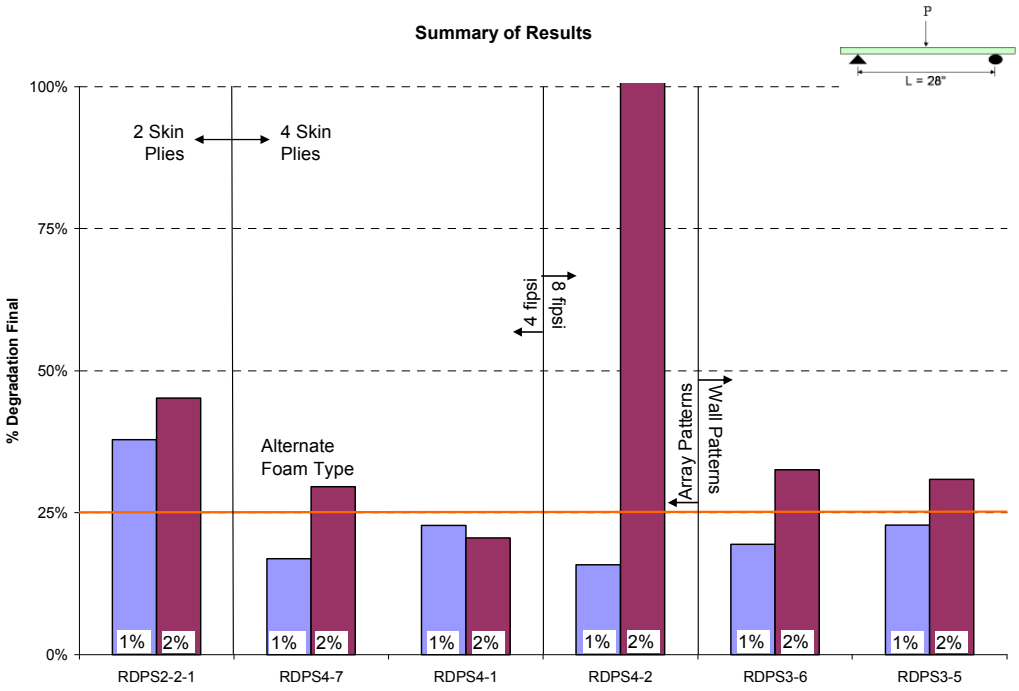

Figure 5.30 Summary of Fatigue Results L=28"

Chapter 6

6 Conclusions and Future Work

6.1 Conclusions

This research program investigates the structural behavior of the innovative 3-D GFRP pultruded sandwich panels in two-way action under static loading condition and one-way action under fatigue loading conditions. The research consists of an extensive experimental program complemented by analytical models to examine the panel's behavior. The main parameters considered in this study included: overall thickness, number of skin plies, insertion pattern and density, and foam type. Based on the scope of this research the following design considerations were drawn for the two-way bending behavior and fatigue performance of these types of sandwich panels.

6.1.1 Two-Way Behavior

The experimental program indicated that the tested panels exhibited a highly nonlinear load-deflection behavior under a two-way bending configuration. The observed nonlinear behavior of the sandwich panels subjected to two-way bending is affected by the development of membrane forces in the panel's skins. The membrane forces were developed due to the large deflection exhibited by the panel. The relative magnitude of the membrane forces is sensitive to the magnitude of the panel's deflection. For relatively small deflections the behavior is linear and governed by the flexural behavior. As the deflection becomes large the behavior becomes nonlinear and is significantly affected by membrane action. Failure of the panel was due to buckling of the edge of the panel at the support was observed due to the

compressive forces induced by the large deflections. Additional capacity of the panels could be developed by constraining the panel's edges in each vertical direction to prevent the buckling failure mode.

The research included a finite element analysis which was calibrated to predict the experimental results of the panels tested in two-way bending. The model was able to capture the nonlinear behavior, however, was not capable to capture the buckling failure mode. The calibrated FE model was utilized to study the effect of the parameters on the two-way bending behavior of the 3-D sandwich panels. Analysis of the test results showed that the panel thickness is linearly related to the total deflection of the sandwich panels at high load levels. The effect of the thickness can be increased by enhancing the composite action by increasing the core shear modulus through increased levels of fipsi. Also, the degree of nonlinearity of the load-deflection behavior due to membrane forces can be reduced by providing the panel with sufficient flexural and shear rigidity.

It was observed that increasing the amount of fipsi will increase the shear stiffness of the panel. However, the effect is negligible for thin panels since the behavior of the panel is governed by flexural and membrane action with little contribution from the shear behavior. As the panel thickness is increased, the relative contribution of the shear deformation increases. Therefore, increasing the core shear modulus by increasing the fiber insertion density has a more pronounced effect on the overall behavior of thicker panels. The results indicated also that the behavior is independent of the level of applied load.

The elastic modulus of the panel's skins can greatly affect the two-way bending behavior of the 3-D sandwich panels by increasing the flexural rigidity and effect of membrane action. The nonlinear relationship between in the skin stiffness and total deflection is due to the coupled effect of the skin stiffness on the bending and membrane behavior of the panel's skins, which is dependent on the applied load level. Also, the effect of the elastic modulus on the membrane behavior can be reduced by increasing the level of fipsi.

The analysis showed also that the aspect ratio of the 3-D sandwich panels subjected to two-way bending is linearly related to the panel's total deflection for aspect ratios between 1 and 2. Increasing the aspect ratio decreases the effect of membrane action and the behavior eventually reduces to the one-way behavior.

The FE model was also used to develop membrane action curves for the proposed design method. The proposed method is based on serviceability of the sandwich panels. The design uses Yen's linear solution for sandwich plate bending and the given membrane action curve to model the nonlinear load-deflection behavior of the panels. By using this method the total load required to achieve a given level of deflection can be calculated as:

$$P_{total} = \frac{1}{1 - \%P_{mem}} P_{bend}$$

where P_{total} is the predicted load due to plate bending and membrane action, $\%P_{mem}$ is the percentage of the total load resisted by membrane action for the given deflection from the membrane action curve, and P_{bend} is the load resisted by the flexural and shear rigidity of the

sandwich panel. This method offers sufficient accuracy and can be easily applied using spreadsheet software. It was determined that the span length of the square panels did not have a significant effect on the percentage of load carried by membrane action. Therefore, a single membrane action curve can be used to predict the behavior for a panel configuration with various span lengths. Increasing the aspect ratio of the panel significantly reduced the effect of membrane action since the behavior shifts toward one-way action.

6.1.2 Fatigue Performance Conclusions

The overall fatigue behavior of the sandwich panels subjected to service load levels suggests a high initial rate of degradation over the first 10,000 cycles. The rate of degradation decreases as the number of cycles is increased up to 100,000 cycles and remains at a low almost constant rate for the remainder of its service life. Degradation of the panel's material properties is due to the deterioration of the insertion's connection to the GFRP skins and a reduction of the shear modulus of the core due to the formation and propagation of microcracks. The condition of the softened connection is more similar to a "pinned" connection after the repeated loading than its original "fixed" state. Softening of the fiber insertions is caused by the propagation of microcracks in the insertions at their connection. The crimped nature of the insertions at their connection to the sandwich panel's skins causes the microcracks to form and the repetitive load causes accumulation of damage over time which can lead to failure of the panels subjected to high load levels.

Based on the findings of the experimental program, it was found that the fatigue performance of the 3-D GFRP sandwich panels is primarily affected by the intensity of the

applied shear stress and the panel's shear behavior. Under an applied load equivalent to 1% core shear strain the degradation is limited to 25% of the initial deflection. Increasing the applied load level to induce a shear strain of 2% resulted in a much higher level of degradation. This is due to the highly nonlinear nature of the localized shear stress-shear strain behavior of the core which resulted in localized strains much higher than predicted. The excessive shear strain induced in the panels significantly increased the percentage of degradation with respect to the initial deflection and the variability of the test results. Fatigue behavior of the panels also indicates clearly that the type of foam used to produce the core is critical when the panels are subjected to 2% core shear strain. Panels constructed using 2 skin plies provided less "fixation" of the insertion connection causing a higher amount of degradation, over 25%, when subjected to the 1% core shear strain service load. To avoid any degradation greater than 25% for panels loaded a service load of 1% core shear strain the panels should have a minimum of 4 skin plies to provide proper connection between the skins. Also, it was determined that increasing the number of fipsi would enhance the composite action between the sandwich layers and reduce the amount of degradation. By doubling the fipsi the average reduction in degradation was on the order of 35% for a 1% service loading condition. For these reasons, the service load level should be limited to 1% core shear strain to prevent any excessive deflection under the applied service load which could lead to failure. Based on the power law model for each specimen, an equation for the average degradation for all panels loaded to 1% core shear strain was formulated as follows:

$$\frac{\delta_{avg} - \delta_0}{\delta_0} = 0.0163 i^{0.1855}$$

Therefore, given the initial static displacement (δ_o), the average increased deflection (δ_{avg}) due to the degradation caused by the repeated service loading can be determined after the ith cycle.

6.2 Recommended Future Research

The present research answers several issues related to the structural behavior of the 3-D sandwich panels in question. However, it is the nature of research in general to always progress and inform. There are numerous ways in which this research could be extended and improved upon such that the innovative material can be more commonly used in practice.

Prediction of the buckling failure mode of the two-way bending specimens could be predicted using more advanced finite element techniques. The incorporation of the failure mode into the two-way design would allow engineers to design the panels for based on strength along with this proposed serviceability design method.

Further experimental investigation to determine the panel's various parameters affect on the overall fatigue performance of the sandwich panels. Based on the influence of parameters such as overall thickness, skin plies, insertion pattern, and insertion density the panels could be optimized for certain applications. Verification of the connection softening mechanism, which is believed to be the cause of the panels fatigue behavior, could be determined through small scale experimental testing of a singe insertion. It may also be applicable to apply multi-scale modeling to the sandwich panels. Small scale modeling of

the connection softening phenomenon could be used to verify the mechanism and then applied to large scale models predicting the panels fatigue performance.

A study of the impact behavior of the sandwich panels should be conducted since the panels can undergo significant deformation. Large deformation of the panels suggests high energy absorption capabilities and a potential market for them in infrastructure blast protection and transportation crash safety.

Preliminary test results indicate that the incorporation of transverse shear webs in the core of the sandwich panel significantly increase the panel's resistance to shear deformation. The shear webs are constructed using the same GFRP material as the panel's skins and are similar in shape to metal decking. The webs are adhesively bonded to each skin and filled with foam and mechanically anchored using the GFRP fiber insertions. Incorporation of the shear webs makes these sandwich panels a much more viable option for other structural applications such as structural decking, temporary mats, and truck trailer components in which serviceability of the panels is critical.

REFERENCES

Allen, H. G., and Feng, Z., Classification of Structural Sandwich Panel Behavior, Mechanics of Sandwich Structures, Kluwer Academic Publishers, 1998.

Allen, Howard G., Analysis and Design of Structural Sandwich Panels, Pergamon Press, Oxford, 1969.

Bitzer, Tom, Honeycomb Technology, Chapman and Hall, London, 1997.

Boresi, Arthur P., and Richard J. Schmidt. Advanced Mechanics of Materials, Sixth Edition. New York, NY: John Wiley and Sons, Inc., 2003.

Brebbia, C. A., and W. P. Wilde. High Performance Structures and Materials II. Boston, Mass: WIT Press, 2004.

Davies, J. M. Lightweight Sandwich Construction. Malden, MA: Blackwell Science, Inc., 2001.

Kim, Jongman, and Stephen R. Swanson. "Design of Sandwich Structures for Concentrated Loading." Composite Structures 52 (2001): 365-373.

Marguerre, Karl, and Hans-Theo Woernle. Elastic Plates. Waltham, Mass.: Blaisdell Publishing Company, 1969.

Meyer-Piening, H. R., and Dan Zenkert. Sandwich Construction 5 Volume II. United Kingdom: Engineering Materials Advisory Services LTD, 2000.

Patrick J. F., "Fundamental Characteristics of 3-D GFRP Pultruded Sandwich Panels." Master's Thesis, North Carolina State University, Raleigh, North Carolina. 2005.

Plantema, Frederik K. Sandwich Construction, the Bending and Buckling of Sandwich Beams, Plates, and Shells. New York, NY: John Wiley and Sons, Inc., 1966.

Reis, E. M., "Characteristics of Innovative 3-D FRP Sandwich Panels for Transportation and Civil Infrastructure." Ph.D. Dissertation, North Carolina State University, Raleigh, North Carolina. 2005.

Shenoi, R. A., H. G. Allen, and S. D. Clark. "Cyclic Creep and Creep-Fatigue Interaction in Sandwich Beams." Journal of Strain Analysis 32.1 (1997).

Swanson, Stephen R. "Response of Orthotropic Sandwich Panels to Concentrated Loading." Journal of Sandwich Structures and Materials 2 (2000): 270-287.

Timoshenko, S., and J. N. Goodier. Theory of Elasticity. New York, NY: McGraw-Hill Book Company, Inc., 1951.

Timoshenko, S., and S. Woinowsky-Krieger. Theory of Plates and Shells. New York, NY: McGraw-Hill Book Company, Inc., 1959.

Ugural, Ansel C. Stresses in Plates and Shells, Second Edition. Boston, Mass: McGraw-Hill Book Company, Inc., 1999.

Yen, Juo T., and Frederick V. Pohle. Deflections of a Simply Supported Rectangular Sandwich Plate Subjected to Transverse Loads. Washington: NACA, 1951.

Zenkert D., The Handbook of Sandwich Construction, Chameleon Press Ltd, London, United Kingdom, 1997.

APPENDICES

APPENDIX A

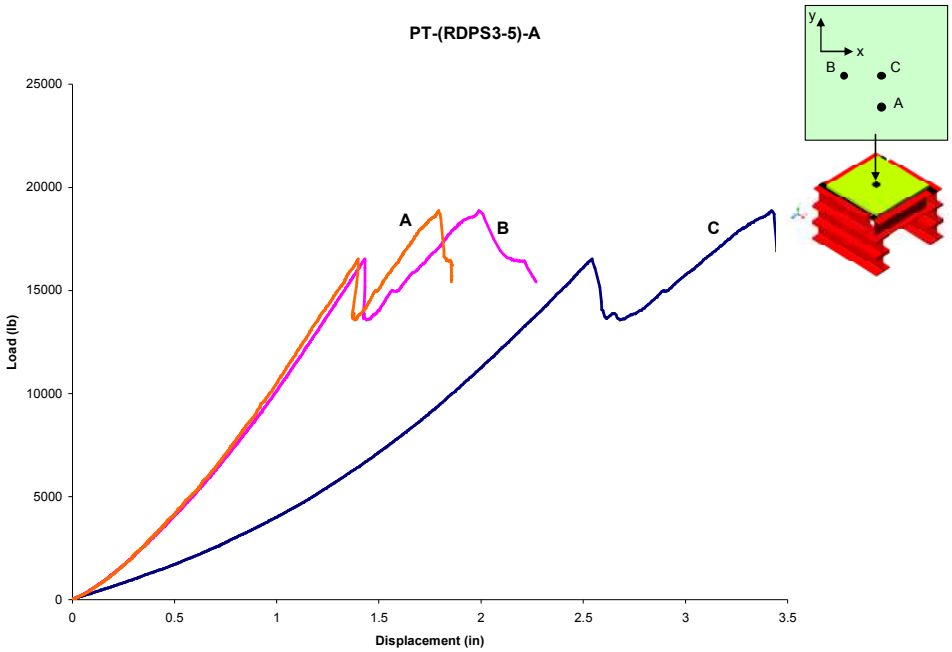

Figure A.1 Two-Way Load vs. Displacement RDPS3-5

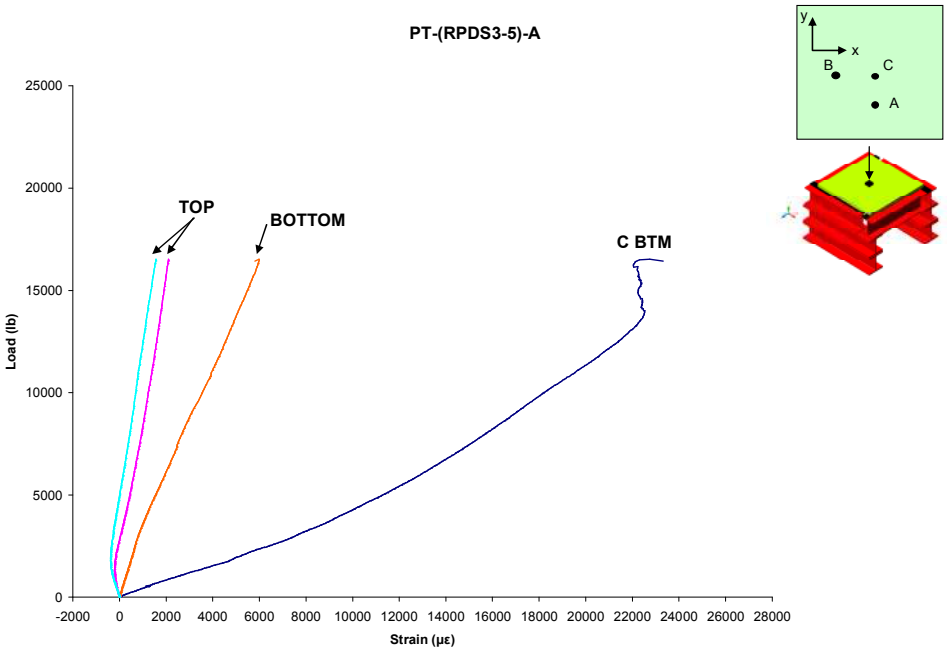

Figure A.2 Two-Way Load vs. Strain RDPS3-5

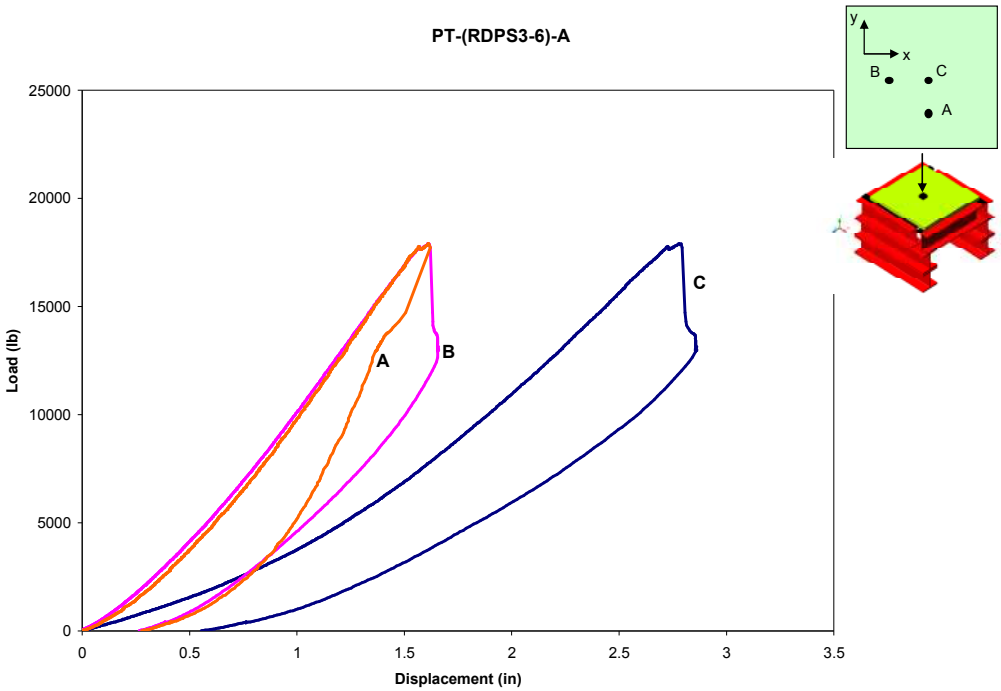

Figure A.3 Two-Way Load vs. Displacement RDPS3-6

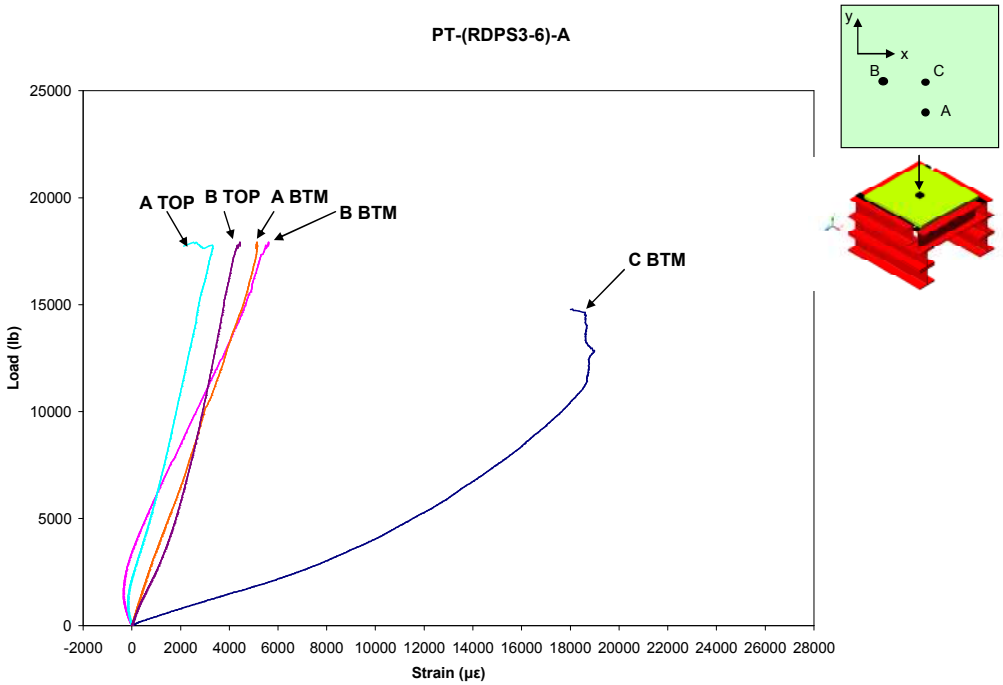

Figure A.4 Two-Way Load vs. Strain RDPS3-6

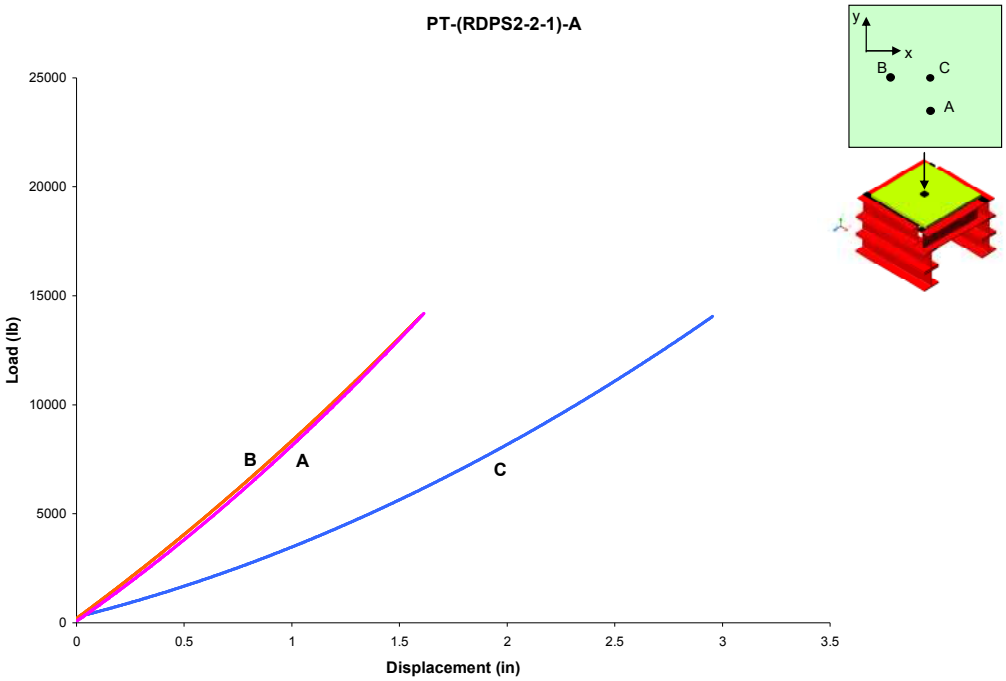

Figure A.5 Two-Way Load vs. Displacement RDPS2-2-1

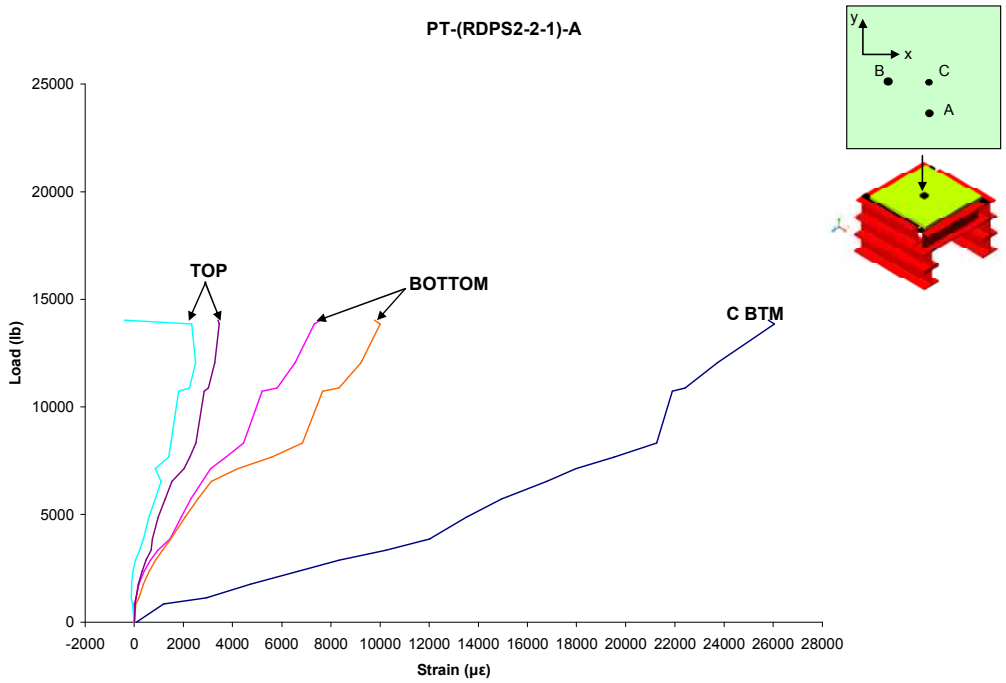

Figure A.6 Two-Way Load vs. Strain RDPS2-2-1

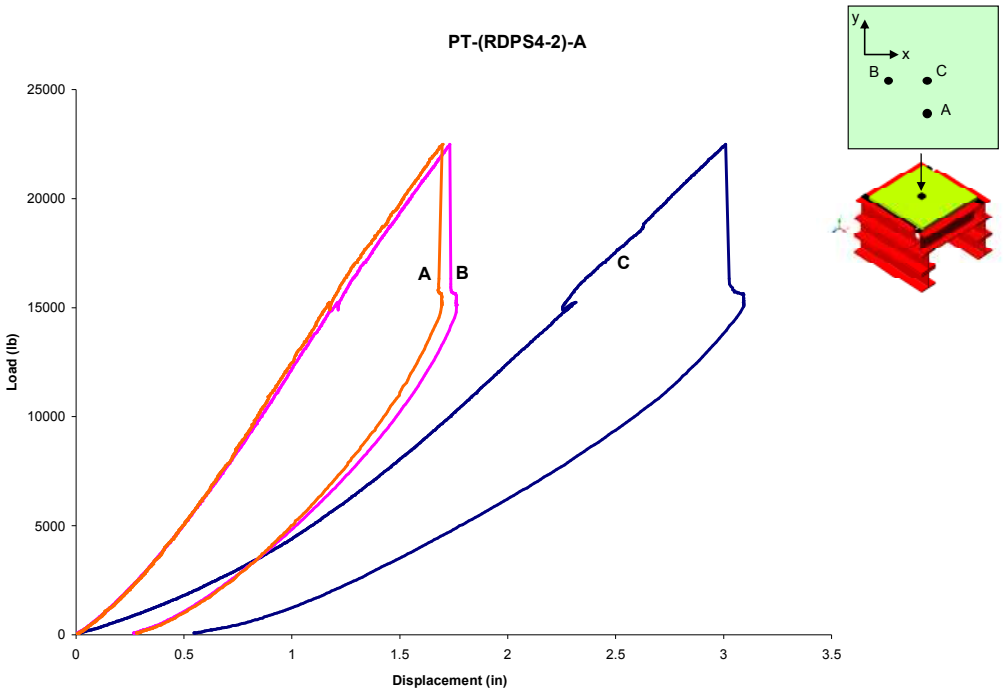

Figure A.7 Two-Way Load vs. Displacement RDPS4-2

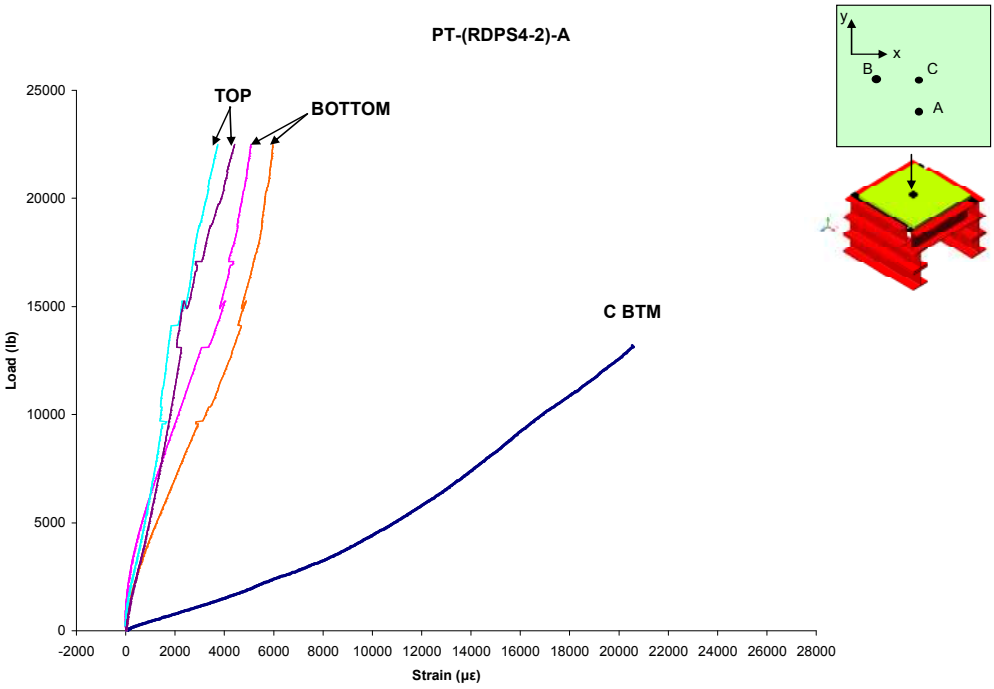

Figure A.8 Two-Way Load vs. Strain RDPS4-2

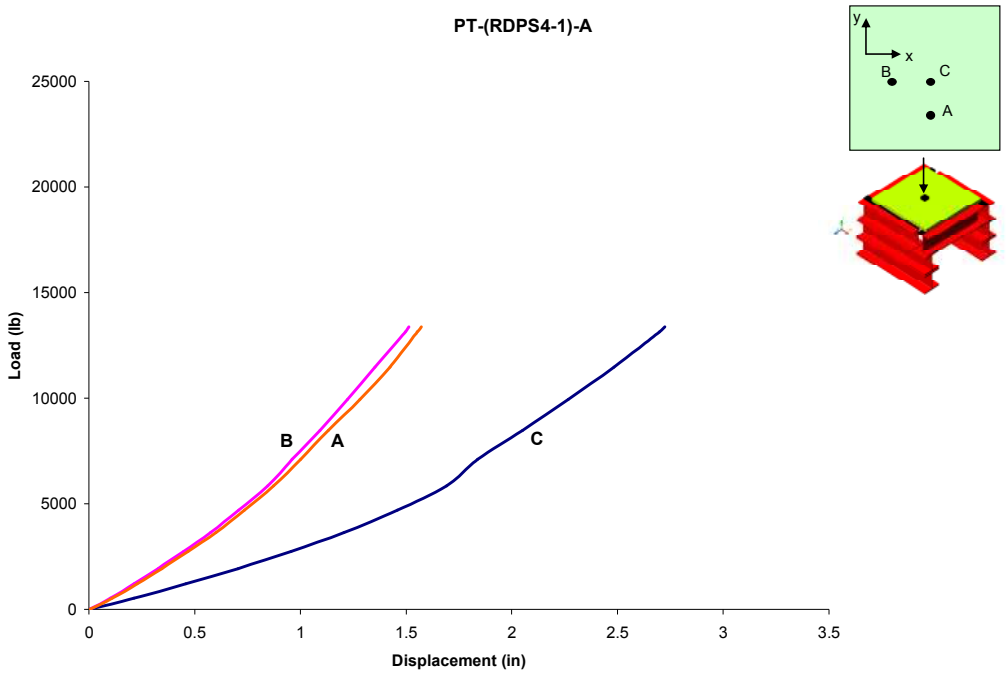

Figure A.9 Two-Way Load vs. Displacement RDPS4-1

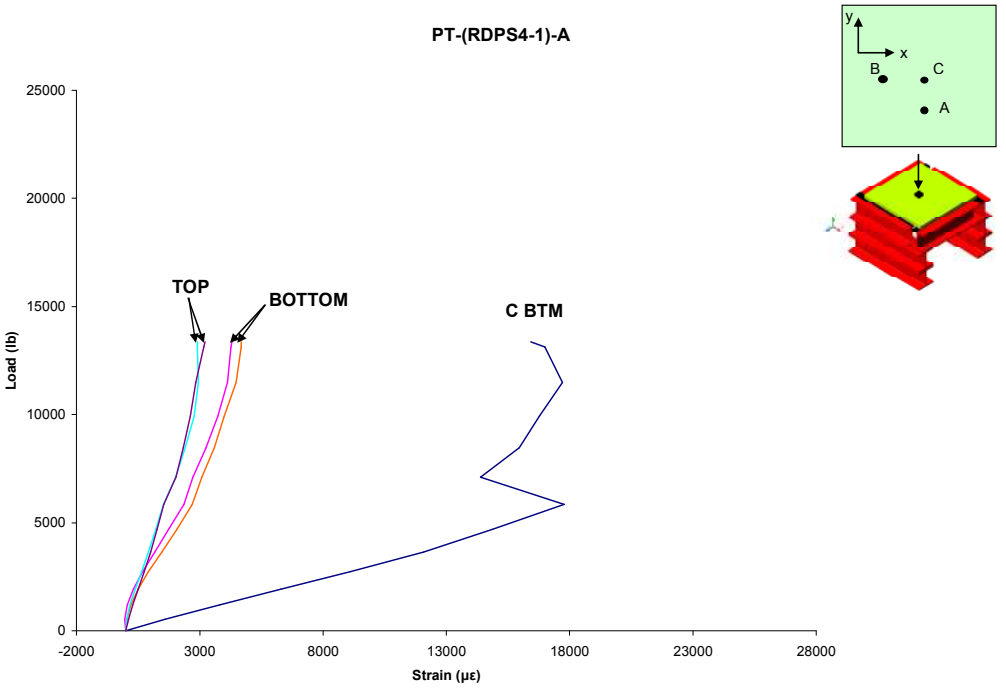

Figure A.10 Two-Way Load vs. Strain RDPS4-1

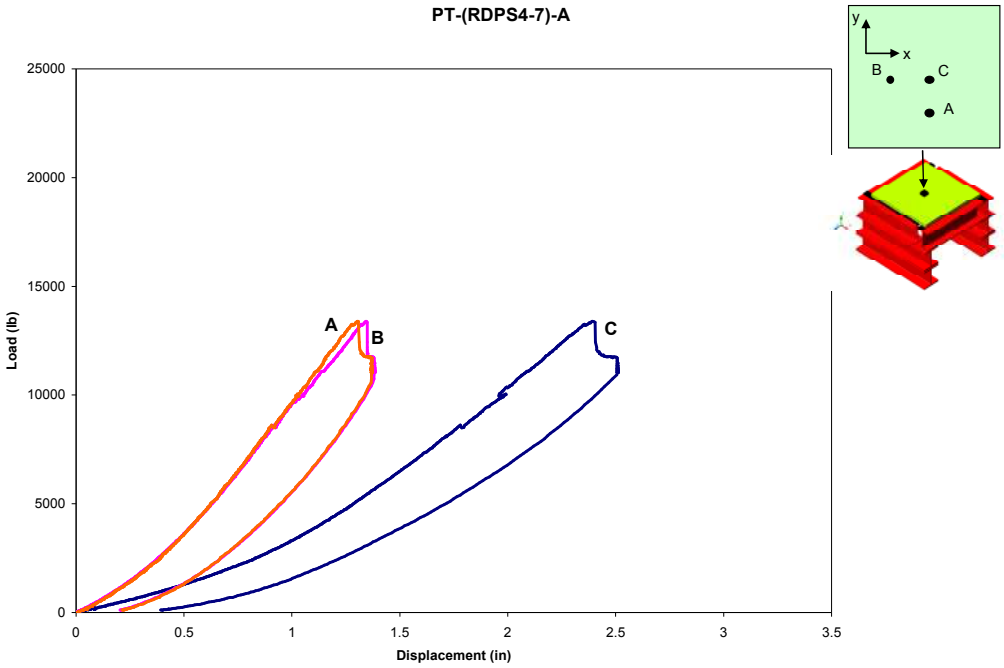

Figure A.11 Two-Way Load vs. Displacement RDPS4-7

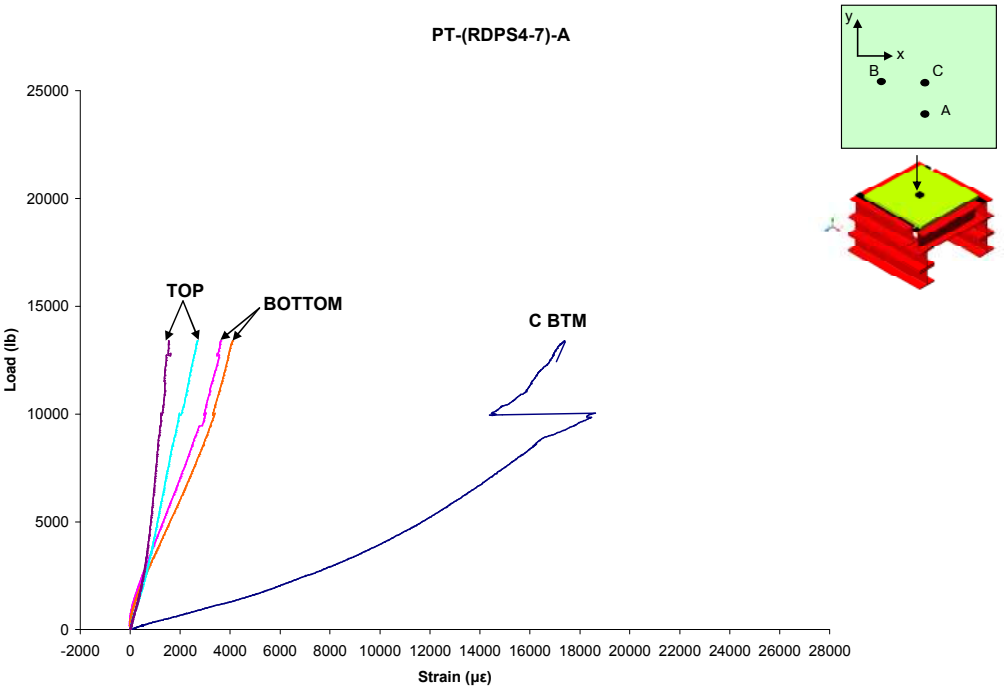

Figure A.12 Two-Way Load vs. Strain RDPS4-7

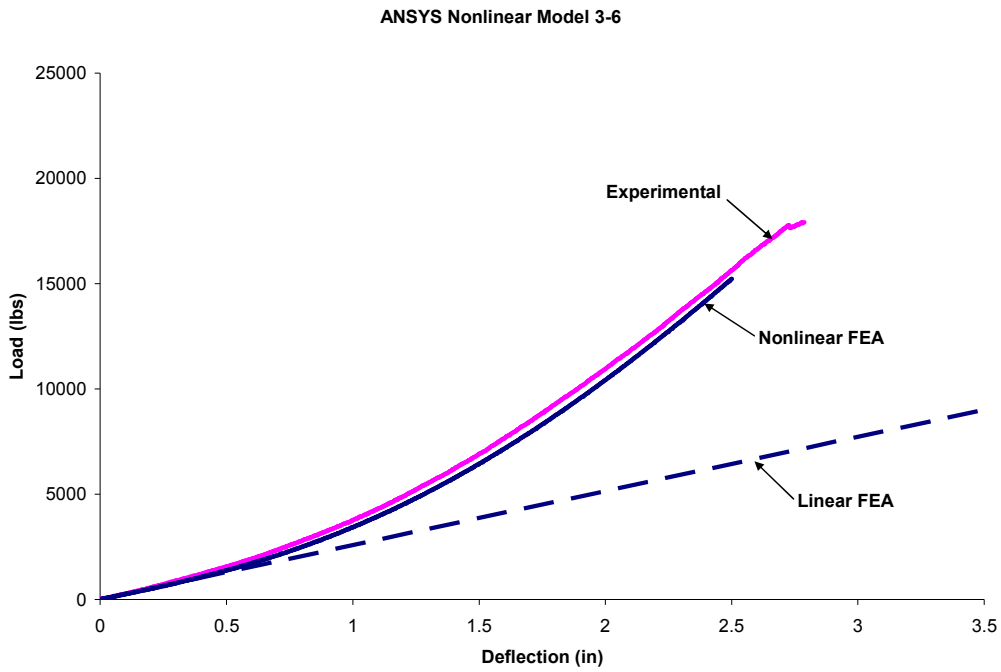

Figure A.13 Nonlinear ANSYS Model for the RDPS3-6 Panel

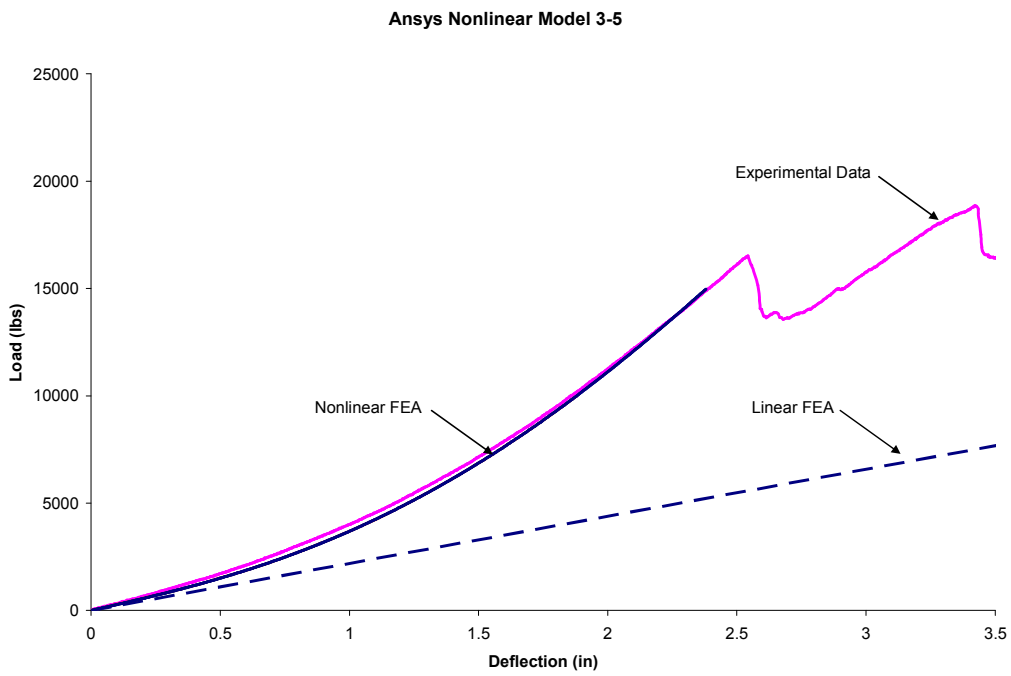

Figure A.14 Nonlinear ANSYS Model for the RDPS3-5 Panel

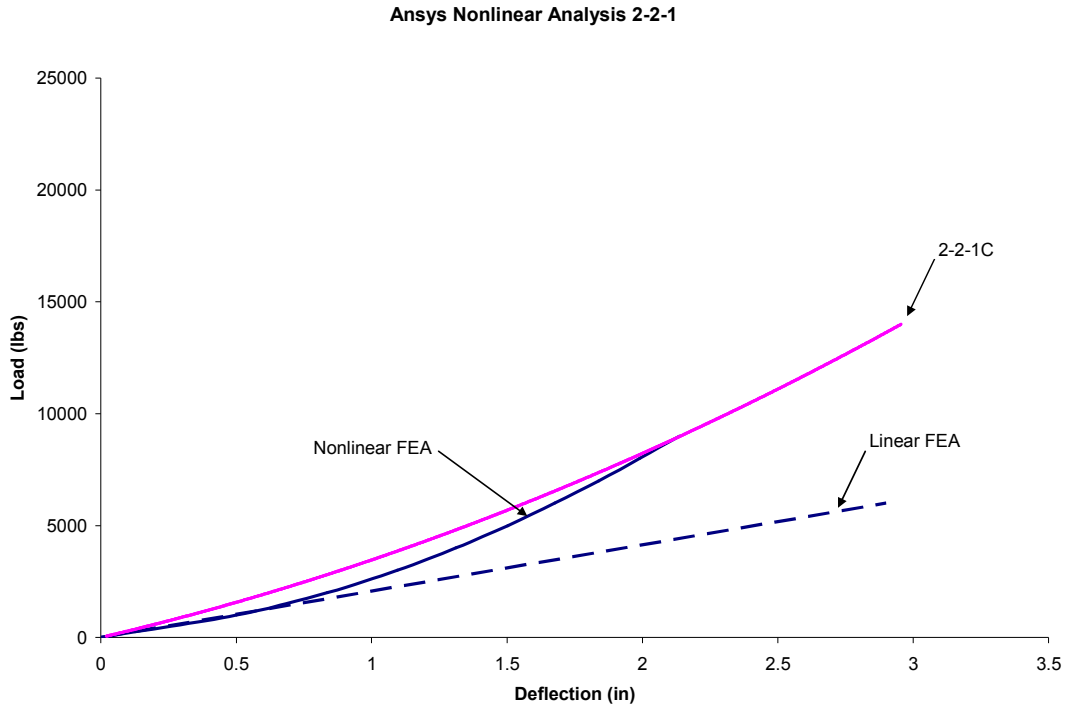

Figure A.15 Nonlinear ANSYS Model for the RDPS2-2-1 Panel

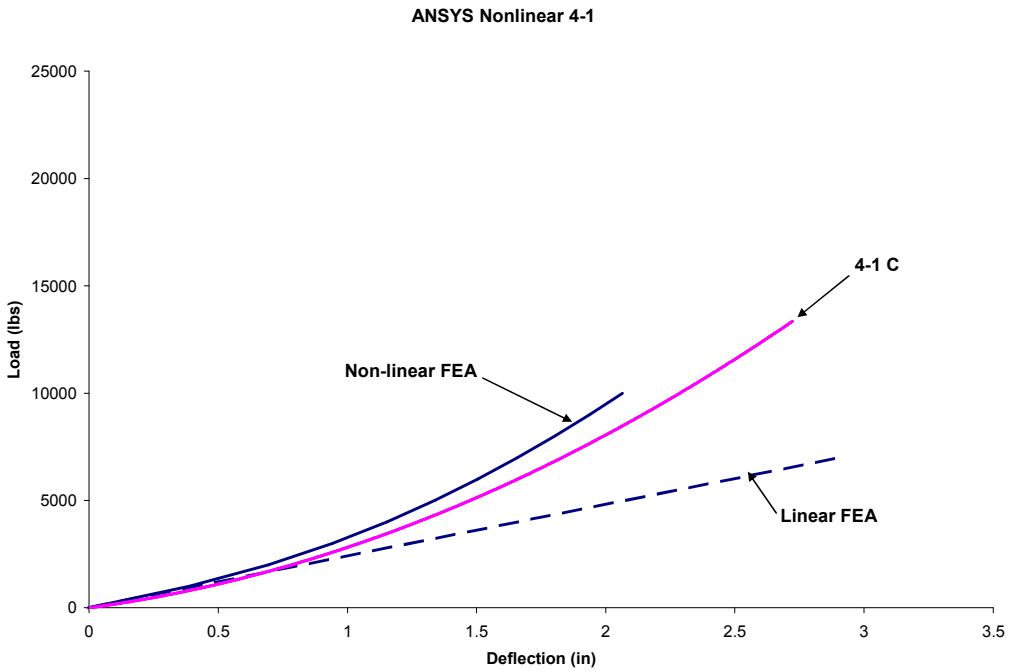

Figure A.16 Nonlinear ANSYS Model for the RDPS4-1 Panel

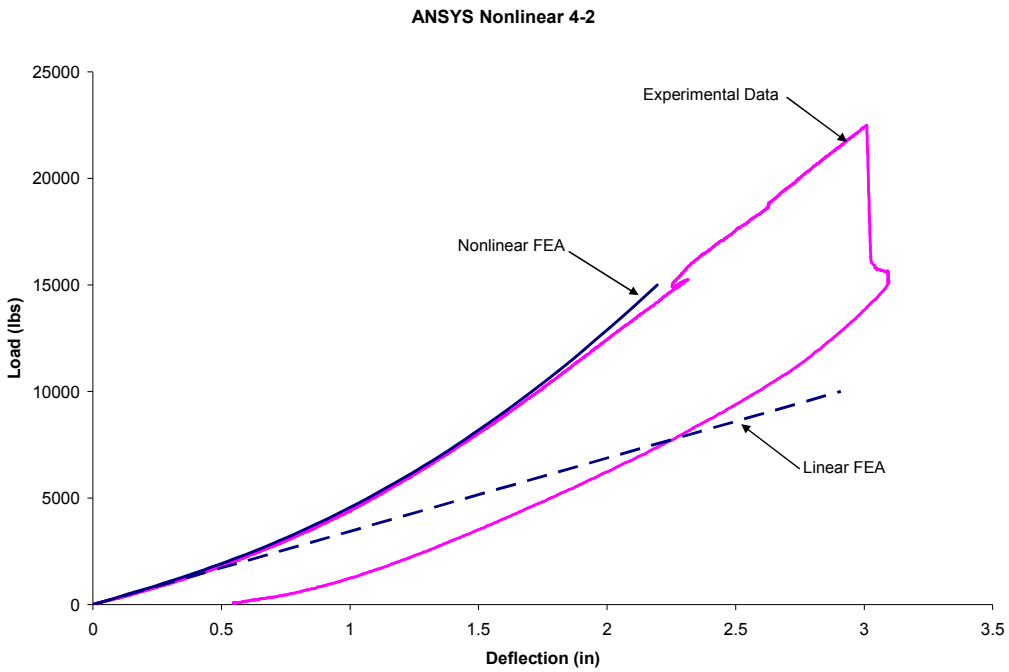

Figure A.17 Nonlinear ANSYS Model for the RDPS4-2 Panel

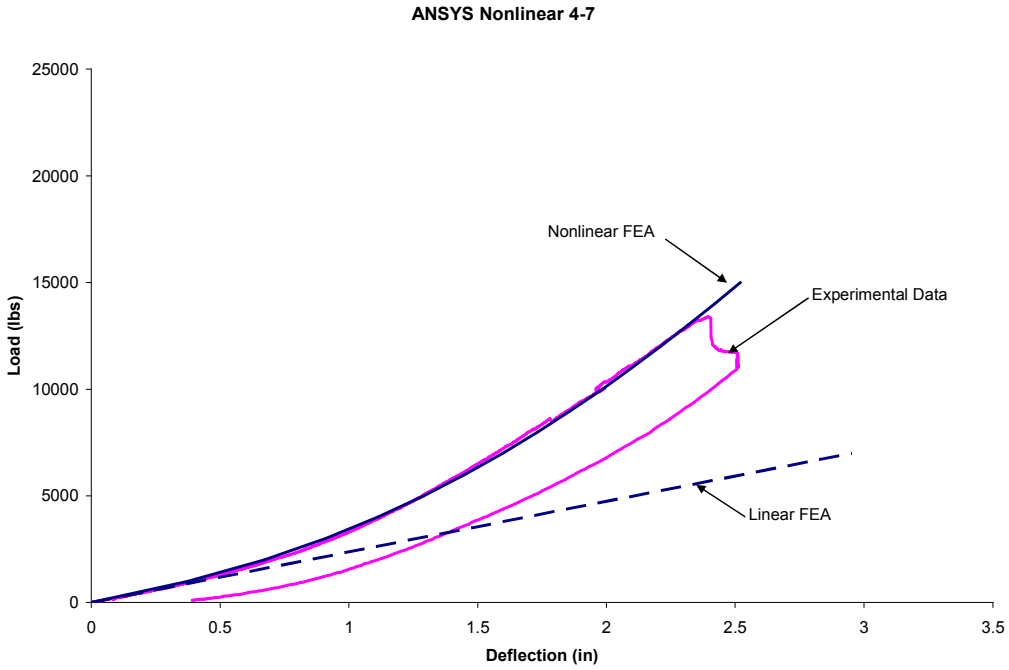

Figure A.18 Nonlinear ANSYS Model for the RDPS4-7 Panel

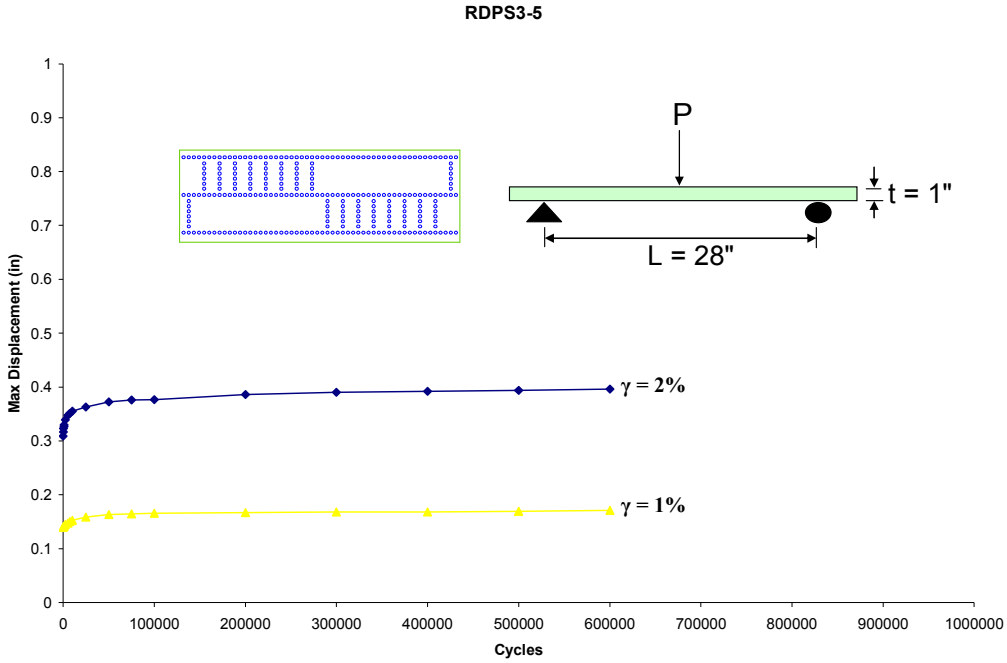

Figure A.19 Max Deflection vs. # of Cycles RDPS3-5 L=28"

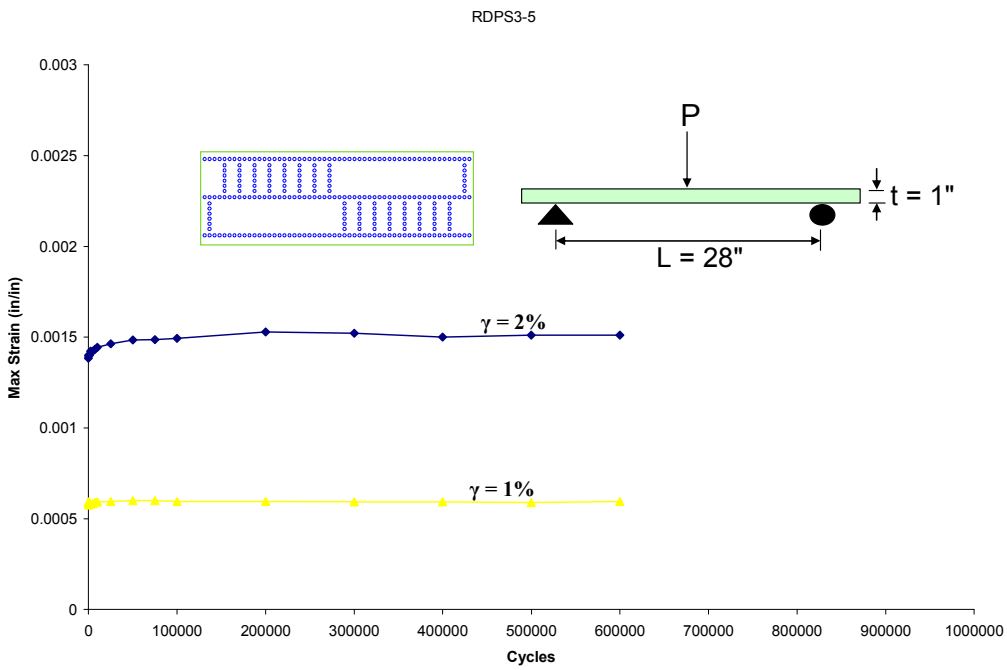

Figure A.20 Max Strain vs. # of Cycles RDPS3-5 L=28"

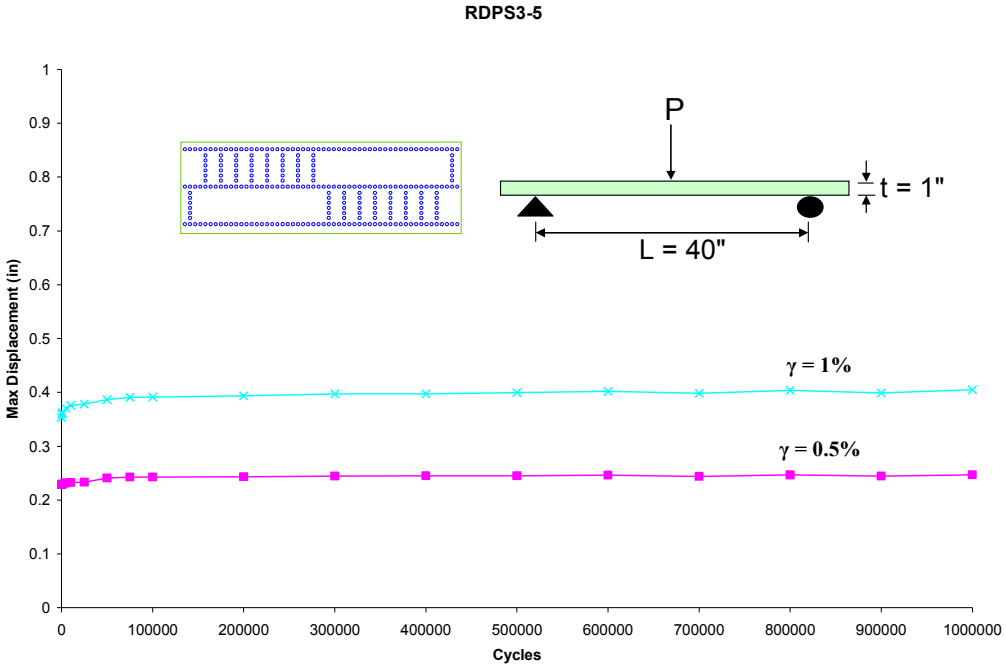

Figure A.21 Max Deflection vs. # of Cycles RDPS3-5 L=40"

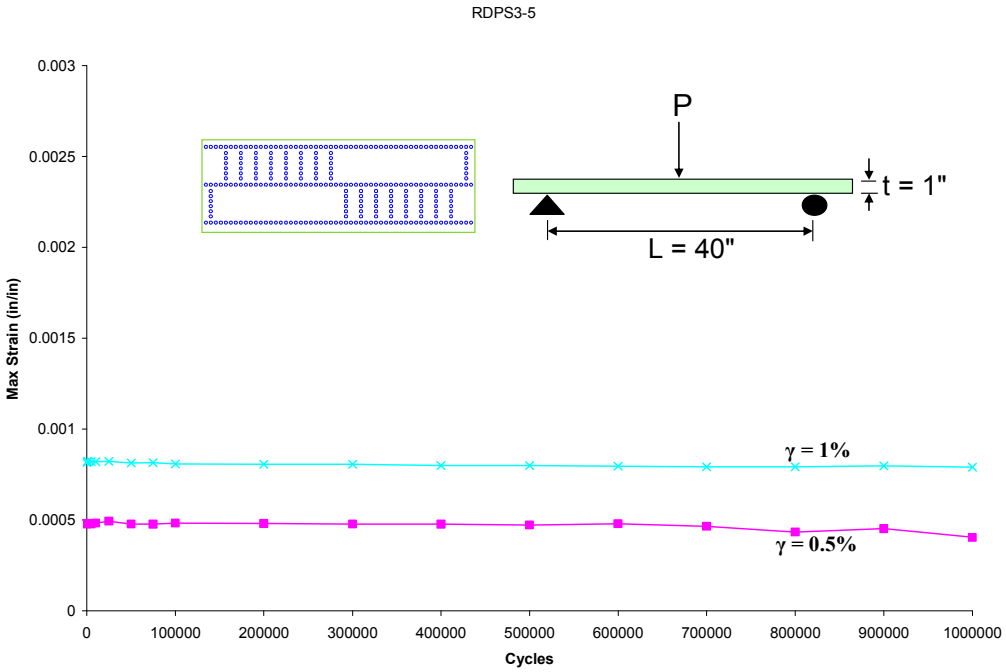

Figure A.22 Max Strain vs. # of Cycles RDPS3-5 L=40"

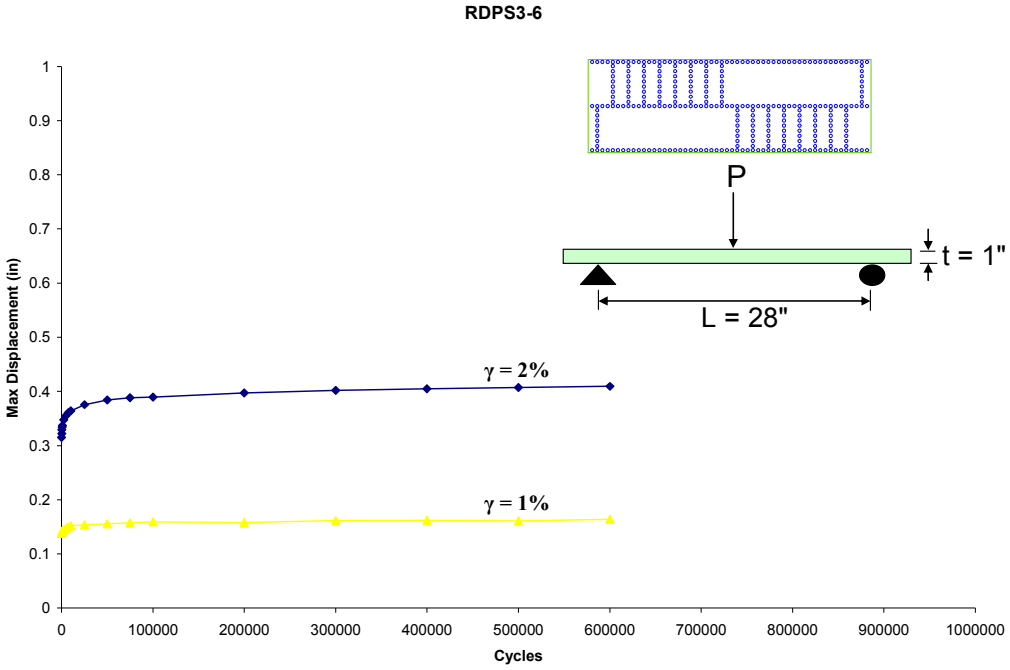

Figure A.23 Max Displacement vs. # of Cycles RDPS3-6 L=28"

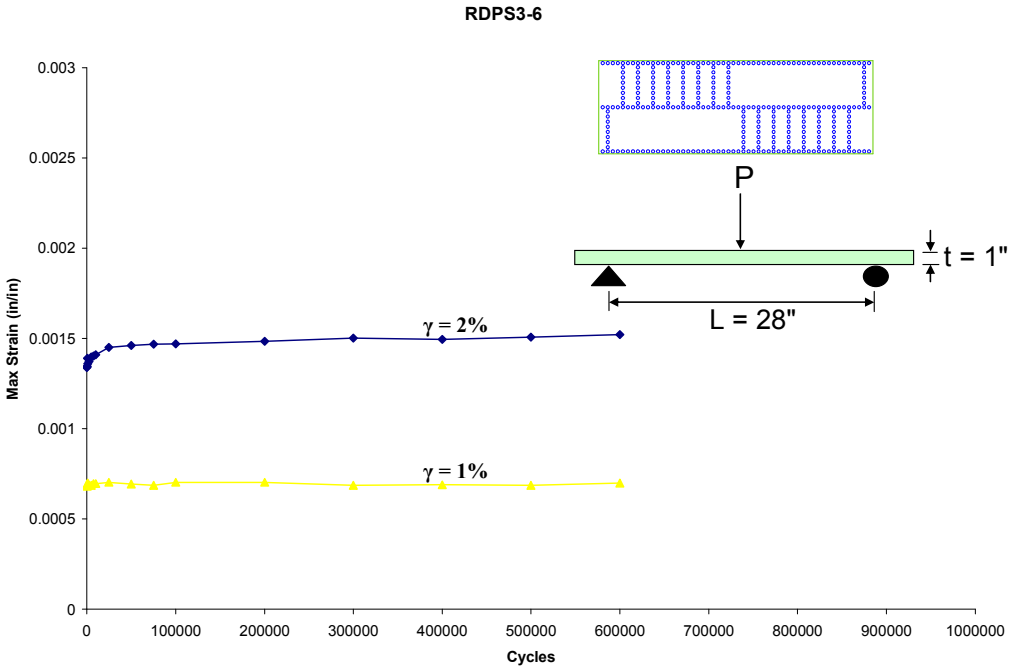

Figure A.24 Max Strain vs. # of Cycles RDPS3-6 L=28"

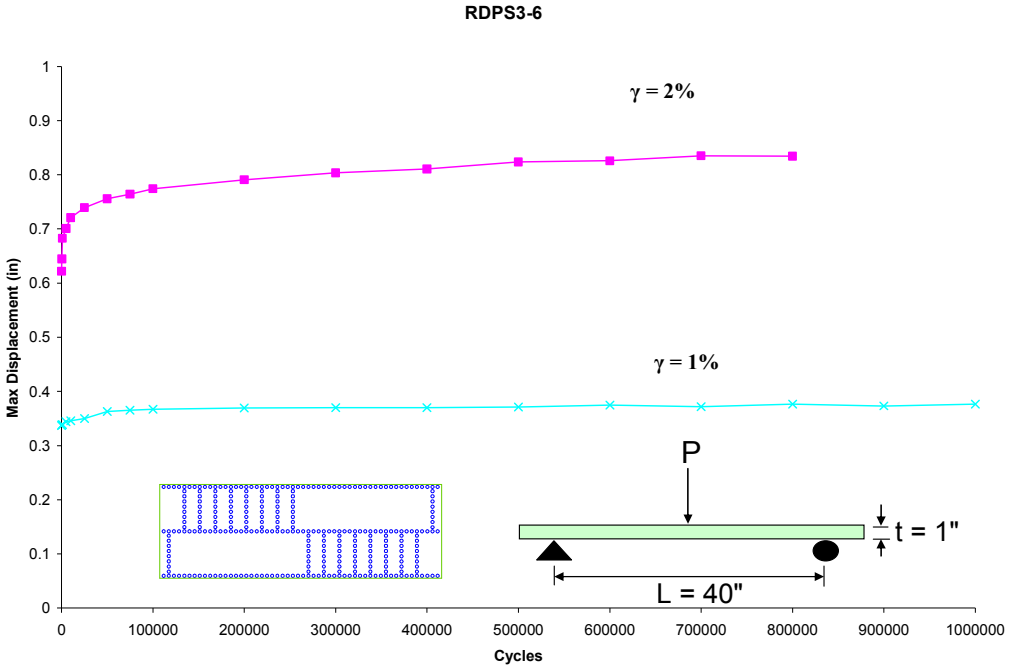

Figure A.25 Max Displacement vs. # of Cycles RDPS3-6 L=40"

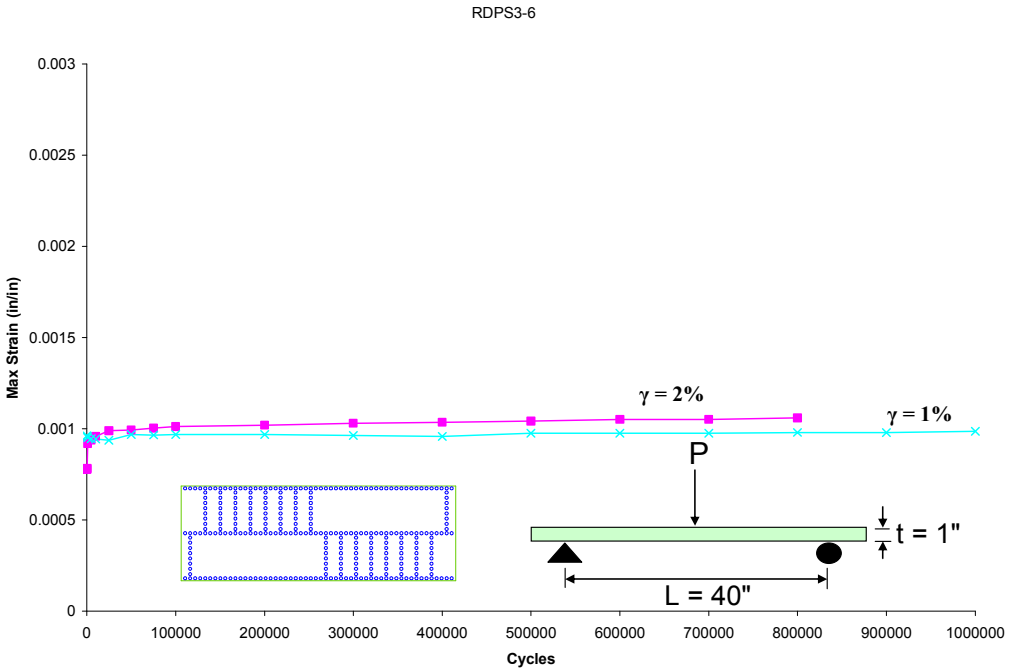

Figure A.26 Max Strain vs. # of Cycles RDPS3-6 L=40"

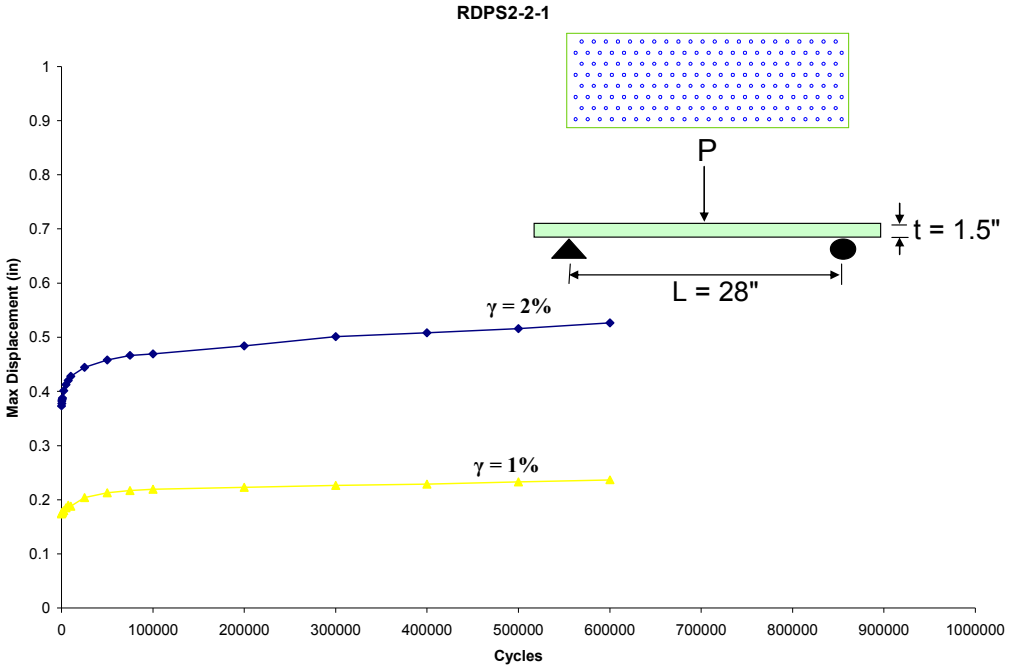

Figure A.27 Max Displacement vs. # of Cycles RDPS2-2-1 L=28"

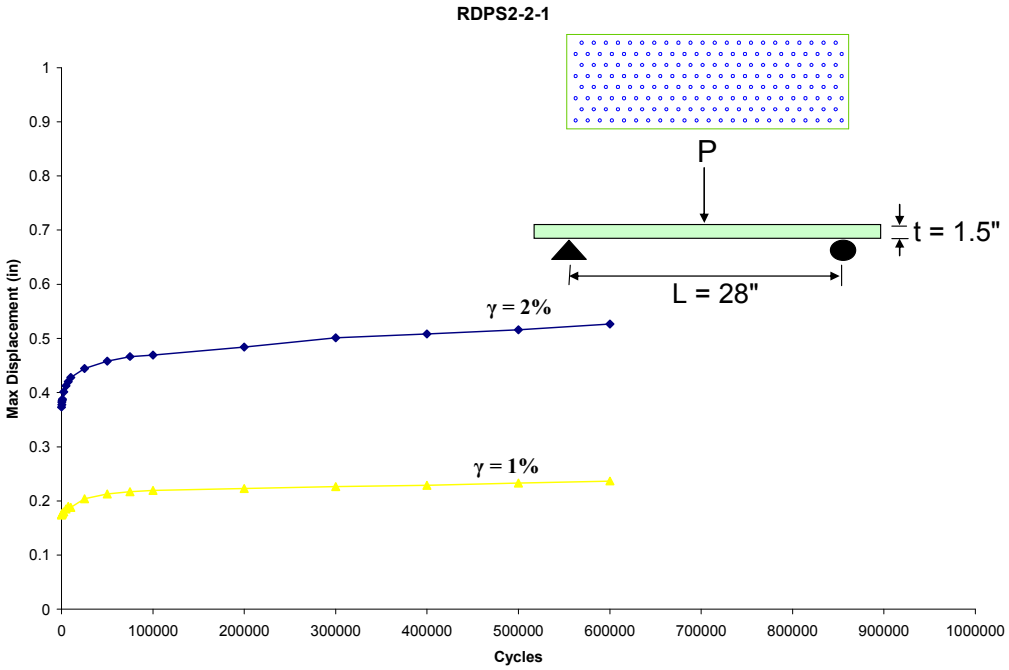

Figure A.28 Max Strain vs. # of Cycles RDPS2-2-1 L=28"

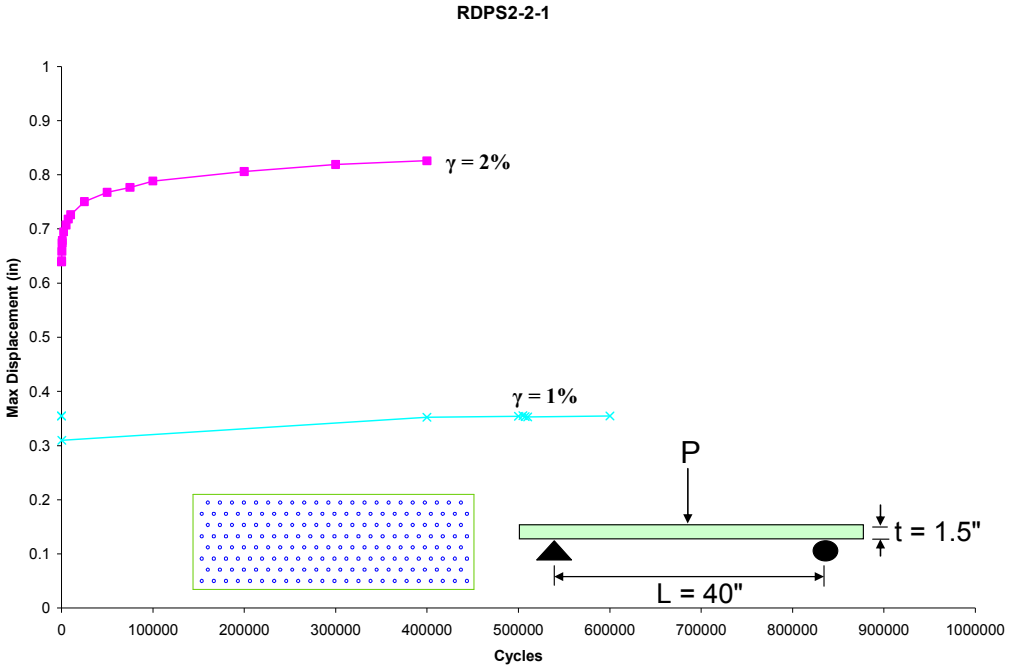

Figure A.29 Max Displacement vs. # of Cycles RDPS2-2-1 L=40"

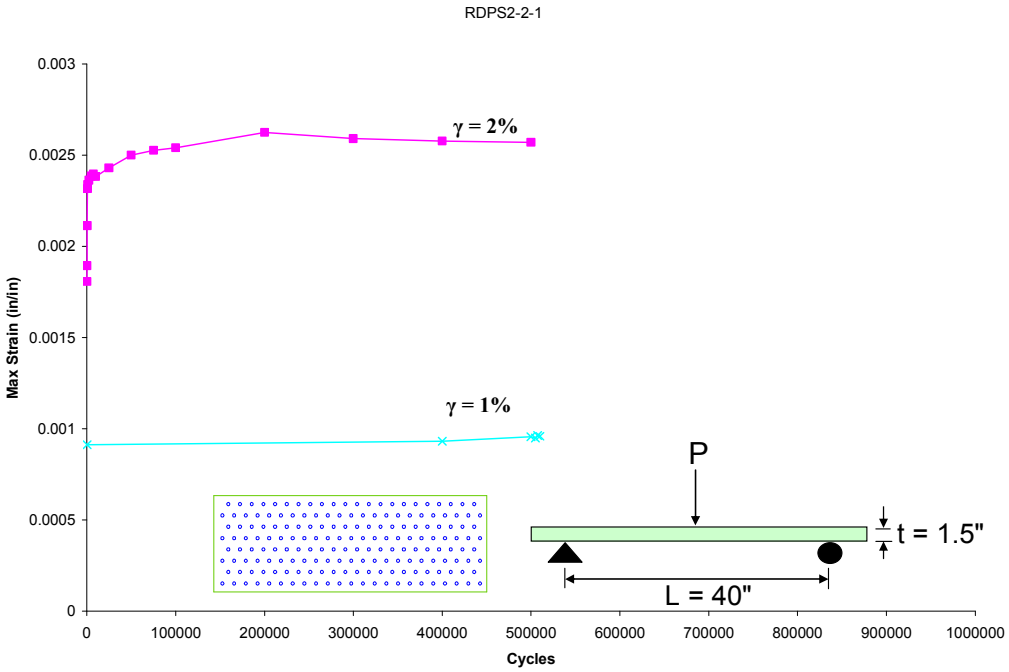

Figure A.30 Max Strain vs. # of Cycles RDPS2-2-1 L=40"

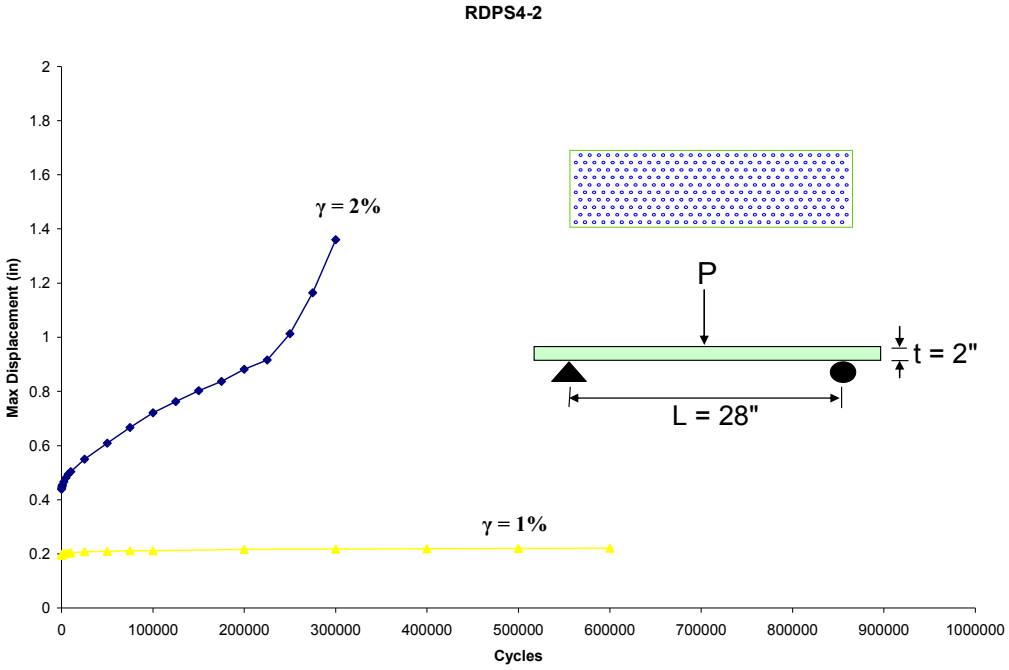

Figure A.31 Max Displacement vs. # of Cycles RDPS4-2 L=28"

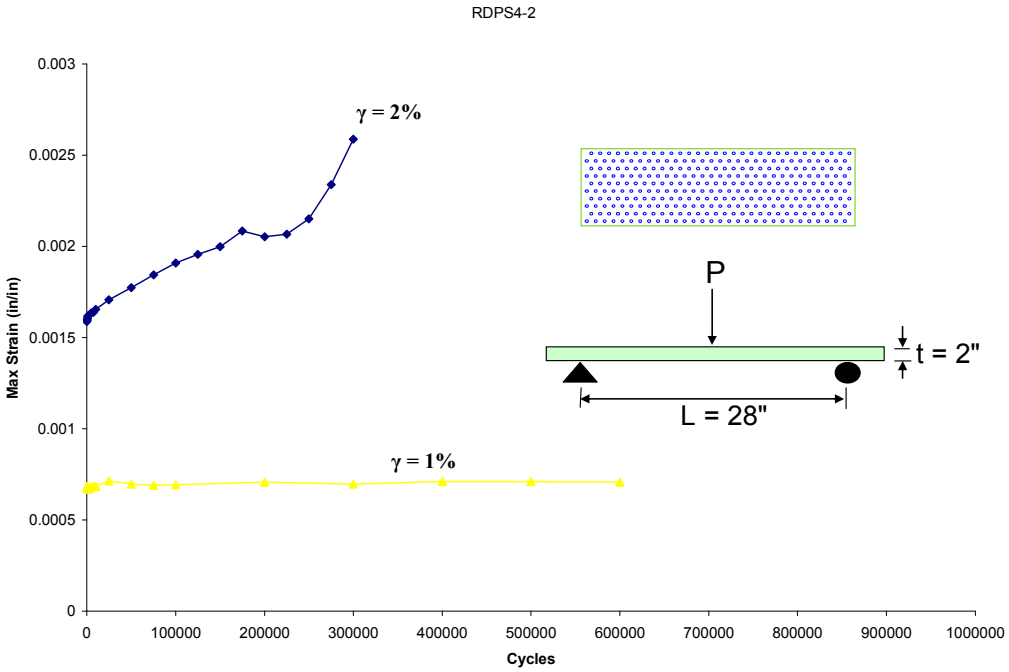

Figure A.32 Max Strain vs. # of Cycles RDPS4-2 L=28"

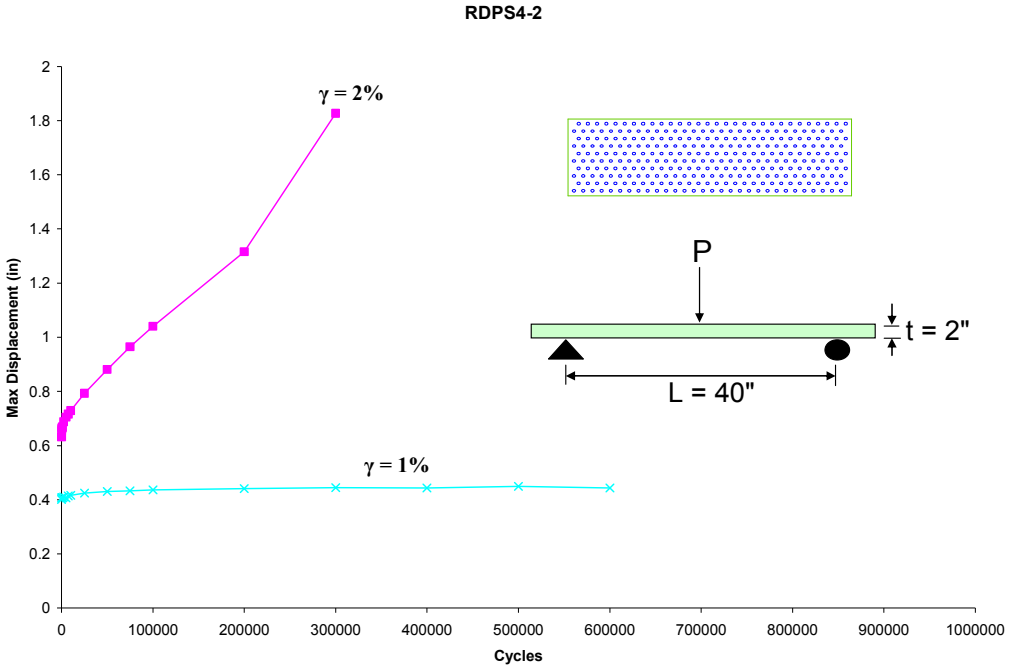

Figure A.33 Max Displacement vs. # of Cycles RDPS4-2 L=40"

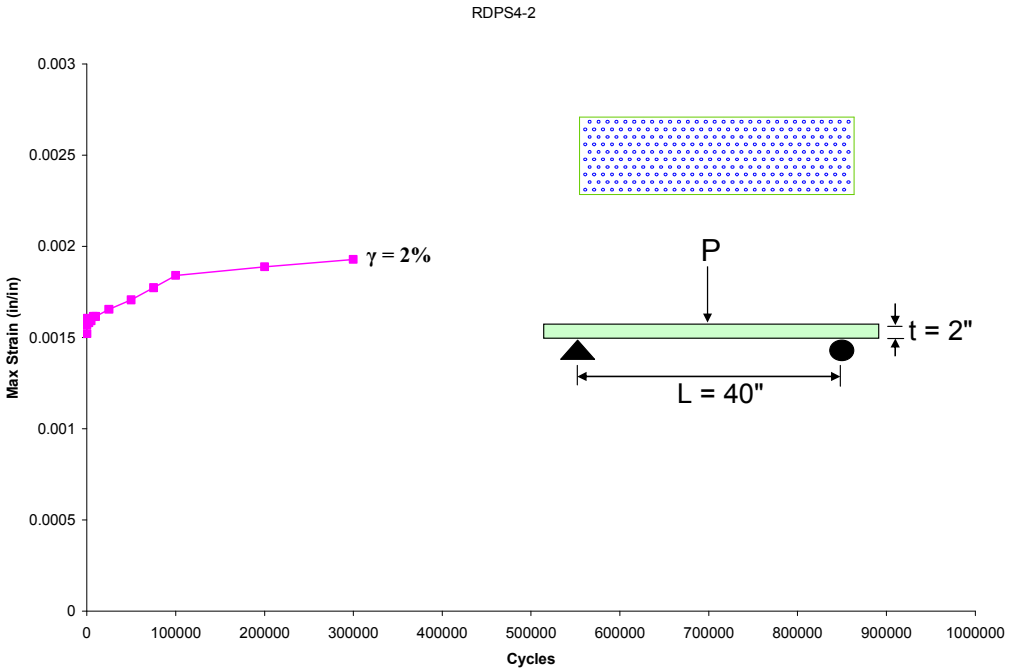

Figure A.34 Max Strain vs. # of Cycles RDPS4-2 L=40"

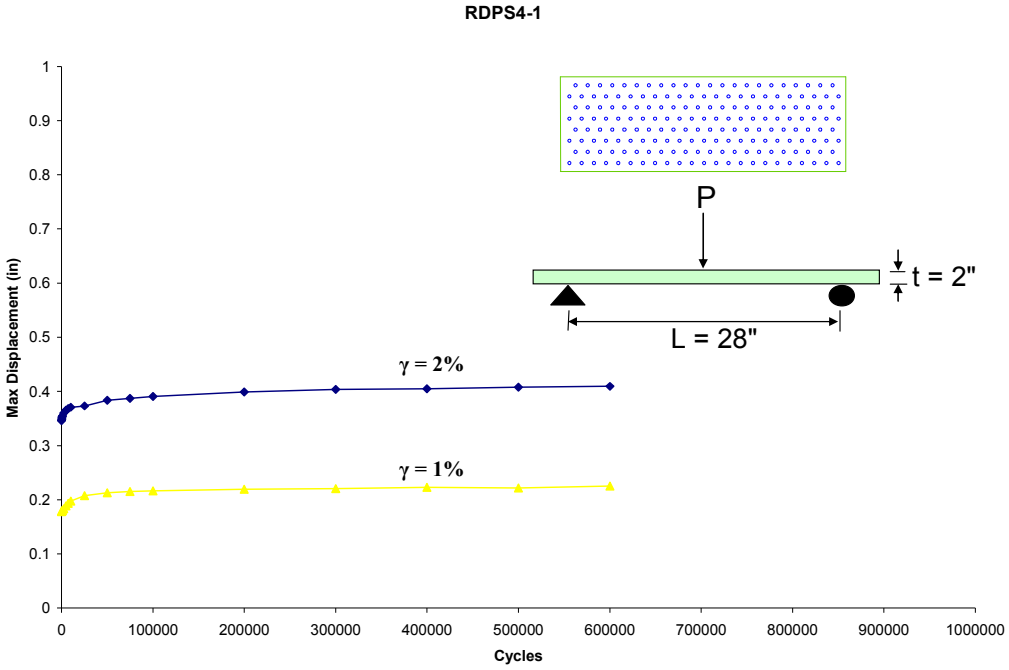

Figure A.35 Max Displacement vs. # of Cycles RDPS4-1 L=28"

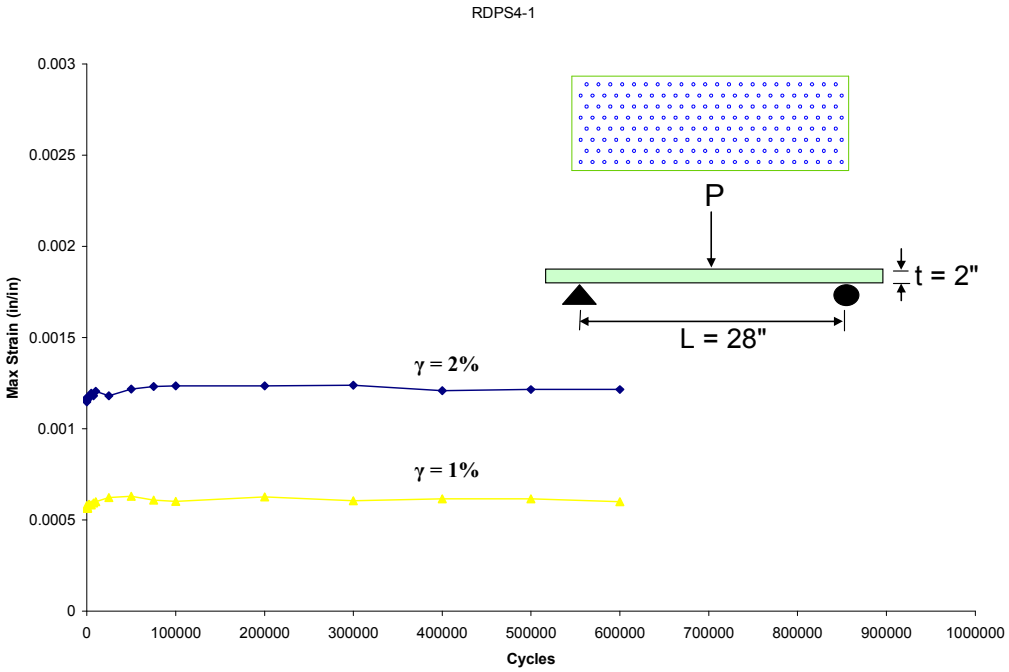

Figure A.36 Max Strain vs. # of Cycles RDPS4-1 L=28"

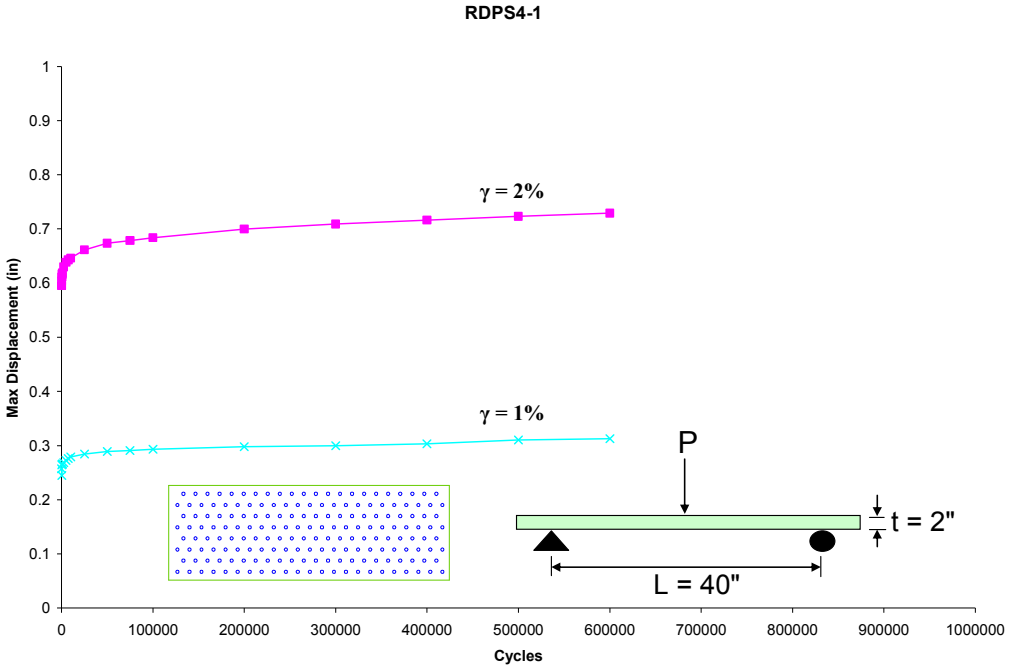

Figure A.37 Max Displacement vs. # of Cycles RDPS4-1 L=40"

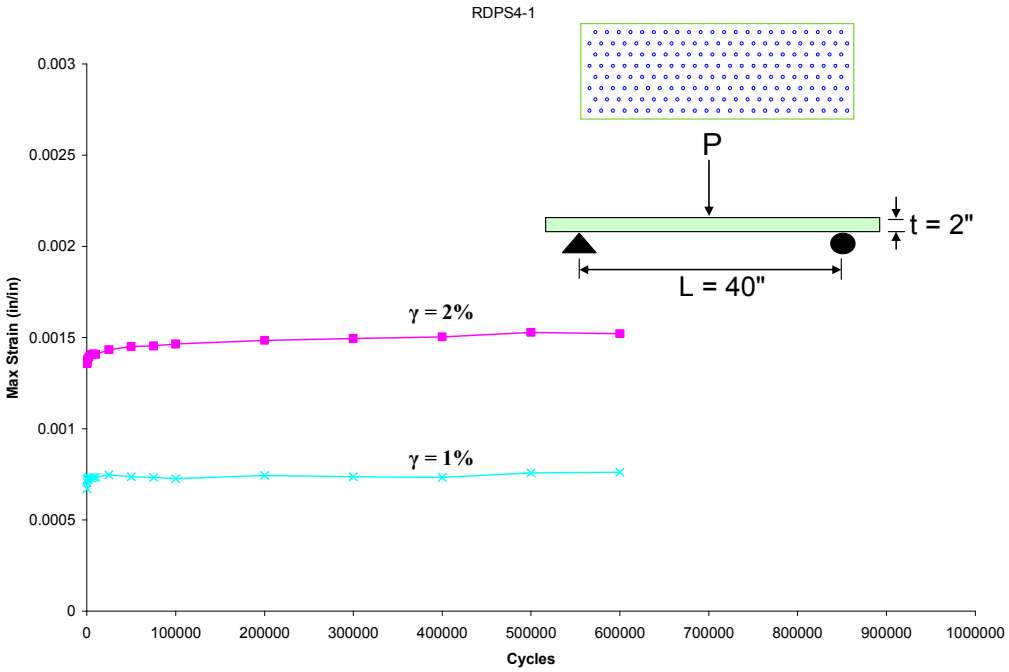

Figure A.38 Max Strain vs. # of Cycles RDPS4-1 L=40"

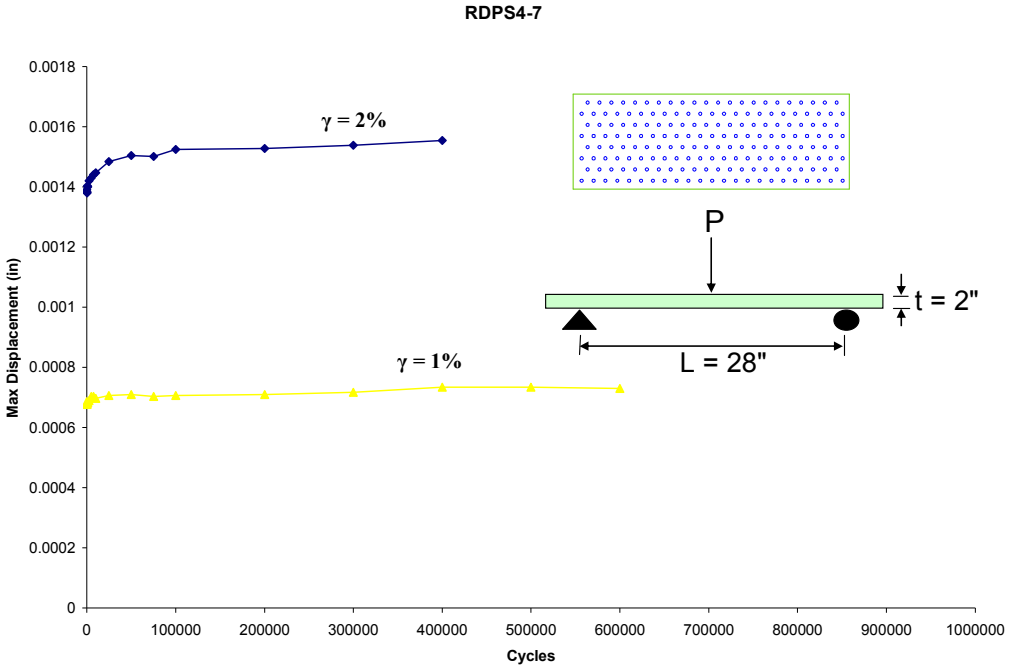

Figure A.39 Max Displacement vs. # of Cycles RDPS4-7 L=28"

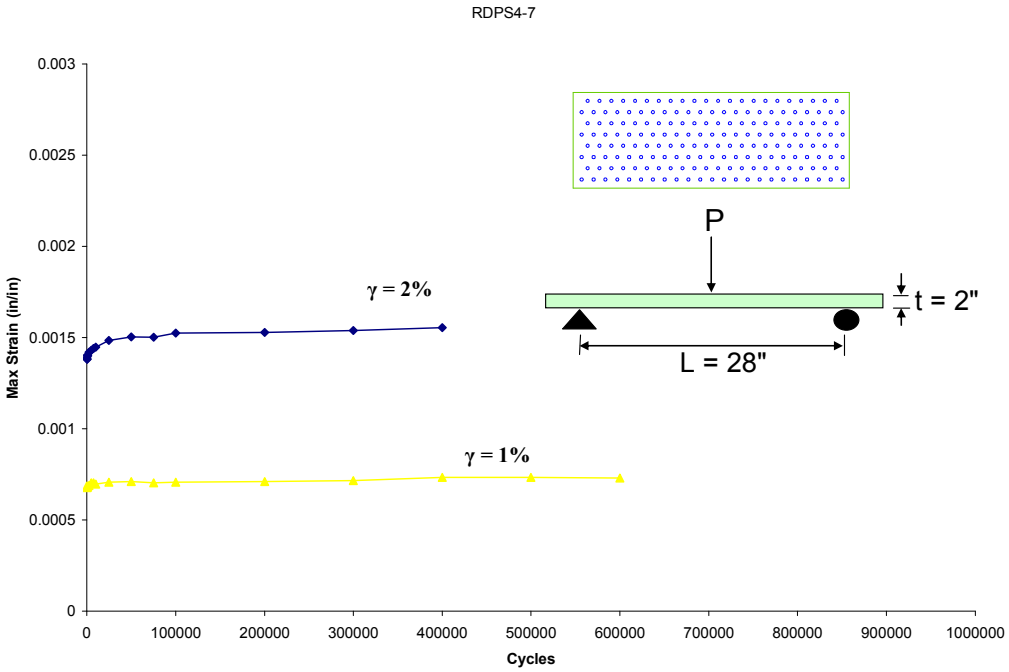

Figure A.40 Max Strain vs. # of Cycles RDPS4-7 L=28"

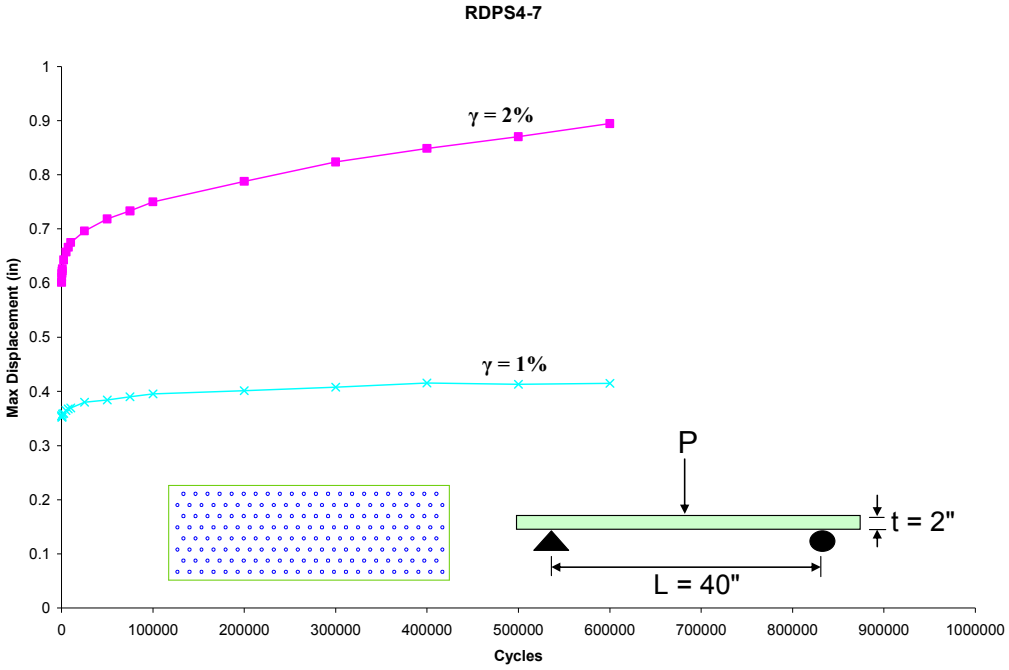

Figure A 41 Max Displacement vs. # of Cycles RDPS4-7 L=40"

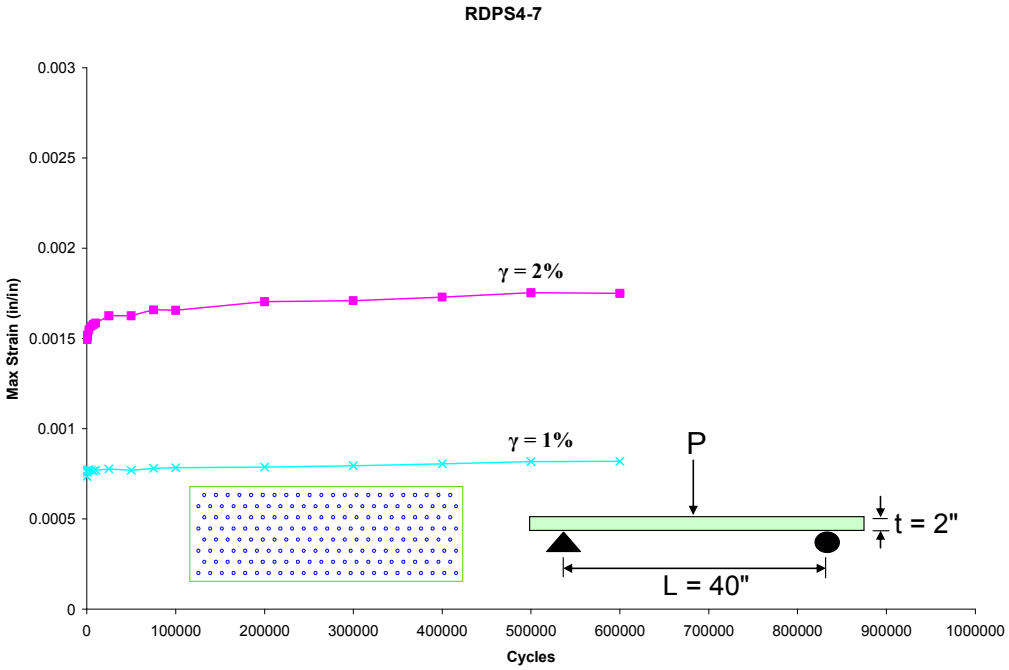

Figure A.42 Max Strain vs. # of Cycles RDPS4-7 L=40"

APPENDIX B

```
FINISH
/CLEAR,NOSTART
/PREP7
MSHKEY,1
!
L1=44
W1=44
L=L1/2
W=W1/2
Material = 'RDPS3.6'
e=4       !ESIZE distance
!
! Initial settings
!
/INPUT,Settings.txt
!
! Element types
!
ET,1,SHELL281
ET,2,SOLID186
ET,3,BEAM188
ET,4,LINK10,,0,1  !Compression Only Spar
ET,5,LINK10,,0,0  !Tension Only Spar
!
! Define material number 1 and 2
!
*USE,%Material%.mac,1,2
!
num = 4
!
MP,EX,num,1E7   !psi (Compresion only supports)
!
num = 5
!
MP,EX,num,1000   !psi (Tension only supports)
!
R,20,0.1,0
R,21,0.1,0
```

```
!
! Define a "section"
!
num = 10
!
SECTYPE,num,SHELL
SECOFFSET,MIDDLE
!-------------------------------------------------------------------------------!
!  SECDATA,A,B,C,D --> A --> Thickness, in                                      !
!                  B --> Material number                                        !
!                  C --> Angle                                                  !
!                  D --> Integration points                                     !
!-------------------------------------------------------------------------------!
SECDATA  , ts/4 ,  1  ,  0.0  ,  3  ! 1 (z = 0)
SECDATA  , ts/4 ,  1  ,  0.0  ,  3  ! 2
SECDATA  , ts/4 ,  1  ,  0.0  ,  3  ! 3
SECDATA  , ts/4 ,  1  ,  0.0  ,  3  ! 4
!-------------------------------------------------------------------------------!
!
ESIZE,1
!
! Create an area geometry
!
K,1,L,0,W    ! --> Keypoint 1
K,2,L,0,-W   ! --> Keypoint 2
K,3,-L,0,-W  ! --> Keypoint 3
K,4,-L,0,W   ! --> Keypoint 4
!
L,1,2  ! --> Line 1
L,2,3  ! --> Line 2
L,3,4  ! --> Line 3
L,4,1  ! --> Line ! 4
!
AL,1,2,3,4  ! --> Area 1
!
! Create a volume geometry
!
K,,L,h,W    ! --> Keypoint 5
K,,L,h,-W   ! --> Keypoint 6
K,,-L,h,-W  ! --> Keypoint 7
K,,-L,h,W   ! --> Keypoint 8
```

```
!
V,1,2,3,4,5,6,7,8
!
!Loading
!4" wide supports constraining translation in the verticle direction only.
!4"x4" loading area
!
nl=L1/e-1
nw=W1/e-1
!
!Create compression only Supports
K,,L,-1,W
*GET,kp6,KP,,NUM,MAX
K,,L,-1,-W
*GET,kp4,KP,,NUM,MAX
KFILL,kp6,kp4,nw,,1
K,,L,-1,-W
*GET,kp3,KP,,NUM,MAX
K,,-L,-1,-W
*GET,kp4,KP,,NUM,MAX
KFILL,kp3,kp4,nl,,1
K,,-L,-1,-W
*GET,kp3,KP,,NUM,MAX
K,,-L,-1,W
*GET,kp4,KP,,NUM,MAX
KFILL,kp3,kp4,nw,,1
K,,-L,-1,W
*GET,kp3,KP,,NUM,MAX
K,,L,-1,W
*GET,kp4,KP,,NUM,MAX
KFILL,kp3,kp4,nl,,1
!
!Create compression only Supports
K,,L,0,W
*GET,kp3,KP,,NUM,MAX
K,,L,0,-W
*GET,kp4,KP,,NUM,MAX
KFILL,kp3,kp4,nw,,1
K,,L,0,-W
*GET,kp3,KP,,NUM,MAX
K,,-L,0,-W
```

```
*GET,kp4,KP,,NUM,MAX
KFILL,kp3,kp4,nl,,1
K,,-L,0,-W
*GET,kp3,KP,,NUM,MAX
K,,-L,0,W
*GET,kp4,KP,,NUM,MAX
KFILL,kp3,kp4,nw,,1
K,,-L,0,W
*GET,kp3,KP,,NUM,MAX
K,,L,0,W
*GET,kp4,KP,,NUM,MAX
KFILL,kp3,kp4,nl,,1
!
LSEL,U,,,ALL
n1=kp6
nn=n1+L1/e+W1/e+L1/e+W1/e
N=nn-n1
C=nn-1
*DO,i,n1,C
  L,i,(i+N),1
*ENDDO
CM,Clines,LINE
ALLSEL
!
!Create 1 tension only support
LSEL,U,,,ALL
KSEL,U,,,ALL
K,,2,h,2
*GET,kp1,KP,,NUM,MAX ! Get the highest keypoint number in the selected set
K,,2,-3,2
*GET,kp2,KP,,NUM,MAX
L,kp1,kp2,1
CM,Tlines,LINE
ALLSEL
!
NUMMRG,KP,(0.0001)
!
esize,e
!
! Mesh areas 1 and 6 with Shell elements
!
```

```
TYPE,1
SECN,10
AMESH,1
AMESH,6
!
! Mesh volume 1 with Solid elements
!
TYPE,2
MAT,2
VMESH,1
!
! Mesh the compression only lines
!
TYPE,4
MAT,4
REAL,20
LMESH,Clines
!
! Mesh the tension only lines
!
TYPE,5
MAT,5
REAL,21
LMESH,Tlines
!
NUMMRG,NODE,(0.0001)
!
!Apply Constraints
!
! Compression only elements
ALLSEL
NSEL,S,LOC,Y,-1  $  NSEL,R,Loc,X,-L  $  D,ALL,UY,0  $  D,ALL,UX,0  $  D,ALL,UZ,0
NSEL,S,LOC,Y,-1  $  NSEL,R,Loc,X,L   $  D,ALL,UY,0  $  D,ALL,UX,0  $  D,ALL,UZ,0
NSEL,S,LOC,Y,-1  $  NSEL,R,Loc,Z,-W  $  D,ALL,UY,0  $  D,ALL,UX,0  $  D,ALL,UZ,0
NSEL,S,LOC,Y,-1  $  NSEL,R,Loc,Z,W   $  D,ALL,UY,0  $  D,ALL,UX,0  $  D,ALL,UZ,0
!
! BCs for the panel corner node
!
NSEL,S,LOC,Y,0.0
NSEL,R,Loc,X,-L
NSEL,R,Loc,Z,-W
```

```
D,ALL,UX,0 $ D,ALL,UZ,0 $ D,ALL,ROTY,0
!
! BCs for the tension only element
!
NSEL,S,LOC,Y,-3
NSEL,R,LOC,X,2
NSEL,R,LOC,Z,2
D,ALL,UY,0  $  D,ALL,UX,0  $  D,ALL,UZ,0
!
!Apply Loads
ALLSEL
!
ftotal = 15000
NSEL,S,LOC,Y,h
NSEL,R,Loc,X,-2,2
NSEL,R,Loc,Z,-2,2
*GET,num,NODE,0,COUNT
fnode = ftotal/num
F,ALL,FY,-fnode
ALLSEL
!
! Create your final load above, then write a "Load Step"
!
LSWRITE,1
!
ftotal = 16000
NSEL,S,LOC,Y,h
NSEL,R,Loc,X,-2,2
NSEL,R,Loc,Z,-2,2
*GET,num,NODE,0,COUNT
fnode = ftotal/num
F,ALL,FY,-fnode
ALLSEL
!
! Create your final load above, then write a "Load Step"
!
LSWRITE,2
!
! Non-Linear Solution
!
/INPUT,NLSolve.txt
```

```
!
! Write the data file
!
/INPUT,WriteData.txt
!
! End of file

! Settings.txt
!
/VIEW,1,1,1,1
/ANG,1
/REP,FAST
!
/PREP7
!
! Mesh setting
!
MSHKEY,1
!
! Print results to the .out file (available through the GUI)
!
OUTPR,NSOL,ALL
OUTPR,RSOL,ALL
OUTPR,ESOL,ALL
!
! Write results to the .db file
!
OUTRES,NSOL,ALL
OUTRES,RSOL,ALL
OUTRES,ESOL,ALL
!
! End
!

!Material Properties
ts=0.178
h=2.0
!
! Define material number 1
!
num = arg1
```

```
!
MP,EX,num,2.70E+06
MP,EY,num,2.70E+06
MP,EZ,num,1.00E+06
!
MP,PRXY,num,0.15
MP,PRYZ,num,0.35
MP,PRXZ,num,0.35
!
MP,GXY,num,0.350E+06
MP,GYZ,num,0.30E+06
MP,GXZ,num,0.30E+06
!
! Define material number 2, RDPS4-1, Core
!
num = arg2
!
MP,EX,num,10.0E+03   !-->  psi
MP,EY,num,50.1E+03   !-->  psi
MP,EZ,num,10.0E+03  !-->  psi
!
MP,PRXY,num,0.200
MP,PRYZ,num,0.050
MP,PRXZ,num,0.050
!
MP,GXY,num,0.40E+03  !-->  psi
MP,GYZ,num,0.40E+03  !-->  psi
MP,GXZ,num,0.450E+03  !-->  psi
!
!END

! NLSolve.txt
! Enter the solution processor
!
/SOLU
!
! Geometric nonlinearity
!
NLGEOM,ON
!
SOLCONTROL,ON
```

```
!
! Number of sub-steps per load step
!
AUTOTS,OFF
!
ALLSEL
!
! Read the load step file
!
LSREAD,1
!
nss = 10
!
NSUBST,nss
!
! Solve the load step
!
SOLVE
!
LSREAD,2
!
nss = 10
!
NSUBST,nss
!
SOLVE
!
FINISH
!
! End
```

```
! WriteData.txt
!
/POST1
!
```

```
*CFOPEN,data,txt
!
*DO,i,1,2
*DO,j,1,nss
!
SET,i,j
PLNSOL,U,Y
*GET,defl,PLNSOL,0,MIN
*VWRITE,i,(-1*defl)
%2I %G
!
*ENDDO
*ENDDO
!
*CFCLOS
!
! End
```